COMPRESSIBILITY OF HYDRATED AND ANHYDROUS SODIUM SILICATE-BASED LIQUIDS AND GLASSES, AS ANALOGUES FOR NATURAL SILICATE MELTS, BY BRILLOUIN SCATTERING SPECTROSCOPY

A DISSERTATION SUBMITTED TO THE GRADUATE DIVISION OF THE UNIVERSITY OF HAWAI'I IN PARTIAL FULFILLMENT OF THE REQUIREMENTS FOR THE DEGREE OF

DOCTOR OF PHILOSOPHY

IN

GEOLOGY AND GEOPHYSICS

AUGUST 2005

By

Sergey Nikolayevich Tkachev

Dissertation Committee

Murli H. Manghnani, Chairperson
Li Chung Ming
Julia E. Hammer
Bruce F. Houghton
Cromwell S. Crawford

ACKNOWLEDGMENTS

I am very grateful to my research advisor and Chair of the dissertation committee, Murli Manghnani, for his strong moral support, guidance and encouragement. Without his passionate determination to jump into something challenging and unknown, the results of my dissertation would have been extremely difficult to achieve. I would like to express my deep appreciation to the members of my Ph.D. committee for giving me a new valuable outlook on the development of the research as well as advice on the way I should present the data. Comments and suggestions generously provided by Li Chung Ming and Julia Hammer helped me immensely to understand how to emphasize the strong points of the dissertation and make improvements to clarify the aspects associated with future directions of the research. The time I spent with Li Chung Ming discussing the technical subject of using the externally heated diamond anvil cell gave me a better vision on how to achieve the results outlined in Chapter 3. The outstanding level of Bruce Houghton's knowledge and his optimism and personal warmth were important factors that positively affected my overall performance during the preparation of my defense and the defense itself. I deeply appreciate the courage and insightful thinking of the outside committee member, Cromwell Crawford, who was not afraid of asking questions and giving valuable recommendations on a subject that was not related to his professional area of research. The success of my research would not be possible without the expertise and knowledge of the permanent mechanical engineer, John Balogh. His solid, right-to-the-point guidance in all technical (and other) aspects — from maintenance of the equipment to the overall psychological climate in the laboratory — were extremely

helpful and always kept challenging situations under control. Numerous discussions with Quentin Williams of the results presented in the dissertation strengthened the scientific ideas and provided bases for my publications in the highly acclaimed scholarly journals. Fengying Li and Yuchang Wang were selflessly helpful by discussing with me various aspects of pressure-induced glass behavior. John Sandercock and Burkard Hillebrands made invaluable contributions to design, installation and troubleshooting, combined with practical suggestions on alignment and maintenance of our state-of-the-art Brillouin scattering system. My understanding and knowledge of various Raman scattering systems were substantially enhanced through technical support provided by Alex Goncharov, Viktor Struzhkin, and Emmanuel Leroy. The samples of float glass and sodium silicate solutions were kindly supplied by Tim Holmquist (Network Computing Service Inc., Minneapolis) and the PQ® Corporation, respectively. John Phair (Federal Highway Administration) played a major role in preparing the samples of alkaline-calcium hydrogels and, then, in studying their structural properties. A fiber-optic system to measure the pressure inside the diamond anvil cell was solely designed and installed by Tom Cooney. Major parts of my dissertation were dramatically improved after I received critical reviews from Vadim Brazhkin, Mark Ghiorso, Yingwei Fei, and anonymous referees from the *Journal of Geophysical Research – Solid Earth* and from *Physical Review Letters*. Initial stages of experiments on water were conducted under supervision and in collaboration with Jay Bass, Stas Sinogeikin, and Andrey Kalinichev. This research was financially supported by U.S. National Science Foundation (Grant No. EAR-0074285; M. H. Manghnani, PI), U.S. Army Research Office (U.S. Army Contract No. DAAD 19-00-1-0569; M. H. Manghnani, PI) and through numerous fruitful

materials science research projects in collaboration with Pavel Zinin, Vladimir Solozhenko, and Stan Vepřek, as well as under a grant from the Federal Highway Administration.

I am forever indebted to my dear wife Maria for her wholehearted support and my father and mother, the best parents in the world, for being always there for me, no matter what turn of events would have come around. The time spent in the magically beautiful Hawai'ian Islands is one of the most precious experiences we have ever had in our lives!

ABSTRACT

A mathematical formalism was tested on compressibility studies of water, before applying it to the high pressure-temperature compressibility studies of hydrated and anhydrous sodium silicate-based liquids and glasses. The hypersonic sound velocity, refractive index and attenuation coefficient obtained using Brillouin light scattering spectroscopy technique were in agreement with literature data. From the measured sound velocities, the pressure dependence of the bulk moduli and density of liquid water were calculated, using Vinet equation of state. The formalism was extended to the Brillouin scattering studies of the elastic properties of alkaline-calcium silica hydrogels and float glass, which exhibits a dramatic increase in the pressure dependence of longitudinal velocity and a discontinuity in the compressibility at about 6 GPa. It is demonstrated that an apparent second-order transition to a new amorphous phase can form via the abrupt onset of a new compressional mechanism, which may be triggered by a shift in polymerization of the glass or an onset of a change in coordination of silicon.

Brillouin scattering measurements were carried out on an aqueous solution of Na_2O-$2SiO_2$ and anhydrous Na_2O-$2SiO_2$ glass and liquid at high P-T conditions. The "modified" platelet scattering geometry has allowed a determination of the longitudinal velocity independently from refractive index, and hence the adiabatic compressibility and density of liquids as a function of pressure and temperature. The observed increase in density of the melt and glass phases formed at high P-T conditions is likely associated with structural effects. The large values of K_S' of the liquid phase illustrate that the means of compaction of the liquid differs substantially from that of the glass, and that the liquid

is able to access a wider range of compaction mechanisms. The measured bulk modulus of Na_2O-$2SiO_2$ aqueous solution is closer to values of silicate melts than to that of end-member water at high pressures. Thus, water-rich silica-bearing solutions present at depth are likely to be difficult to seismically distinguish from anhydrous silicate melts based solely upon their sound velocities. The data on water-bearing compounds allow the pressure dependence of the partial molar volume of water to be assessed to upper mantle depths.

TABLE OF CONTENTS

LIST OF FIGURES

Chapter 1

GENERAL INTRODUCTION

1.1 ELASTICITY OF THE SILICATE MELTS IN THE EARTH'S INTERIOR

The composition of silicate melts within the Earth is dominated by the oxides SiO_2, Al_2O_3, FeO, MgO, CaO, Na_2O and K_2O. Various mixtures of these oxides, with 40-80-mol% SiO_2, make up the granites of the crust, basalt and rhyolite magmas, and plume-associated melts in the mantle. The majority of binary and ternary oxide melt compositions investigated in the laboratory have bulk moduli ranging from 15 to 25 GPa at 1 atmospheric pressure (10^5 Pa) [*Rivers and Carmichael,* 1987; *Secco et al.,* 1991]. Ultrasonic studies [e.g., *Rivers and Carmichael*, 1987*; Kress et al.,* 1988*; Secco et al.,*1991*; Webb and Courtial,* 1996] have provided data that elucidate the composition dependence of compressibility of silicate melts at ambient pressures.

Our understanding of both magmatic processes and the differentiation history of the Earth's mantle is dependent on the physical properties of silicate melts under simultaneous high pressure and temperature conditions. The behavior of such melts at pressure depends on their composition (and thus their structure), as well as the surrounding mineral assemblage [*Mysen,* 1990]. A number of studies have shown that at high pressures, silicon in silicate melts plausibly undergoes a change from four- to six-fold coordinate with respect to oxygen [e.g., *Stolper and Ahrens,* 1987]. Shock wave studies on silicate melts have indicated that at depths of 150-200 km in the upper mantle,

the density of melts could be higher than the surrounding rocks due to pressure-induced coordination changes [*Stolper and Ahrens,* 1987*; Rigden et al.,* 1988, 1989].

Indeed, coordination changes of silicon provide the most plausible mechanism for generating the 20% (or more) increase in silicate melt density inferred to occur in the upper mantle of the planet: this change in density is considerably in excess of that likely to occur from either pressure-induced shifts in chemical partitioning or structural transformations associated with other elements. The implications of the density difference between melts and their surrounding rocks, and the role of these differences in the early differentiation and evolution of the Earth and planetary interiors have been discussed by numerous authors [*Rigden et al.,* 1984, 1988, 1989*; Jeanloz,* 1989*; Miller et al.,* 1991*; Circone and Agee,* 1996].

The thermodynamic and viscoelastic properties of silicate melts are essential for modeling the generation, flow and transport of magmas in the Earth's upper mantle. In terms of the most fundamental of questions about magmas, whether they will buoyantly rise or sink, the most important parameters are the composition and structural dependence of the melt density (ρ), its bulk modulus (K_S), and pressure derivative of the bulk modulus (dK_S/dP) at high pressures. Indeed, such data have relevance not only for processes of mantle differentiation and primordial stratification, but also for the magnitude of the buoyancy forces that drive the upwelling silicic magmas in the deep crust. Ultrasonic measurements (at ambient pressure) have provided excellent data on density-bulk modulus systematics for a variety of both natural and synthetic silicate melts [*Sato and Manghnani,* 1985*; Rai et al.,* 1981*; Kress et al.,* 1988, 1989*; Rivers and Carmichael,* 1987*; Lange and Carmichael,* 1987, 1991*; Secco et al.,* 1991*; Webb and*

Courtial, 1996]. Shock-wave studies on the diopside-anorthite system have provided values for densities and the equation-of-state of model basaltic melts to ~ 35 GPa, including constraints on dK_S/dP [*Rigden et al.,* 1984, 1988, 1989]. The implications of the shock-wave data for producing incompatible-element enriched reservoirs in the deep mantle due to downward melt segregation in Earth's early history have been emphasized by *Rigden et al.* [1984]. Static compression [*Agee and Walker,* 1988*; Agee,* 1992a, 1992b*; Circone and Agee,* 1996] data for komatiite, peridotite, fayalite and Ti-rich melts at high pressures (up to 8 GPa) have also provided values for melt densities, thermal expansion, bulk modulus and its pressure derivative for these compositions. The shock-wave and static compression studies of silicate melt densities consistently support the olivine flotation hypothesis of *Stolper et al.* [1981] that basic silicate melts become denser than coexisting crystalline olivines and pyroxenes (at depths of 150-200 km) through their higher compressibility. Such studies also raise the possibility that such density inversions could occur at deeper depths within the Earth's mantle [*Miller et al.,* 1991]. Unfortunately, no static studies of melts sample a pressure (or composition) range over which coordination changes of Si are likely to occur. As such coordination changes plausibly control melt-solid density inversions at depths of the transition zone, few constraints exist on the relationship between the structural changes in a melt under compression, and the rapid changes in elastic properties known to occur in melts under shock-loading. Therefore, an experimental determination of silicate melt/glass/aqueous solution elasticity under the high P-T conditions of the lower crust and upper mantle by means of laser Brillouin light scattering spectroscopy, which can directly probe the changes in elastic properties of melts, in conjunction with the static compression in the

externally heated diamond anvil cell (DAC) will be advantageous from the standpoint of filling the gap in the data between the high pressure dynamic shock loading and large volume static compression experiments.

The two main fluid phases within the Earth's crust and mantle are silicate rock melts and hydrous fluids, which form a continuity of miscible compositions at shallow upper mantle conditions [*Kohn*, 2000; *Shen and Keppler*, 1997]. Even though these phases are physically and chemically different near the surface of the Earth, water and liquid SiO_2 exhibit striking similarities in their structure and behavior [*Angell et al.*, 1982]. For example, the vitrification of aqueous binary solutions under pressure and low temperature [*Angell*, 2002; *Kanno*, 1987] support the notion that water- and silica-rich liquid systems may have similar structural mechanisms responsible for their anomalous thermodynamic properties [http://www.btinternet.com/~martin.chaplin/anmlies.html; *Polian et al.*, 2002] which distinguish them from normal liquids [*Wolf and McMillan*, 1995]. In this regard, the effect of alkalis, which lower the melting temperatures (and glass transitions) of natural silicate liquids and, therefore, make the silicate melts experimentally more straightforward to probe, on the thermoelastic properties of binary silicate liquids under pressure is not well constrained. Similarly, virtually no data exist on the effect of dissolved silicate species on the elastic properties of aqueous solutions at more moderate pressures and temperatures.

The goals of this dissertation are two-fold: first, to demonstrate the feasibility of determining the effect of changes in the coordination number of silicon on the elasticity of amorphous silicates at high pressures and temperatures using Brillouin spectroscopy. Second, we wish to constrain whether the elastic properties of silica-rich aqueous fluids

more closely resemble water or silicate melts, particularly at the high pressure and temperature conditions under which silicate melts and hydrous fluids may be completely miscible.

1.2 ORGANIZATION OF CHAPTERS

In Chapter 2, the high-pressure experimental studies of liquid water, alkaline-calcium silica hydrogel and anhydrous silicate glass by Brillouin scattering spectroscopy are presented and accompanied by an introduction into the Brillouin scattering technique as well as analysis of the conventional scattering geometries used to extract acoustic velocities of the liquids and solids. Further analysis is given with regard to the elastic moduli obtained from the measured pressure dependencies of the acoustic velocities. The results on liquid water have been presented at the International Conference on High Pressure Science and Technology (AIRAPT-17), held in Honolulu, Hawaii, USA, July 25-30, 1999 [*Tkachev and Manghnani*, 2000], whereas work on elastic and structural properties of alkaline-calcium hydrogels has been published in the *Journal of Materials Research* in February 2005 [*Phair et al.*, 2005] and carried out in collaboration under a grant from the Federal Highway Administration.

In Chapter 3, the approach developed in Chapter 2 is applied to the high-pressure and high-temperature studies of hydrated and anhydrous Na_2O-$2SiO_2$ liquid, and glass using Brillouin scattering technique. A concept of the "modified" platelet scattering geometry, that has been successfully used in elastic modulus determination and is described in the work published in *Physical Review B* in August 2003 [*Tkachev et al.*, 2003a], is introduced. The results of these studies, that also include a recent assessment

of partial molar volume of water to upper mantle depths, have been presented at the COMPRES (Consortium for Materials Properties Research in Earth Sciences) 3rd Annual Meeting, held in Lake Tahoe, California, USA, June 19-22, 2004, while the preliminary results without the data on partial molar volume of water were presented at the Fall 2003 meeting of the American Geophysical Union (AGU) in San Francisco [*Tkachev et al.*, 2003b].

Results on float glass presented in Chapter 2 and those on hydrated and anhydrous Na_2O-$2SiO_2$ liquid and glass from Chapter 3 have formed bases of two manuscripts recently accepted for publication in *Physical Review Letters* and in the *Journal of Geophysical Research – Solid Earth*, respectively.

Chapter 2

HIGH-PRESSURE BRILLOUIN SPECTROSCOPIC STUDIES OF PURE WATER, ALKALINE-CALCIUM SILICA HYDROGELS AND ANHYDROUS SILICATE GLASS

2.1 SOUND VELOCITY AND ATTENUATION IN STABLE AND METASTABLE LIQUID WATER TO 1.2 GPA BY BRILLOUIN SPECTROSCOPY AND CASE STUDY OF ALKALINE-CALCIUM SILICA HYDROGELS

2.1.1 *INTRODUCTION*

At the end of the sixties, viscoelastic properties of water were investigated by ultrasonic methods [*Heydemann and Houck*, 1969; *Holton et al.,* 1968]. The use of Brillouin light scattering spectroscopy in combination with static compression in the diamond anvil cell (DAC) provided an additional powerful tool for investigation of viscoelastic behavior of water in a different frequency range and at higher pressures [*Grimsditch et al.,* 1996; *Polian and Grimsditch,* 1983; *Rouch et al.,* 1976].

Recent interest in metastable (i.e., outside its stability field) water [*Mishima and Stanley,* 1998a,b; *Poole et al.,* 1992] prompted us to conduct Brillouin scattering spectroscopy studies on stable and metastable water in DAC up to 1.2 GPa at room temperature.

Two main OBJECTIVES of this Section are:

- To investigate viscoelastic properties (sound velocity, sound absorption and equation of state) of water in stable and metastable regions within the frequency scale of the laser light Brillouin scattering spectroscopy.

- To investigate the elastic and structural properties of alkaline-calcium silica hydrogels using the formalism developed by meeting the first objective.

2.1.2 *THEORETICAL BACKGROUND*

Brillouin spectroscopy is based on measuring the frequency shift (Fig. 2.1) between elastically scattered light (Rayleigh peak) and inelastically scattered light (Brillouin peaks). The elastically scattered light has the same frequency as incident light while the inelastically scattered light has its frequency shift due to the Doppler effect resulting from the interaction of light with propagating acoustic waves (phonons). In general, the thermodynamic theory defines two types of density fluctuations (the departure of the density from its average value in a small volume, the linear dimensions of which are small in comparison with the wavelength of the light, but it contains a sufficient number of molecules that it can be subjected to statistical analysis [*Fabelinskii*, 1968]) that cause the scattering of light in matter. The Raleigh peak is resulting from density fluctuations at constant pressure, while the Brillouin peaks are resulting from those at constant temperature [*Mountain*, 1966]. Since Doppler-shifted light photons scattered on thermally excited acoustic phonons (sound waves) of the sample produce peaks in the Brillouin spectrum (Fig. 2.1), the sound velocity (V is either longitudinal, V_P, or shear, V_S, velocity) can be expressed via:

$$V = \frac{\lambda \nu}{2n \sin(\theta/2)} \tag{2.1.1}$$

where ν is the Brillouin frequency shift; λ is the wavelength of the laser (514.5 nm); n is the refractive index; θ is the scattering angle.

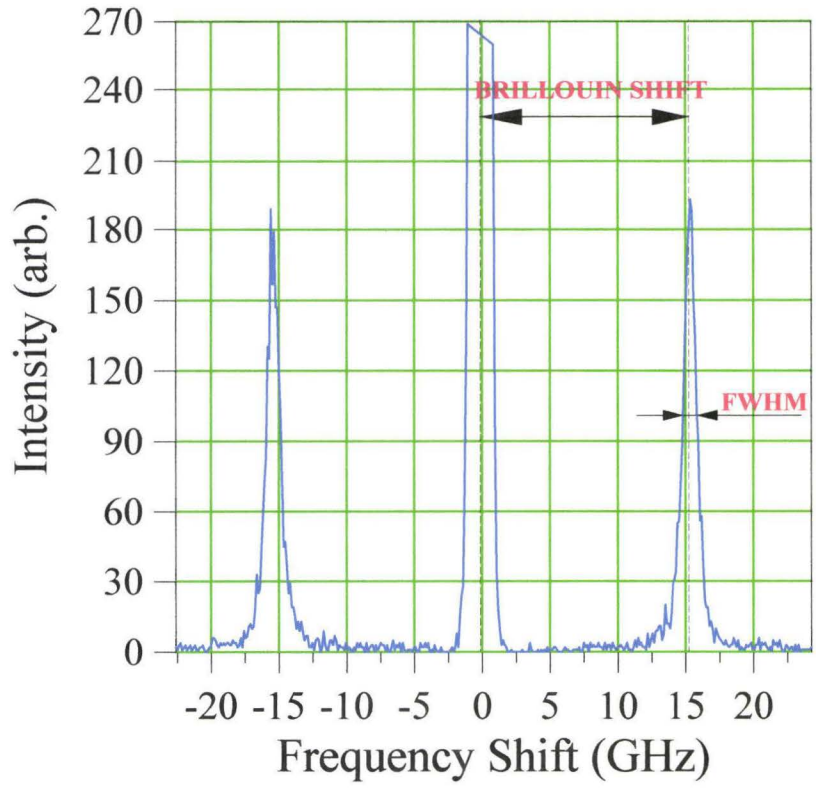

Figure 2.1.

Brillouin spectrum of liquid water (metastable phase) at 1.16 GPa and room temperature. Central Rayleigh peak (truncated) originates from the elastic scattering of photons, while the two Brillouin peaks are due to inelastic scattering of photons. Positions of the Rayleigh peak and one of the Brillouin peaks are indicated by dashed vertical lines. The Brillouin shift is a frequency shift between the Rayleigh peak and Brillouin peak. FWHM is the full-width at half maximum of the Brillouin peak. The Y axis is the integral intensity of accumulated photons, while the X axis represents the corresponding frequency shift from the position of the Raleigh peak (zero point).

For Brillouin peaks, density fluctuations also dissipate with time. This process of dissipation results in broadening of the peaks, due to attenuation of acoustic waves (phonons). A full-width at half maximum (FWHM) of the Brillouin peak (Fig. 2.1) serves as a measure of viscous dissipation in liquid medium.

For our measurements of the viscoelastic constants of liquid water, we used a six-pass tandem Fabry-Perot interferometer [*Sandercock*, 1982]. A spectrum of incident light was produced by a single-mode argon-ion laser with a wavelength of 514.5 nm, operating at 40 mW. The scattered light was recorded on a 1024-channel multichannel analyzer. From this instrument, the spectra were downloaded to a computer for curve-fitting of the peaks and deconvolution of the instrumental contribution [*Oliver et al.*, 1992] to the Brillouin width.

Brillouin scattering data on double distilled liquid water were obtained at 22.5°C in a DAC (Fig. 2.2) between atmospheric pressure and 1.2 GPa (Fig. 2.3). The diameter of the diamond anvil flat was 0.7 mm. An Inconel-718 gasket (thickness of 0.315 mm) with a 0.31 mm diameter sample chamber was used. In most cases, the gasket was pre-indented to a thickness of about 0.2 mm. The Merrill-Bassett-type DAC [*Merrill and Bassett,* 1974] and also Bassett-type DAC [*Jayaraman,* 1983] allowed us to perform measurements in a backscattering (180°) geometry and also in a symmetric (90°) platelet geometry [*Whitfield et al.,* 1976; *Xu and Manghnani,* 1992; *Tkachev et al.*, 1995b]. A simplified view of the setup for symmetric platelet geometry is shown in Figure 2.2. For this geometry, the sound velocity, V, is related to the Brillouin frequency shift ν by

$$V = \frac{\lambda \nu}{2 \sin \theta}, \qquad (2.1.2)$$

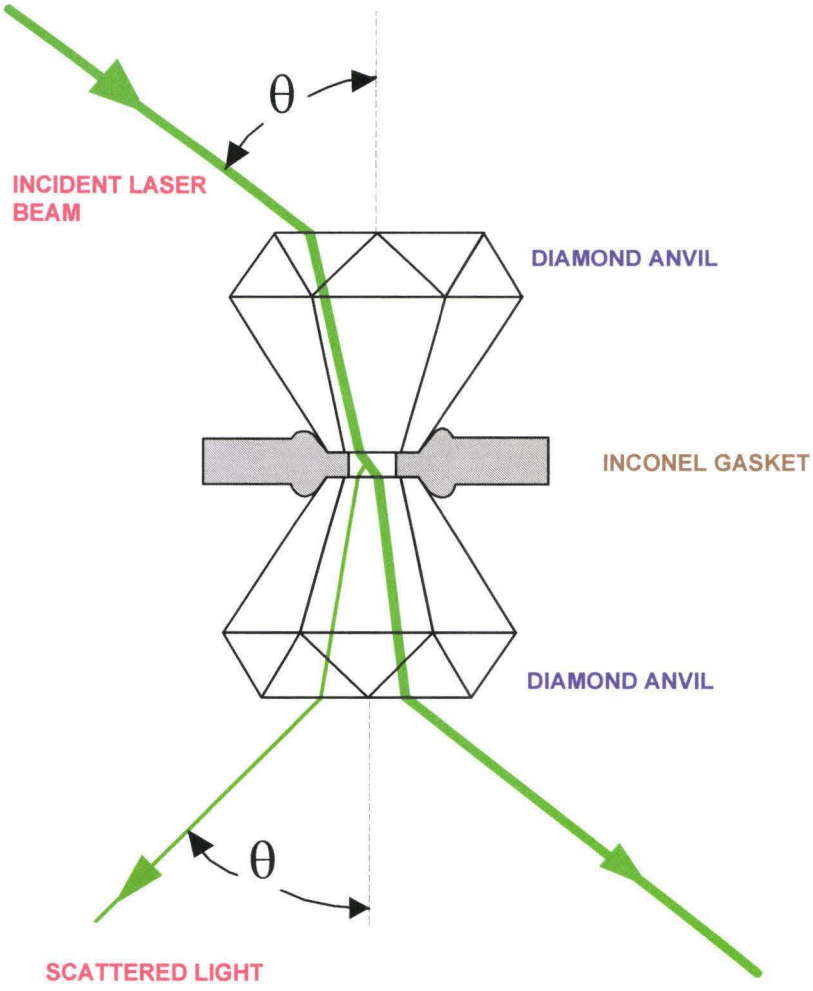

Figure 2.2.

Sketch of the experimental setup. The high pressure diamond anvil cell (DAC) is represented by two diamond anvils (upper and lower) and an Inconel gasket, with a central hole, which serves as a miniature container for the sample. The external scattering angle θ is the angle between the incident laser beam, which passes through the transparent diamonds in the same direction as it enters DAC after refractions on the surfaces of the diamonds, and a normal to the base of a diamond. A dashed line shows the normal to the base of a diamond.

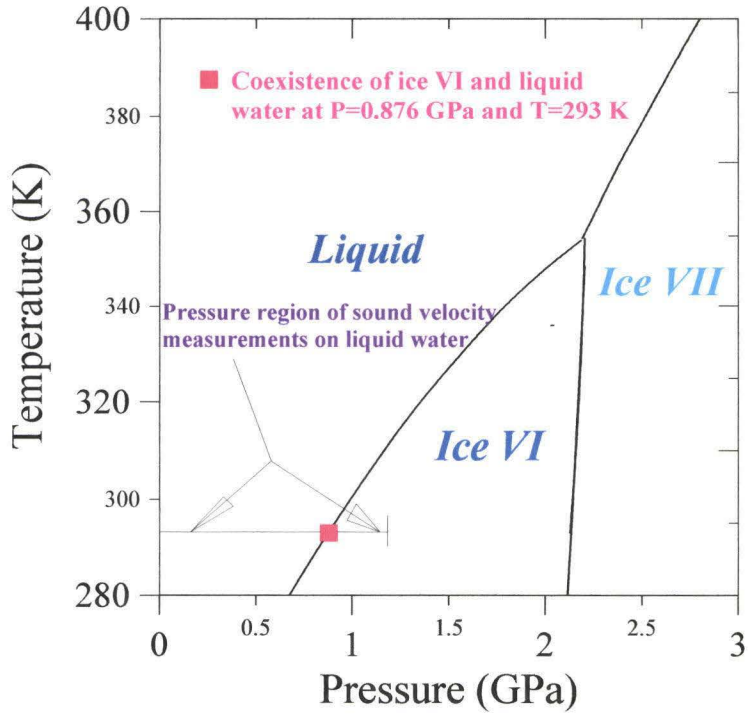

Figure 2.3.

Pressure region of sound velocity measurements in the phase diagram of water. A thick solid line shows the P-T phase boundaries of water in the vicinity of the triple point Liquid -Ice VI - Ice VII [*Pistorius et al.*, 1968]. A thin horizontal solid line marks the region of Brillouin scattering spectroscopy measurements (present study) of liquid water at room temperature. The red solid square represents coexistence between liquid water and crystals of ice VI, obtained in the vicinity of the phase boundary between liquid water and ice VI. The portion of the thin horizontal solid line, which lies in the field of stability of ice VI, to the right of the red solid square, represents the region of measurements on metastable liquid water. Metastable liquid water undergoes phase transition to ice VI [*Tkachev et al.*, 1995a, 1996] at pressures above 1.16 GPa.

where λ is the incident laser wavelength (514.5 nm) and θ is the external scattering angle. For the backscattering (180^0) geometry, the sound velocity is related to the Brillouin frequency shift through the refractive index n of the scattering medium by $n\mathrm{V} = 0.5\nu\lambda$.

In order to obtain the equation of state (EOS) from sound velocity data, we expressed the pressure dependence of the sound velocities through commonly used parameters of the EOS: K_{0T} (isothermal bulk modulus at atmospheric pressure) and K_{0T}' (pressure derivative of the isothermal bulk modulus at atmospheric pressure).

The longitudinal and shear sound velocities can be expressed through the adiabatic (constant entropy) bulk modulus K_S and the density ρ:

$$\mathrm{V}_\mathrm{p}^2 - \frac{4}{3}\mathrm{V}_\mathrm{s}^2 = \frac{K_s}{\rho}. \qquad (2.1.3)$$

In general, the equation of state contains an isothermal bulk modulus, K_T, rather than the adiabatic bulk modulus K_S. The adiabatic bulk modulus was derived from the isothermal bulk modulus [*Brown et al.,* 1988]:

$$\frac{1}{K_S} = \frac{1}{K_T} - \alpha\left(\frac{\mathrm{dT}}{\mathrm{dP}}\right)_S, \qquad (2.1.4)$$

where α is the coefficient of thermal expansion. The thermal expansion coefficient was calculated from P-V-T data on liquid water [*Hilbert et al.,* 1981] using the definition of this parameter [*Stacey,* 1977], while the pressure derivative of temperature for water was taken from the literature [*Boehler and Kennedy,* 1977].

We measured the attenuation of sound in liquid water, using the Brillouin linewidths. The final expression for the Rayleigh-Brillouin spectral density [*Rouch et al.,*

1976] defines the full-width at half maximum (FWHM) of the Brillouin peaks (Fig. 2.1), 2Γ, as quadratically dependent on the frequency ν. Therefore, to get a comprehensive picture of results obtained from different experimental techniques, varying in frequency ranges, we used formulation involving the frequency-independent attenuation coefficient [*Herzfeld and Litovitz*, 1959] $\frac{\alpha_D}{\nu^2}$ (where α_D is energy decay constant), which is related to the FWHM by:

$$\frac{\alpha_D}{\nu^2} = \pi \frac{\Gamma}{V\nu^2}. \tag{2.1.5}$$

This term allows for a more direct comparison of results from various types of experiments.

The ruby fluorescence technique [*Piermarini and Block*, 1975] was used to measure pressure at the center and edges in the sample. The pressure uncertainties did not exceed 0.05 GPa.

2.1.3 *RESULTS*

Pressure dependencies of sound velocities and refractive index of liquid water were measured up to 1.2 GPa at room temperature. Present hypersonic results shown on Figures 2.4 and 2.5 are in agreement with literature data on ultrasonic measurements of sound velocity [*Heydemann and Houck,* 1969; *Holton et al.,* 1968] and on optical interferometric measurements of refractive index [*Vedam and Limsuwan,* 1978] in liquid water at high pressures. It can be seen that the region of transition between stable and metastable water is not marked by discontinuities in sound velocity and refractive index. On the contrary, the jump in longitudinal sound velocity at ~ 1.2 GPa reflects the first-

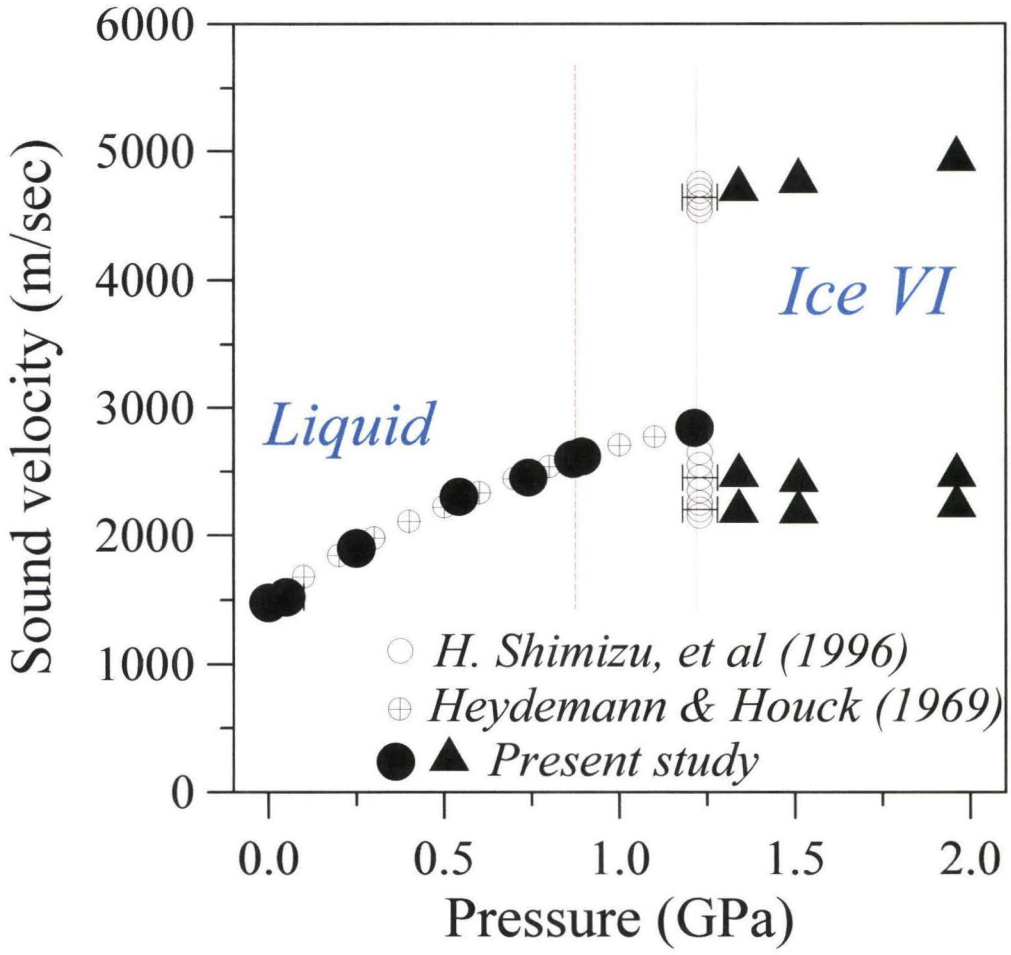

Figure 2.4.

Pressure dependence of sound velocities in liquid water and Ice VI obtained using the ultrasonic technique [*Heydemann and Houck,* 1969] and Brillouin scattering spectroscopy [present study; *Shimizu et al.,* 1996b]. The dashed and dotted vertical lines represent the phase boundaries between liquid water, metastable water and ice VI.

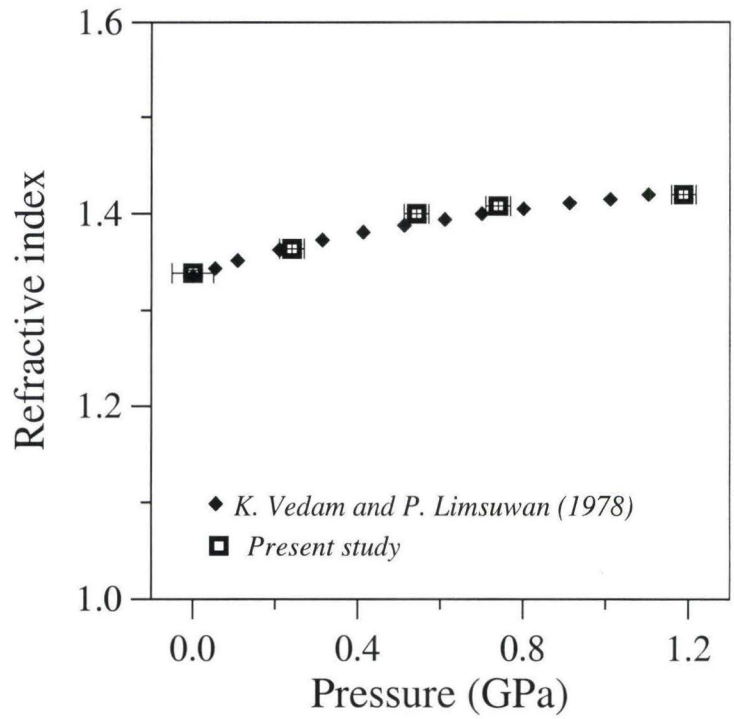

Figure 2.5.

A good agreement is found between the results on the pressure dependence of refractive index of liquid water determined by optical interferometry and our Brillouin spectroscopy.

order phase transition between metastable water and Ice VI (the first-order phase transition from Ice VI to liquid water occurs at the phase boundary between the stability fields of Ice VI and liquid water [*Tkachev et al.*, 1995a, 1996]).

The best fit to the existing volumetric data on water has been obtained by utilizing the universal Vinet EOS, which is based on the universal relationship between binding energies and the distance between atoms [*Rose et al.,* 1981]. This EOS successfully used in case of organic liquids [*Oliver et al.,* 1991] is expressed as:

$$P(X) = 3K_{0T}\left(\frac{1-X}{X^2}\right)e^{\eta(1-X)}, \tag{2.1.6}$$

where $X \equiv \sqrt[3]{\left(\frac{\rho_0}{\rho}\right)}$, $\eta \equiv \frac{3}{2}\left(K_{0T}' - 1\right)$, and ρ_0 is the density at ambient pressure. For this type of EOS, an expression for the isothermal bulk modulus as a function of strain is given by:

$$K_T(X) = \frac{K_{0T}}{X^2}(2 + (\eta - 1)X - \eta X^2)e^{\eta(1-X)}, \tag{2.1.7}$$

Available data on pressure dependencies of the thermal expansion [*Hilbert et al.,* 1981] and pressure derivative of temperature [*Boehler and Kennedy,* 1977] for water allow us (Equation 2.1.4) to determine [*Brown et al.,* 1988] $K_{0T} = 2.17 \pm 0.05$ GPa and $K_{0T}' = 7.0 \pm 0.8$. These values are in good agreement with literature values: $K_{0T} = 2.18 \pm 0.02$ GPa [*Fine and Millero,* 1973] and $K_{0T}' = 6.67 \pm 0.03$ [*Heydemann and Houck,* 1969].

Figure 2.6 demonstrates the difference between K_S calculated from present sound velocity data and K_T calculated using Equation 2.1.7 increases with pressure and becomes as large as 10 % or more at 1.2 GPa.

Figure 2.7 shows an excellent agreement between densities calculated from present sound velocity data and *Bridgman*'s [1913] volumetric measurements. It should be noted that this is not a fit to Bridgman's data. This figure contains two completely independent sources of data.

Figure 2.8 demonstrates that the attenuation coefficient for liquid water decreases with increasing pressure, in qualitative agreement with ultrasonic measurements [*Litovitz and Carnevale,* 1955]. No discontinuity has been observed between the regions of stable and pressure-induced metastable water.

2.1.4 *A CASE STUDY: ELASTIC AND STUCTURAL PROPERTIES OF ALKALINE-CALCIUM SILICA HYDROGELS*

2.1.4.1 *Experimental*

Alkaline-calcium silica hydrogels, also referred to as the alkali-silica reaction (ASR) gel, were synthesized by the addition of calcium hydroxide (Aldrich, AR grade) powder to solutions of sodium silicate (Aldrich, ~ 27 % SiO_2, ~ 14% NaOH, density = 1.390 g/cm^{-3}) diluted with distilled water to a concentration of [SiO_2] = 1.5 M. Solutions were sonicated for 5 minutes to fully disperse the suspension. Two alkaline-calcium silica gels of different $Ca(OH)_2$ concentration were prepared, one with initial [$Ca(OH)_2$] equal to 0.08 M (referred to as sample A) and the other with initial [$Ca(OH)_2$] equal to 0.8 M

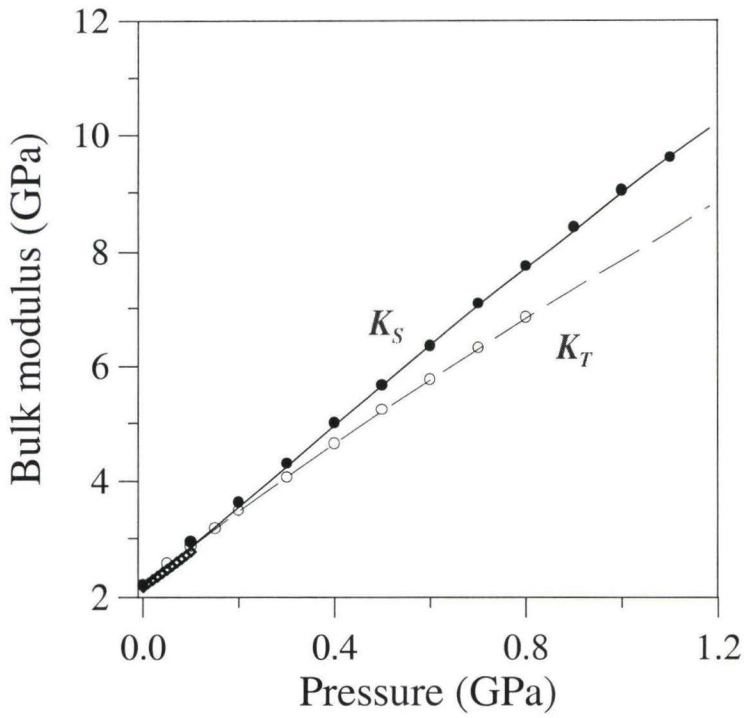

Figure 2.6

Pressure dependence of adiabatic bulk modulus (K_S) and isothermal bulk modulus (K_T) of liquid water. Solid line and solid circles represent adiabatic bulk moduli determined in present study and by *Heydeman and Houck* [1969], respectively. K_T is shown by dashed line (present study), open circles [*Bridgman,* 1913], and open rhombs [*Chen et al.,* 1977].

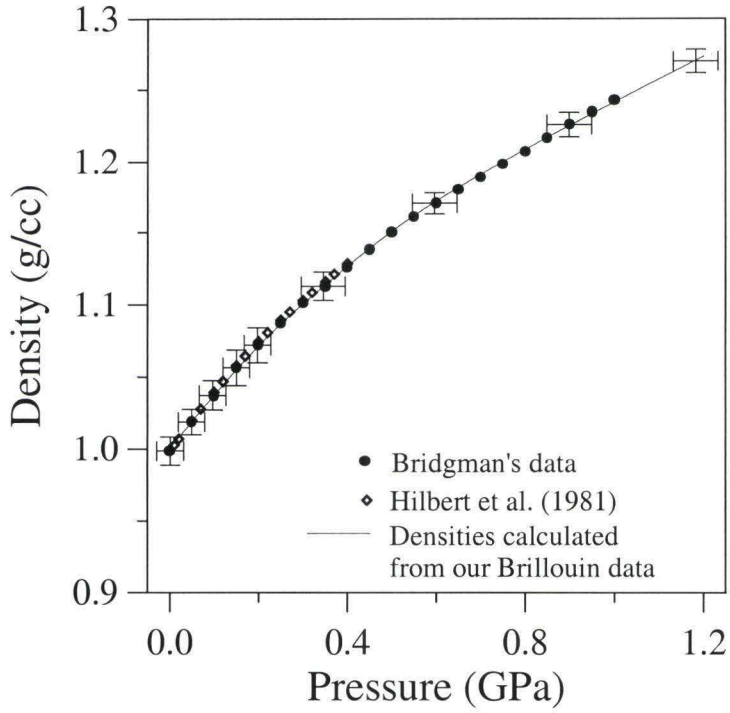

Figure 2.7.

Comparison between the measured density values [*Bridgman,* 1913; *Hilbert et al.,* 1981] and those calculated (solid line) from the Brillouin scattering pressure dependence of sound velocity of liquid water.

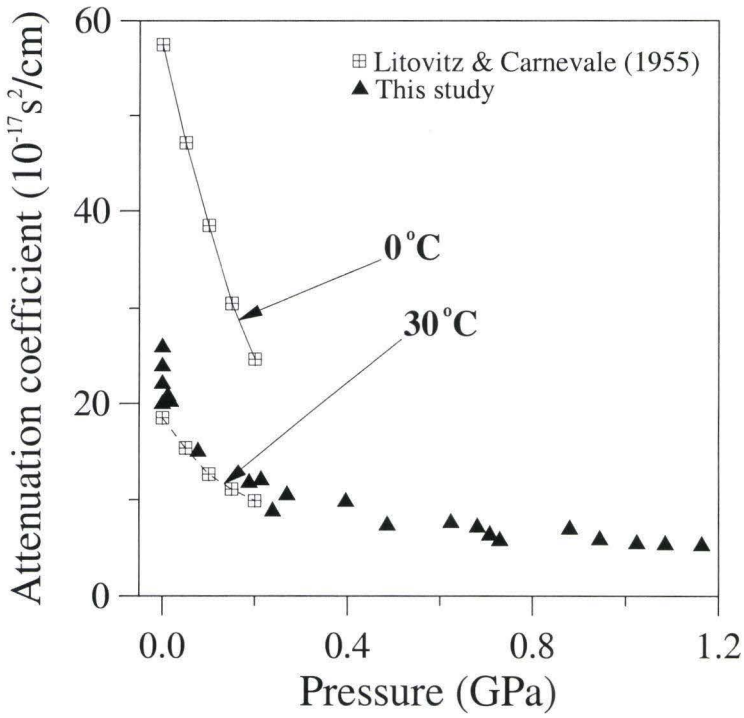

Figure 2.8.

Comparison between ultrasonic measurements [*Litovitz and Carnevale,* 1955] of attenuation coefficients and present measurements of attenuation coefficients for liquid water. Present results at 22.5 °C lie between the ultrasonic data at 0 °C and 30 °C, closer to 30 °C, thus demonstrating a good agreement with ultrasonic measurements. Standard deviations are represented by sizes of symbols.

(referred to as sample B). To the best of our knowledge this will be the first study of the bulk elastic moduli for this type of alkaline-calcium silica hydrogel.

Brillouin scattering measurements were conducted on the alkaline-calcium silica hydrogels placed inside a diamond anvil cell (DAC) at 22.5 °C, over a pressure range of 0.1 to 1.6 GPa. A Bassett-type DAC [*Jayaraman*, 1983] was used for measurements in both 180° backscattering and 90° symmetric platelet geometries [*Whitfield et al.*, 1976]. Pressure within the DAC was determined using the ruby fluorescence technique [*Piermarini and Block*, 1975], which allowed monitoring at several locations in the sample. The refractive index of the gels was estimated from the comparison of the 180^0 and 90^0 scattering geometry measurements. FTIR spectra were recorded for the samples using a Nicolet Magna-IR 560 Spectrometer equipped with a DRIFT attachment, utilizing OMNIC v 6.0a software for data analysis. Water content of the gels was determined using a TA Instruments thermogravimetric analysis system (TGA) and the density was measured using a pycnometer.

2.1.4.2 *Discussions*

Figure 2.9 depicts the effect of pressure on the longitudinal (V_P) and shear (V_S) sound wave velocities as well as the product of the refractive index and longitudinal wave (nV_P), for both alkaline-calcium silica hydrogels. However, no shear wave velocities could be observed for sample A due to the fact that its viscosity was too low. In any case, both samples exhibited a gradual increase in the longitudinal wave velocity with increasing pressure. The presence of pressure-induced irreversible changes, occurring in sample B upon compression (dashed lines), was confirmed during the decompression

cycle (solid lines). Increasing pressure seemed to have less of an effect on the shear wave velocities determined for sample B. Notwithstanding, the longitudinal wave velocity for sample B (between ~4000 and ~5000 m/sec) was typically twice that observed for sample A (between ~2000 and ~2500 m/sec). Figure 2.9 displays also the longitudinal wave velocity and product of the refractive index and longitudinal wave velocity fitted to a second order polynomial for sample B. Recording the product of the refractive index and the longitudinal wave velocity is useful for indicating whether there is a second order phase transition (e.g. glass transition) in the material [e.g., *Askarpour and Manghnani*, 1994; also: Section 3.3 in Chapter 3]. This can easily (usually as a change in slope) be traced by measuring pressure/temperature dependencies of nV_P.

The empirical equations for these fits relating the pressure (P) to $n\mathrm{V_P}$ and $\mathrm{V_P}$ are as follows: $n\mathrm{V_P}(P) = 5759.90 + 2194.99P - 316.46P^2$, and $\mathrm{V_P}(P) = 3900.60 + 1574.70P - 372.44P^2$.

The fact that a negative value for the second derivative was observed is empirically consistent with normal compression behavior of liquids under pressure, for example, in pentane [*Tkachev and Bass*, 1996]. From the plot of $n\mathrm{V_P}$ against pressure in Figure 2.9, it is also clear that, for the present samples, no second order phase transition could be observed.

Values for the density, bulk modulus and compressibility for both gels are presented in Figures 2.10, 2.11, and 2.12, respectively. The data values have also been fitted to second-order polynomials to serve as a guide to the eye. In viewing Figure 2.11, it is of interest to note that the bulk modulus (K_S) values for sample B are approximately 2 to 3 times larger than for sample A. This trend is largely in agreement with previous

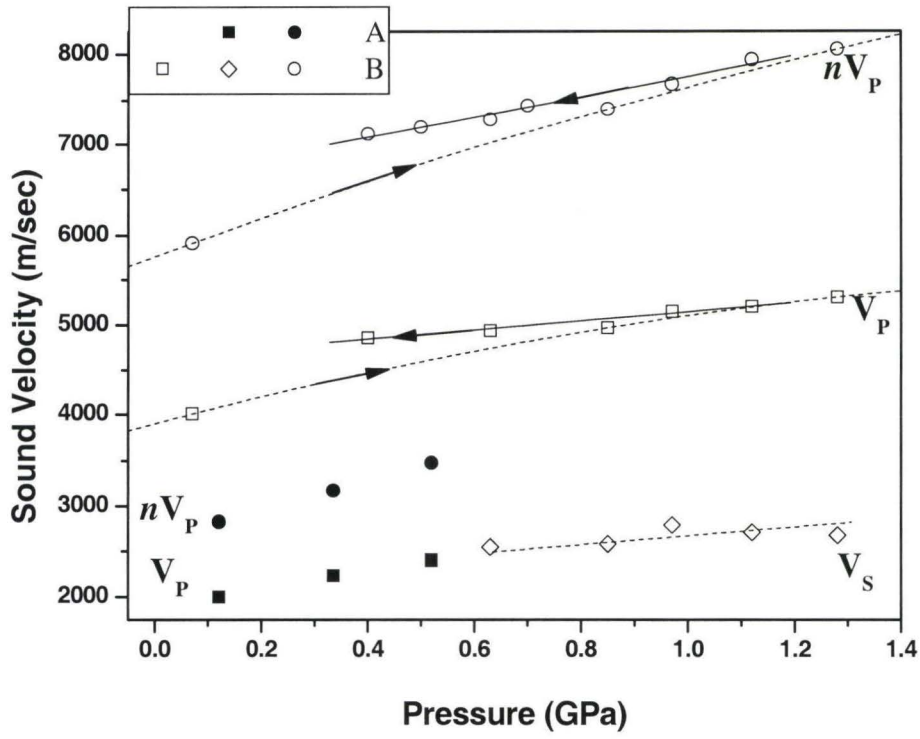

Figure 2.9.

Longitudinal (square) and shear (diamond) sound wave velocities, and nV_P (circle) for alkaline-calcium silica hydrogel. Sample A is represented by closed symbols. Sample B is represented by open symbols. Polynomial and linear fits for sample B are also provided with dashed lines passing through data points collected on compression and solid lines passing through data points collected on decompression, respectively (no difference between compression and decompression data has been observed for sample A).

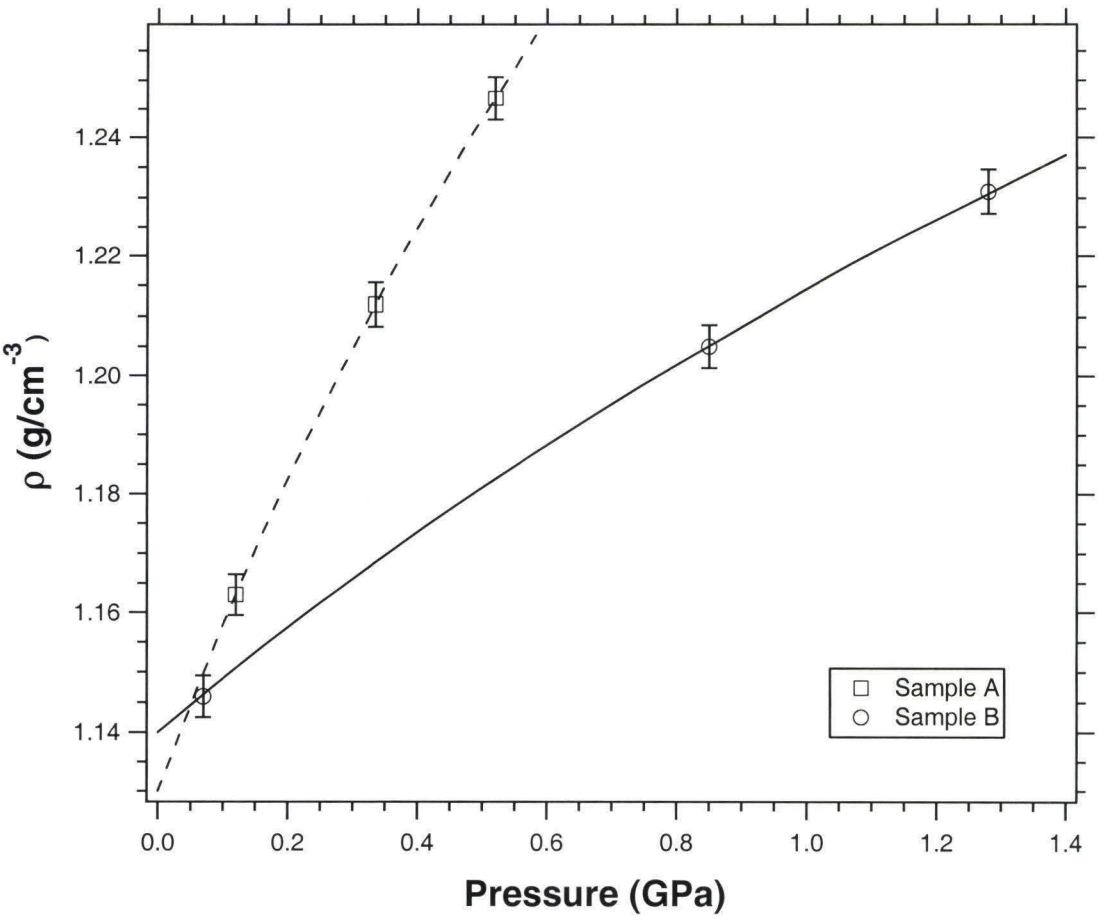

Figure 2.10.

Density (ρ) of alkaline-calcium silica hydrogels as a function of pressure.

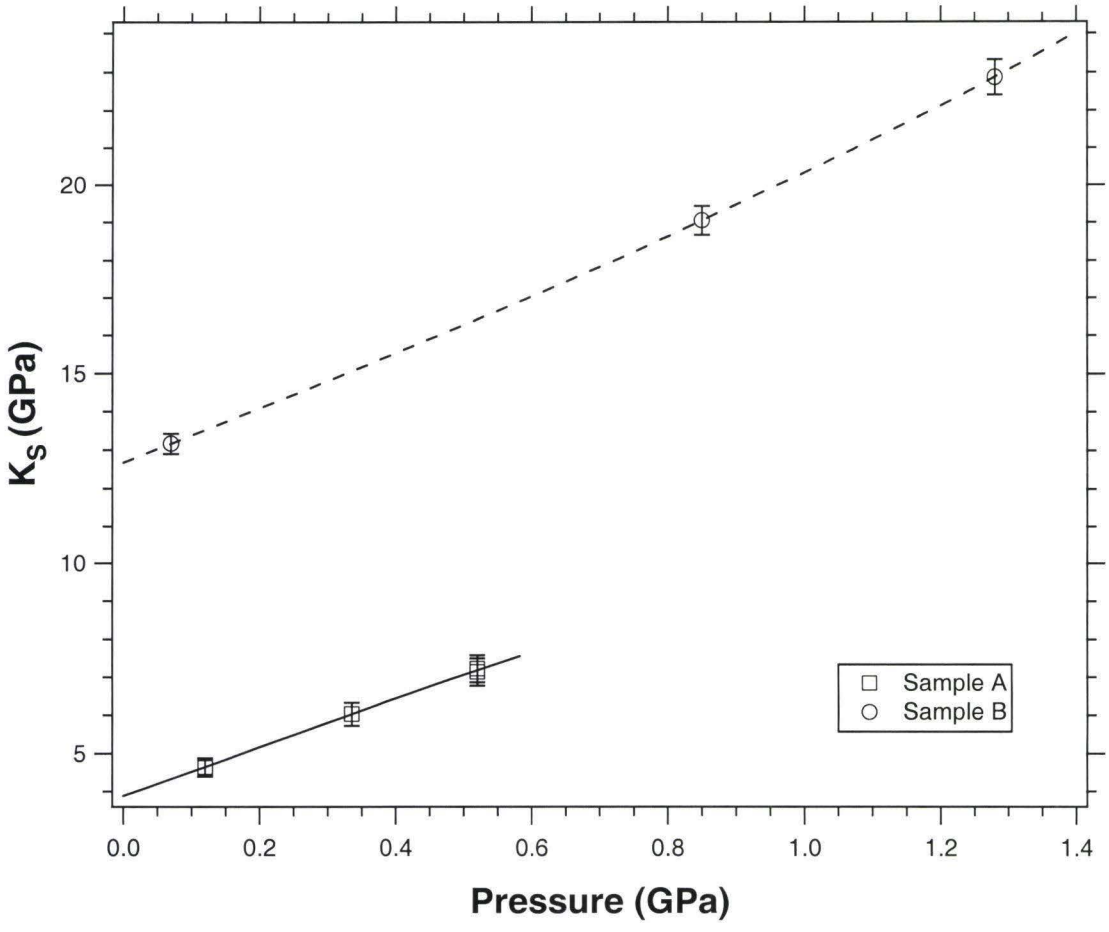

Figure 2.11.

Bulk modulus (K_S) of alkaline-calcium silica hydrogels as a function of pressure.

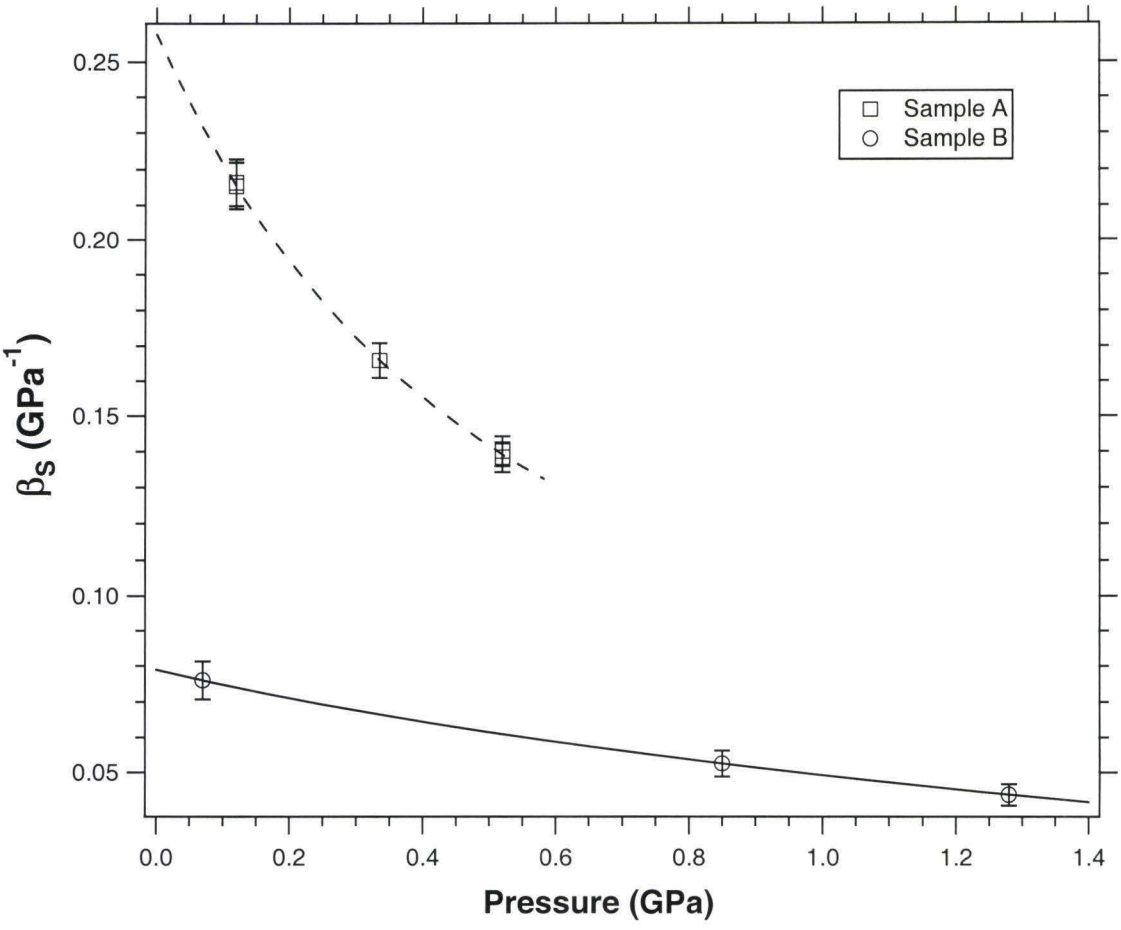

Figure 2.12.

Compressibility (β_S) of alkaline-calcium silica hydrogels as a function of pressure.

data [*Gaboriaud et al.*, 2002]. While no published data are available for the bulk modulus (K_S) of $Ca(OH)_2$ containing ASR gels, complex (storage and loss) shear moduli have been reported [*Gaboriaud et al.*, 2002]. In all instances, it was observed that increasing the $Ca(OH)_2$ concentration caused an increase in the relative moduli. Storage moduli of 0.1 KPa and 70 KPa have been recorded for ASR gels containing 0.08 and 0.5 M $Ca(OH)_2$ respectively [*Gaboriaud et al.*, 2002]. Bulk moduli, on the other hand, represent a fundamentally different parameter and as a consequence, their absolute values are different. It must also be noted that previously reported storage moduli for ASR gels were measured on gels synthesized from different alkali metal hydroxides and at lower SiO_2/Na_2O values than those used in the present study. As such, the differences in moduli are to be expected.

Given that there is no comparable increase in the bulk modulus with increasing calcium hydroxide concentration, this suggests that the increase in the bulk modulus is not a simple concentration effect. Further experimentation is required to explain the increase in the bulk modulus with increasing $Ca(OH)_2$ concentration.

By referring to the supplementary FTIR data presented in Figure 2.13, it is possible to gather molecular structure information to explain the differences in the elastic moduli between the two ASR gels. The absence of any peak associated with crystalline structure confirms the amorphous nature of the material. Neither out of plane Si-O bending (520-545 cm^{-1}) nor in plane Si-O bending (450-465 cm^{-1}) peaks could be observed, which would be indicative of crystalline structure in the silica. Moreover, the fact that most of the peaks are generally broad and diffuse suggests a highly random structure.

While four major peaks can be observed in Figure 2.13, only two are of interest for explaining structural changes that accompany any variation to the elastic properties of the material. The first peak of interest, observed at approximately 900-915 cm^{-1}, may be assigned to nonbridging free Si-O^- bending modes [*Marinangeli et al.*, 1978]. While this is a broad peak, it was not possible to deconvolve this peak into neighboring peaks such as the Si-O(H) bond stretching vibration at approximately 950 cm^{-1}. Nevertheless, the peak at 900-915 cm^{-1} gives information on the size of the Si-based species, since it predominates only in clusters of average size smaller than the dimension of $(SiO)_6$ rings [*Almeida and Pantano*, 1990; *Viart et al.*, 1997].

Silica polycondensation reactions go through a stage where if the hydrogel nano- and micro-scale particles are small enough, they will promote the formation of broken Si-O^- bonds and thus contribute to the peak intensity at 900-915 cm^{-1} [*Chmel et al.*, 1990]. According to Figure 2.13, sample A demonstrates a considerably peak at approximately 900 cm^{-1}, suggesting the presence of significant amounts of smaller particles. For sample B, the reduced intensity of the 900 cm^{-1} peak absorption is consistent with greater progress in network formation and polycondensation reactions [*Chmel et al.*, 1990], which causes the small oligomers to condense to form larger structures.

The second infrared band of importance in Figure 2.13 is between 1040 and 1200 cm^{-1} and may be assigned to the asymmetric stretching mode of Si-O(-Si) bonds arising from the formation of a silica network [*Bass and Turner*, 1997]. Typically, this band can be deconvoluted into four or five peaks at approximately 1040, 1080, 1100, 1160, and 1200 cm^{-1}. The peaks at 1040, 1100, and 1160 cm^{-1} are commonly assigned to stretching vibrations of Si-O-(Si) and belong to structures that are more linear than they are

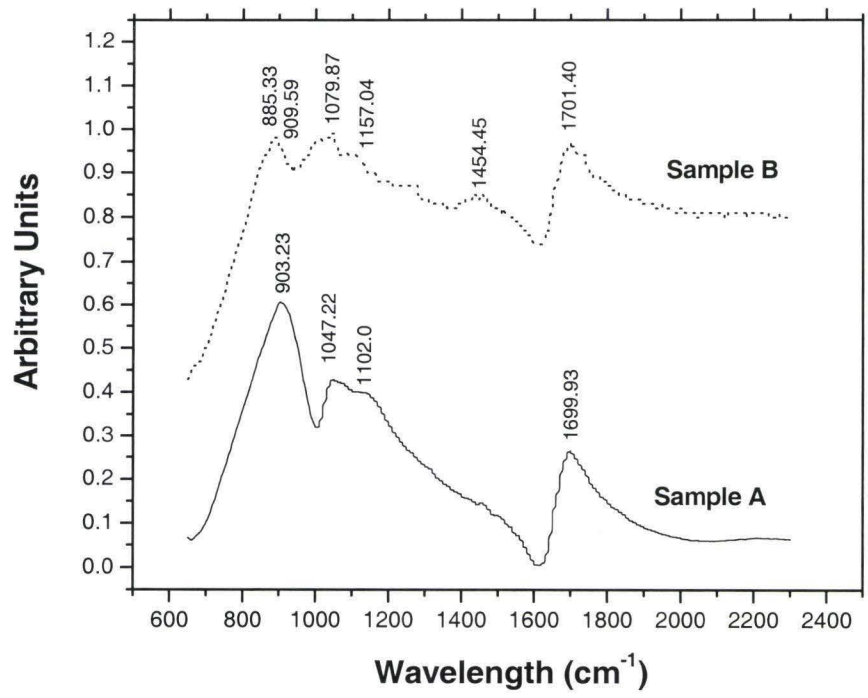

Figure 2.13.

FTIR spectra of alkaline-calcium silica hydrogels. Solid line represents sample A while dashed line represents sample B. Lines are displaced arbitrarily for ease of viewing.

crosslinked [*Viart et al.*, 1997]. Peaks at 1080 and 1200 cm^{-1} vibrations, on the other hand, have been assigned to Si-O-(Si) stretching in cyclic structures [*Viart et al.*, 1997; *Chmel et al.*, 1990]. Referring to Figure 2.13, the Si-O(-Si) band in sample A appears to be dominated by peaks at 1040 and 1100 cm^{-1}, suggesting a more linear and less interconnected structure. Sample B in addition to the peak at approximately 1160 cm^{-1}, has a significant peak at approximately 1080 cm^{-1}, which suggests the presence of more complex cyclic structures that maybe associated with greater silica network formation or polycondensation reactions [*Ortego et al.*, 1991].

The two remaining peaks of note within the spectra are observed at 1450 and 1700 cm^{-1}. The first peak is associated with carbonation while the second peak may be assigned to absorbed water on the gel surface [*Hughes et al.*, 1994].

Taking into account the infrared peak assignments and relative peak intensities, it is possible to deduce from Figure 2.13 that sample B has undergone more polycondensation (i.e., Si-O-Si network formation) than sample A. In addition, more smaller silica oligomers predominate in sample A compared to sample B, as demonstrated by the relative intensities of the $Si\text{-}O^{-}$ bending mode peak. Both these points indicate that calcium promotes the formation of the siloxane network and may subsequently explain the observed increase in the bulk modulus of the gel. This explanation largely follows the mechanism of formation given previously for similar measurements on ASR gels, in which calcium acts as a silica condensation "catalyst" [*Gaboriaud et al.*, 1999].

Of further interest is the fact that both the bulk modulus (K_S) and the density (ρ) of the two gels smoothly increased with increasing pressure while the compressibility

(β_S) decreased. At the pressures investigated for the present alkaline-calcium silica hydrogels, no phase transition of the gel from liquid state to solid state was observed. It is expected that considerably more pressure (>10 GPa) is required to facilitate this conversion.

Summing up, for the first time, Brillouin spectroscopy has been applied to determine the bulk moduli for alkaline–calcium silica hydrogels. Meaningful differences in the bulk moduli were observed as a function of composition and pressure. In summary, the bulk moduli were found to be dependent upon the cross-link density of the network, which could be controlled by the $Ca(OH)_2$ concentration. Bulk moduli of 4 to 8 GPa, and 16 to 25 GPa were observed for alkaline–calcium silica hydrogels gels synthesized from 0.08 and the 0.8 M $Ca(OH)_2$ solutions respectively. This followed a similar pattern to shear moduli reported previously for a comparable system, as a function of calcium content [*Gaboriaud et al.*, 2002]. Supplementary FTIR measurements determined that increasing calcium concentration promoted the formation of more complex silica species and a more inter-connected silica network, which explains the higher elastic moduli observed for samples with higher calcium concentrations. The present work can be regarded as a clear demonstration of the potential of Brillouin scattering technique for characterizing the elastic properties of ASR gels as a function of composition and pressure.

2.1.5 *CONCLUSIONS*

In summary, the densification curve of water obtained at high pressures by Brillouin scattering measurements is in agreement with Bridgman's volumetric data, and

the formalism applied to the well-known substance (water) has been successfully extended to the Brillouin scattering studies of the relatively less investigated material (alkaline-calcium silica hydrogel). Brillouin Scattering measurements on water to ~ 1.2 GPa have not revealed discontinuity in sound velocity and attenuation, whereas, above 1.2 GPa, a sharp discontinuity represented by a jump in the sound velocity data, has signified the onset of the first-order phase transition from the pressure-induced metastable liquid water to the stable phase of Ice VI as shown on Figure 2.4. No phase transition of the hydrogels from liquid state to solid state has been observed. A consistency between hypersonic (GHz) and ultrasonic (MHz) data (i.e., no frequency dependence in sound velocities has been observed) and continuous decrease in attenuation with pressure (Fig. 2.8) imply a relaxed nature (i.e., the system returns to the equilibrium following displacement caused by laser light photons before the occurrence of the next displacement) of both stable (see also the next Section and the answers to questions 7 and 8 from Appendix for the discussion on systems that are not fully equilibrated) and metastable water phases at room temperature.

2.2 AN *IN SITU* BRILLOUIN SPECTROSCOPIC STUDY OF A PRESSURE-INDUCED APPARENT SECOND ORDER TRANSITION IN A SILICATE GLASS

2.2.1 *INTRODUCTION AND EXPERIMENTAL*

The study of phase transitions in amorphous solids is of importance in condensed matter physics [*Huang and Kieffer*, 2004], geophysics [*Williams and Jeanloz*, 1988], and materials science [*Gaskell*, 1977]. A variety of experimental methods have been deployed

to investigate the elastic, vibrational and structural properties [*Meade et al.*, 1992; *Gromnitskaya et al.*, 2001; *Hemley et al.*, 1986] of amorphous polymorphs formed in solids and liquids at high pressure and/or temperature, providing valuable constraints for the corresponding theoretical simulations [*Zotov et al.*, 1999; *Poole et al.*, 1992]. The means by which amorphous materials densify is among the principal concerns of such studies, with both apparently first-order phase transitions between amorphous phases [*Gromnitskaya et al.*, 2001; *Mishima et al.*, 1985] and gradual densification processes [*Williams and Jeanloz*, 1988; *Meade et al.*, 1992; *Hemley et al.*, 1986] having been documented to occur under compression. The notable aspect of these results on pressurized metastable amorphous phases is that apparent thermodynamic transitions can be observed. These observations, despite the portion of the potential energy landscape occupied by the amorphous phases, and their relationship (or lack thereof) to liquid structures are each remaining enigmatic [*Giovambattista et al.,* 2003].

Being a very sensitive technique, Brillouin light scattering spectroscopy is a very sensitive technique, and has been widely used for characterizing first-order phase transitions [*Shimizu et al.*, 1996a] as well as for detecting phase transitions which are not characterized by a jump in density [*Xu and Manghnani*, 1992], including second-order order-disorder phase transitions in crystals [*Askarpour et al.*, 1993]. Brillouin scattering enables direct measurements of the sound velocities, and hence the elastic properties of materials [*Benedek and Fritsch*, 1966; *Vacher and Boyer*, 1972]. In conjunction with the diamond anvil cell (DAC), Brillouin light scattering is uniquely suitable for characterizing the mixed (amorphous) states existing in materials [*Zha et al.*, 1994], and

for monitoring changes in elasticity occurring during densification of amorphous materials.

During the past two decades, numerous studies focusing on the nature of amorphous-amorphous transitions (AAT) in pure *a*-SiO_2 under high pressure have been conducted by Brillouin scattering [e.g., *Zha et al.*, 1994; *Grimsditch*, 1984, 1986; *Polian and Grimsditch*, 1990, 1993; *Döring et al.*, 1994; *Rau et al.*, 1995] as well as vibrational spectroscopy and NMR, complemented by molecular dynamics (MD) simulations [*Huang and Kieffer*, 2004; *Williams and Jeanloz*, 1988; *Hemley et al.*, 1986; *Stebbins*, 1987, 1991; *Wolf et al.*, 1990; *Lacks*, 1998; *Trachenko and Dove*, 2003]. However, experimental elasticity data are sparse for silica-based glasses, alkali and/or alkaline earth oxides in the tetrahedral network structure, which are not fully polymerized (that is, glasses in which non-bridging oxygen ions, or NBO, are not bound to two silicons). In such glasses (values of NBO per tetrahedral unit, or NBO/T, in these glasses generally span from 0.5 to 1) different mechanisms of densification are available relative to pure silica. In other words, the distribution of non-bridging oxygens around silicons may shift, and coordination changes may initiate more readily than in pure silica glass [*Williams and Jeanloz*, 1988; *Meade et al.*, 1992; *Stebbins*, 1991].

Studies of water-white (NBO/T=0.75) and window glasses (NBO/T=0.67) by Brillouin scattering [*Xu*, 1996] (< 6 GPa) and ultrasonic methods [*Li et al.*, 2000] (< 2 GPa) showed the anomalous shear modulus softening in water-white glass similar to that observed in pure silica below 2 GPa. However, unlike in silica [*Zha et al.*, 1994], the anomalous pressure-induced decrease of longitudinal velocity is not observed in such glasses [*Xu*, 1996]. Moreover, no conclusions on the nature of the transition to the denser

amorphous states were drawn from previous studies [*Xu*, 1996; *Li et al.*, 2000]. Therefore, we were motivated to investigate *in situ* the elastic behavior of float glass (soda-lime silicate glass) during compression and decompression.

Here, we report the first macroscopic evidence of a partially reversible pressure-induced, apparently second-order amorphous-amorphous transition in float glass (NBO/T=0.66) with high silica content [*Holmquist et al.*, 1995] (for comparison, basaltic magmas have NBO/T between 0.9 and 0.6, andesite and dacite have values between 0.5 and 0.3, rhyolite and granite generally have values between 0.2 and 0.05 for anhydrous compositions [e.g., *Mysen et al.*, 1982]):

Chemical composition of float glass (in wt%)							Density
SiO_2	Na_2O	CaO	MgO	Al_2O_3	K_2O	Fe_2O_3	(kg/m^3)
73.7	10.6	9.4	3.1	1.8	1.1	0.2	2530

We used two different DACs, a lever type DAC [*Ming et al.*, 1987] for backscattering geometry [*Grimsditch*, 2001] and a Bassett-type DAC [*Jayaraman*, 1983] for symmetric 90° scattering geometry [*Whitfield et al.*, 1976], coupled with a Brillouin scattering setup similar to those employed in previous studies [*Xu and Manghnani*, 1992; *Tkachev et al.*, 2003a]. In the former case, a ground sample of the glass was loaded without pressure transmitting medium in a 150-μm thick Inconel 718 gasket pre-indented to approximately 70 μm, and the sample was repeatedly cycled to high pressure and decompressed in order to characterize any hysteresis/irreversible densification. In the latter case, a T301 stainless steel gasket (250 μm in thickness) was utilized. Five samples ranging from 90 to 30 microns in thickness and polished on both sides were used for five sequential compression runs at hydrostatic conditions; and a 4:1 mixture of methanol-

ethanol, which is hydrostatic to 10.4 GPa, was used as the pressure medium. The time scales at which the samples were held at pressure between measurements varied between 30 minutes and 7 days; all five samples yielded data that fell along the same trend, thus indicating that time-dependent effects are not significant over these conditions. The ruby fluorescence method was used to determine the pressure [*Piermarini et al.*, 1975] in all experiments. Raman spectra of pressurized glasses were acquired using a setup described previously [*Manghnani et al.*, 2000], with an accumulation time of 30 minutes.

2.2.2 *RESULTS AND DISCUSSIONS*

Results of the Brillouin scattering measurements in backscattering geometry (Fig. 2.14) show pronounced changes in the pressure dependence of nV_P (where n is the refractive index, and V_P is longitudinal sound velocity), suggesting that an amorphous-amorphous transition(s) occurs both during compression and decompression. Such transitions are exhibited in the sound velocity of pure silica [*Grimsditch*, 1984], but it is unclear whether they are associated with a discontinuity in elastic moduli. It has long been recognized that silica-rich glasses show changes in pressure dependence of the elastic moduli that are related to the anomalous elastic behavior of pure silica. These changes quantitatively correlate with silica content [*Manghnani*, 1969; *Manghnani and Benzing*, 1969], but there are distinct differences between float glass and pure a-SiO_2 [*Grimsditch*, 1984] in the pressure-induced changes in nV_P ($nV_P = 0.5\nu\lambda$, where λ = 514.5 nm is the incident laser light wavelength, and ν is a frequency shift defined by the position of the symmetric peaks shown in the upper left inset of Figure 2.15) during compression and decompression.

In the case of pure silica, there is a decrease in nV_P up to about 2 GPa followed by a pronounced increase [*Grimsditch*, 1984]. However, float glass shows no distinguishable change (a "plateau" region, Fig. 2.14) in sound velocity up to 3-4 GPa. Instead there is a larger pressure dependence of nV_P than in the case of silica glass at higher pressures. The nV_P values obtained during decompression approximately correspond to those of pure silica only down to 3 GPa (first decompression cycle on Figure 2.14) and decrease at a steeper rate at lower pressures, almost reaching its initial value, which is characterizing the glass at ambient conditions, prior to being compressed. The pressure dependences of nV_P in the second and third compression cycles are similar, with the nV_P values in the third cycle slightly lower than in the second (Fig. 2.14), but again both appreciably differ from those for pure silica after the onset of permanent densification.

During second decompression cycle of float glass the nV_P values (Fig. 2.14) are different from the corresponding values in pure silica and do not follow the nV_P-P path of the first decompression cycle, in contrast to the behavior of pure silica at high pressure [*Grimsditch*, 1984]. Interestingly, there is evidence for significant time-dependence of glass densification: the first point of the second decompression cycle ($\approx$ 6 GPa, Fig. 2.14) was taken two days after the last point of the second compression cycle ($\approx$ 7 GPa). The sample pressure had relaxed by almost 1 GPa, and nV_P had increased by a well-resolved 270 m/s. Both the pressure drop and velocity increase are consistent with a time-dependent densification of the glass, and this implies that the glass had not fully structurally equilibrated at the end of the second compression cycle (similar observations were made at lower as well as higher pressures during the second decompression and the first compression cycles, respectively, with delay periods varying from two hours to

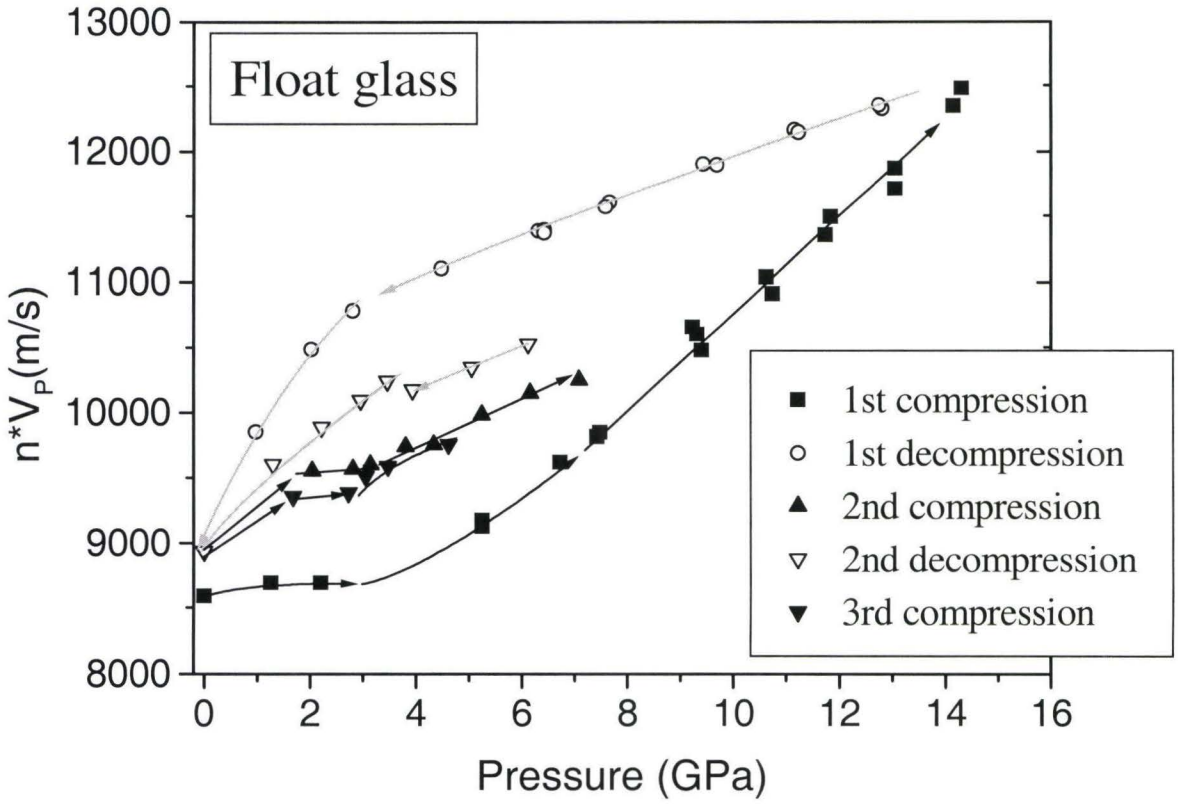

Figure 2.14.

Pressure dependence of nV_P in float glass during three compression and two decompression cycles; the black and gray arrows indicate directions of compression and decompression, respectively. Note that the ambient-pressure decompression value of nV_P is higher than the one obtained before pressurization, signifying an onset of permanent densification in the glass. The accuracy of the measurements determined by the standard deviation of the replicate analysis is within the size of the symbols.

several days). Nevertheless, the reproducibility of the ambient pressure sound velocity for different pressure-time histories (Fig. 2.14) implies that while a range of path-dependent structural states may exist at high pressures, they uniformly return to a similarly densified glass at ambient conditions.

The nV_P "plateau" region (Fig. 2.14) is also observed during the second and the third compression cycles, but it is offset to pressures of ~1.5-2.5 GPa, and is preceded by a relatively strong increase in nV_P. Moreover, the "plateau" region shifts to higher values of nV_P, during the second and third compressional cycles. Clearly, there is a complex interplay between the initial level of densification of the glass at ambient pressure and the anomalous lack of pressure dependence of the longitudinal sound velocity.

Raman scattering data of the densified glasses at ambient pressure are shown in Figure 2.15. No indication of glass devitrification are present in the spectra; an increase in linewidth of a number of the peaks is observed, and there are minor changes in the positions of the major bands identified in the glass. Most of the changes in the peak positions are within ± 10 cm^{-1} of the Raman bands of the glass powder prior to compression. There are shifts in intensities, particularly, of the 525 and 637 cm^{-1} bands. The former band is associated with SiO_4 tetrahedra with 3 bridging oxygens; accordingly, a shift in the distribution of bridging oxygens may occur within the densified glasses [*Xue et al.*, 1991].

The advantage of employing the symmetric Brillouin light scattering geometry is that it allows longitudinal and shear velocities to be measured without knowing the refractive index of the sample [*Whitfield et al.*, 1976]. The velocity values can then be used to estimate elastic parameters of the silicate glass [e.g., *Xu*, 1996]. Importantly, the

present results (Fig. 2.16) are in good agreement with available ultrasonic [*Li et al.*, 2000] and independent DAC strain measurements [*Meade and Jeanloz*, 1987], at ultralow frequencies. Indeed, the strain measurements also predict both an anomalous increase, as well as a "plateau" region, in the bulk modulus (above and below 5 GPa, respectively) for a silicate glass with a slightly different composition from ours.

The interesting aspect of the hydrostatic experiments of Fig. 2.16 is that while the density of the glass appears to monotonically increase with pressure, the bulk modulus clearly shows a discrete discontinuity near 6 GPa, and Poisson's ratio exhibits a distinct decrease (Fig. 2.16). The pressure of this transition is slightly elevated from that observed in the backscattering experiments (Fig. 2.14): this is likely due to the well-known role of shear stresses in triggering transformations at lower pressure [*Brückner*, 1970, 1971] in the non-hydrostatic backscattering experiments. The non-hydrostatic experiments (Fig. 2.14) provide an upper bound on the amount of irreversibility that is shown (Fig. 2.16) on decompression in the hydrostatic experiments, as permanent densification likely occurs more rapidly (and perhaps at lower pressures) under non-hydrostatic stress conditions.

The shift in bulk modulus, but apparently not in density, is in accord with the characteristics of a second-order phase transition. The higher-pressure amorphous material is characterized by markedly different pressure derivatives of the Young's and bulk moduli, and it is at precisely the pressure of this transition that the shear modulus begins to have a normal positive pressure derivative. The likely rationale for the initial decrease in bulk modulus (increase in compressibility) associated with the phase transition is that the glass has accessed a different compressional mechanism at pressures above 6 GPa, which in turn results in a different atomic configuration in the glass

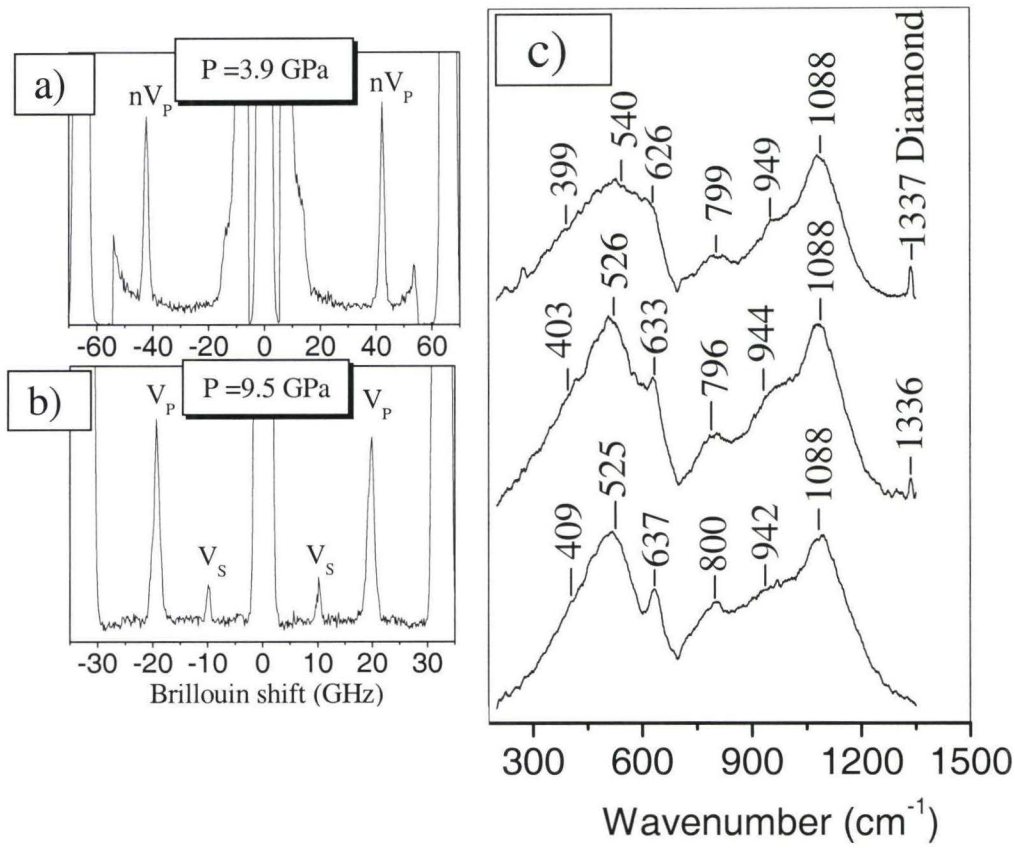

Figure 2.15.

(a) and (b) are typical Brillouin spectra of float glass showing nV_P, longitudinal (V_P) and shear (V_S) wave modes obtained *in situ* from the backscattering [*Grimsditch*, 2001] and symmetric 90° scattering [*Whitfield et al.*, 1976] geometries at 3.9 and 9.5 GPa, respectively. (c) shows unpolarized Raman spectra, from top to the bottom, of float glass after the second decompression cycle, first decompression cycle, and of the glass sample before DAC loading, respectively. Raman shift peak at ~1336 cm^{-1} is from the lower diamond anvil.

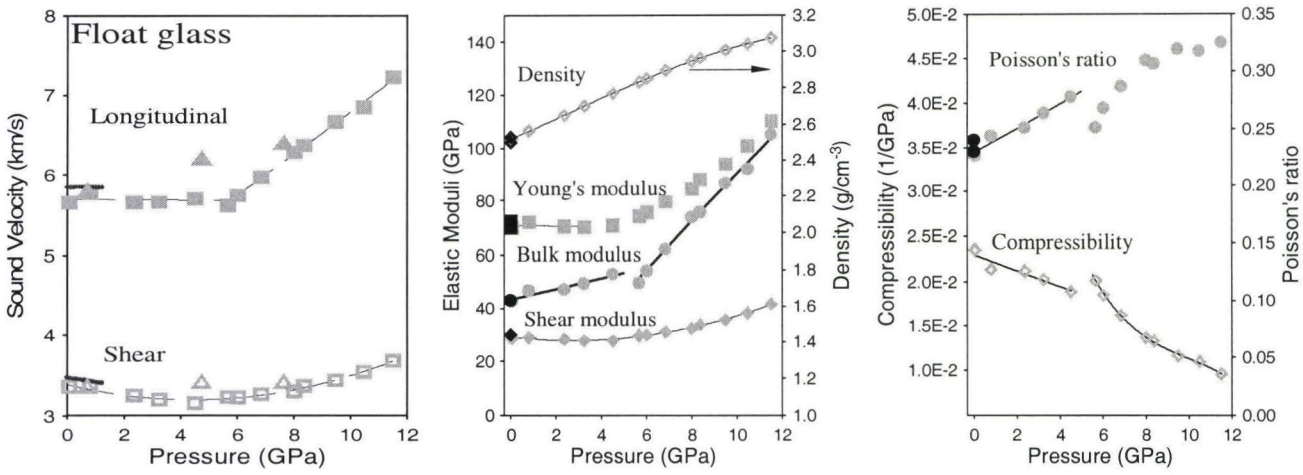

Figure 2.16.

Pressure dependences (first compression cycle, gray symbols) of sound velocities (ultrasonic values [*Li et al.*, 2000] are indicated by small dark-gray symbols on the left plot, and hypersonic values obtained during decompression from about 8 GPa are marked by gray triangles) and calculated elastic moduli and density ρ (lines are guides for the eyes, titles are self-explanatory, black symbols are representative elastic constants of float glass [e.g., http://www.sunmanagement.com/Ats129.pdf]) of float glass. The density values have been calculated using $dP/d\rho \approx V_P^2 - 4/3V_S^2$ (while sample density is not directly measured, the bootstrap technique has been shown to be quite accurate [*Tkachev and Manghnani*, 2000]). Accuracies of experimental and calculated values are within the size of the symbols, making the transition identifiable at about 6 GPa.

structure. The dense, high-pressure configuration may be associated with either disproportionation of SiO_4 species with three bridging oxygens to a mixture of two and four [e.g., *Xue et al.*, 1991], or an onset of highly coordinated silicon [*Williams and Jeanloz*, 1988; *Meade and Jeanloz*, 1987]. The combination of an initially increased compressibility (as denser coordinations are accessed) followed by a markedly large decrease in compressibility with pressure leads us to favor the latter alternative. In other words, the onset of the change in coordination allows more "room" for the sample to be initially compressed than during subsequent increase in pressure, due to the accumulation of denser coordinations in the sample that results in the decreased susceptibility of the sample to the pressure changes.

2.2.3 *CONCLUSIONS*

In summary, Brillouin scattering measurements in both scattering geometries explicitly demonstrate that the onset of an amorphous-amorphous phase transition need not have a discontinuity in the density as pressure is changed, but rather may exhibit anomalous jumps (Fig. 2.16) in Poisson's ratio and compressibility (bulk modulus) under pressure. The pressure dependence of Poisson's ratio is, in turn, clearly consistent with a pressure-induced increase in ductility and a decrease in shear strength at high pressures, as reported [*Meade and Jeanloz*, 1988] for amorphous SiO_2. Moreover, the softening of shear modulus, as is observed during the transformation between amorphous forms of ice [*Gromnitskaya et al.*, 2001], with the minimum shear modulus lying at the pressure of the transition is consistent with the existence of two different amorphous states in float glass. Our results demonstrate that a similar set of phase transition types is available to

amorphous solids on densification as is available to crystalline solids: first order transitions [*Gromnitskaya et al.*, 2001]; apparent second order transitions, as shown by this study; as well as gradual structural changes occurring with densification [*Williams and Jeanloz*, 1988; *Meade et al.*, 1992; *Hemley et al.*, 1986; *Meade and Jeanloz*, 1987]. The likely second-order transformation we documented here is clearly distinct from the well-known thermally-activated second-order glass transition. However, this pressure-induced second order transition does share characteristics with the glass transition: it is associated with the glass accessing a different (and, in this instance) pressure-activated set of structural environments, and this transition is associated with significant time and sample history dependences. The idea that a change in compressional mechanism can generate a glass-to-glass transition is in accord with the underlying concepts behind the "free volume" model of the glass transition [*Cohen and Grest*, 1979]. The significance of amorphous-amorphous phase transitions in silicate glass with regard to the study of Earth by seismic methods has to be viewed from the perspective of the corresponding pressure-induced gradual changes that occur in silicate melt and is addressed in Chapter 3.

Chapter 3

COMPRESSIBLITY OF HYDRATED AND ANHYDROUS Na_2O-$2SiO_2$ LIQUID, AND GLASS TO 8 GPA USING BRILLOUIN SCATTERING

3.1 INTRODUCTION

A knowledge of the viscoelastic properties of molten silicate material generated within the Earth's interior is crucially important for understanding the dynamics of magmatic processes as well as the history of the planet's primordial stratification. Because experimental data on density and bulk modulus play valuable roles in models of the transport and buoyancy of magmas, a variety of spectroscopic, ultrasonic and shock-wave techniques has been applied in numerous studies of natural and synthetic silicate liquids and glasses [*Wolf and McMillan*, 1995] at high temperature (T) and pressure (P).

The two main fluid phases within the Earth's crust and mantle are silicate melts and hydrous fluids, which form a continuum of miscible compositions at shallow upper mantle conditions [*Kohn*, 2000; *Shen and Keppler*, 1997]. Even though these phases are physically and chemically different near the surface of the Earth, water and liquid SiO_2 exhibit striking similarities in their structure and behavior [*Angell et al.*, 1982]. For example, the vitrification of aqueous binary solutions (e.g., aqueous lithium chloride solutions) under moderate pressure and low temperature [*Angell*, 2002; *Kanno*, 1987] supports the notion that silica- and water-rich liquid systems may have similar structural mechanisms responsible for their anomalous thermodynamic properties, which distinguish them from other liquids [*Wolf and McMillan*, 1995] that do not vitrify under

pressure. In this regard, the effect of alkalis on the thermoelastic properties of binary silicate liquids under pressure is not well constrained. Similarly, virtually no data exist on the effect of dissolved silicate species on the elastic properties of aqueous solutions at high pressures and temperatures.

The present study is oriented towards experimentally determining silicate melt/glass/aqueous solution elasticity under high P-T conditions of the lower crust and upper mantle by means of Brillouin scattering spectroscopy in conjunction with the externally heated diamond anvil cell (DAC). Our experimental objectives are to demonstrate the feasibility of determining elastic properties of liquids using Brillouin spectroscopy under extreme conditions, as well as to collect reconnaissance data on the effect of both pressure and dissolved water on the compressibility of silicate liquids. We utilize sodium silicate-based liquids as analogues for chemically complex, naturally occurring liquids. There are two rationales for using such alkali silicate liquids. First, their melting temperatures (and glass transitions) lie far below those of most natural silicate liquids, making their liquids experimentally more straightforward to probe, particularly at pressure. Second, the bonding environment of silicon is known to shift to higher coordination numbers in both crystalline and amorphous alkali silicates at substantially lower pressure conditions than is inferred to occur within natural liquids [e.g., *Farber and Williams,* 1996; *Fleet and Henderson,* 1997]. Accordingly, alkali silicate liquids are likely to undergo structural transitions at substantially lower pressure and temperature conditions than melts containing abundant alkaline-earth cations (Section 3.6 at the end of this Chapter gives more details on how analog studies will be related to Earth's P-T regimes and natural materials).

Pressure-induced coordination changes of silicon with respect to oxygen in natural melts have been inferred from both static measurements as well as shock wave measurements of molten silicates [e.g., *Rigden et al.,* 1988] and also confirmed by numerous Molecular Dynamics studies [*Rustad et al.,* 1990, 1991; *Wasserman et al.,* 1993; *Bryce et al.,* 1997; *Diefenbacher et al.,* 1998; *Nevins and Spera*, 1998]. Such structural changes may generate the density cross-over between silicate liquids and surrounding rocks within the upper mantle [*Stolper and Ahrens*, 1987; *Williams and Jeanloz,* 1988; *Wolf and McMillan*, 1995; *Farber and Williams,* 1996; *Matsui,* 1996]. The coordination change of silicon has been suggested to be largely responsible for generating the 20 % (or more) increase in silicate melt density believed to occur in the Earth's upper mantle. Moreover, the buoyancy forces on the aqueous fluids released from the dehydrating oceanic slab remain ill-constrained. The implications of the density contrasts between liquids and solids in planetary interiors for the differentiation and evolution of the planets are among the outstanding topics in modern geophysics [*Agee*, 1998].

The geophysical goals of this study are two-fold: first, to demonstrate the feasibility of determining the effect of changes in the coordination number of silicon on the elasticity of amorphous silicates at high pressures and temperatures using Brillouin spectroscopy. Second, we wish to constrain the elastic properties of hydrous silicate liquids at high pressures. Indeed, whether the elastic properties of silica-rich aqueous fluids more closely resemble water or silicate melts, particularly at the high pressure and temperature conditions under which silicate melts and hydrous fluids may be completely miscible, is unknown. In this respect, it is notable that the adiabatic bulk modulus of pure

water is near 2.0 GPa at ambient pressure, while those of silicate melts typically lie near 20 GPa [*Shimizu et al.,* 1996b; *Rivers and Carmichael,* 1987]. Accordingly, there is nearly a factor of two difference between the bulk sound velocity of water and silicate melts near their respective melting temperatures. If temperature differences could be taken into account, the discrepancy between the sound velocities would be even larger (sound velocity of water will be significantly lower at those melting temperatures). Whether this difference in sound speeds between these two geochemically important fluids persists at even shallow upper mantle conditions is ill-constrained. Moreover, the pressure dependence of the partial molar volume of water within silicate liquids has been constrained for only a few compositions [e.g., *Ochs and Lange,* 1997; 1999]. Therefore, we examine the constraints provided by our Brillouin data on the high pressure molar volume of water.

3.2 EXPERIMENTAL METHODS

Brillouin scattering spectroscopy employed in the present study is an optical technique that allows direct measurements of acoustic wave velocities by probing the sample with a laser beam (typical Brillouin spectra of the samples under investigation are shown on Figures 3.1a and 3.1b) thus eliminating the necessity of mechanical contact with the sample. The Brillouin scattering experimental setup (Fg. 3.2) and curve-fitting

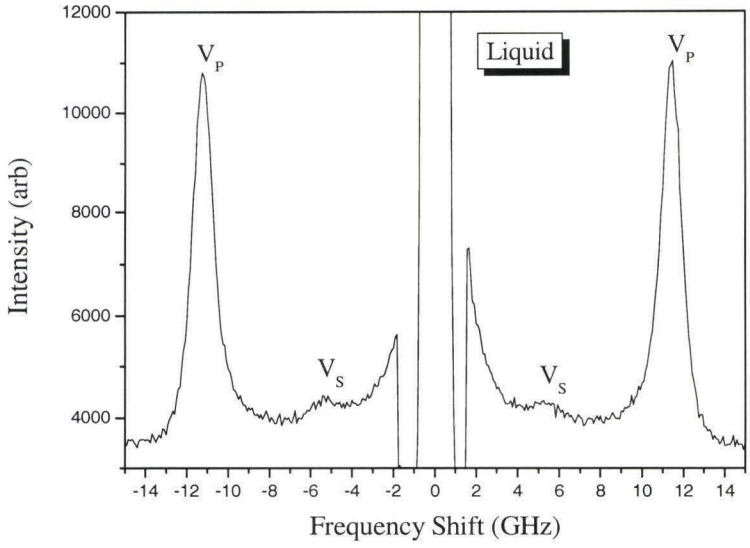

Figure 3.1.a.

Experimental Brillouin spectrum (thin solid lines) of hydrous Na_2O-$2SiO_2$ solution at 0.13 GPa, ambient T, before the glass transition.

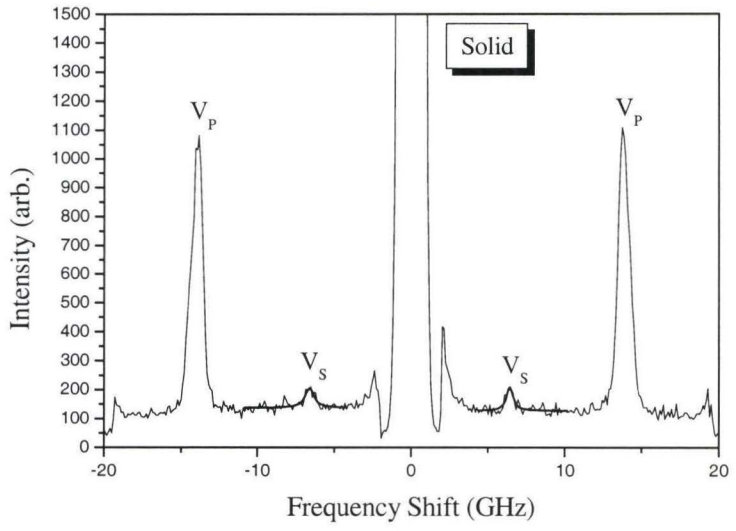

Figure 3.1.b.

Experimental Brillouin spectrum (thin solid lines) of hydrous Na_2O-$2SiO_2$ solution at 2.5 GPa, ambient T, after the glass transition. Thick solid lines are results of curve fitting routine for shear velocity (V_S) peaks. Conventional platelet geometry [*Whitfield et al.*, 1976] has been utilized in both a) and b).

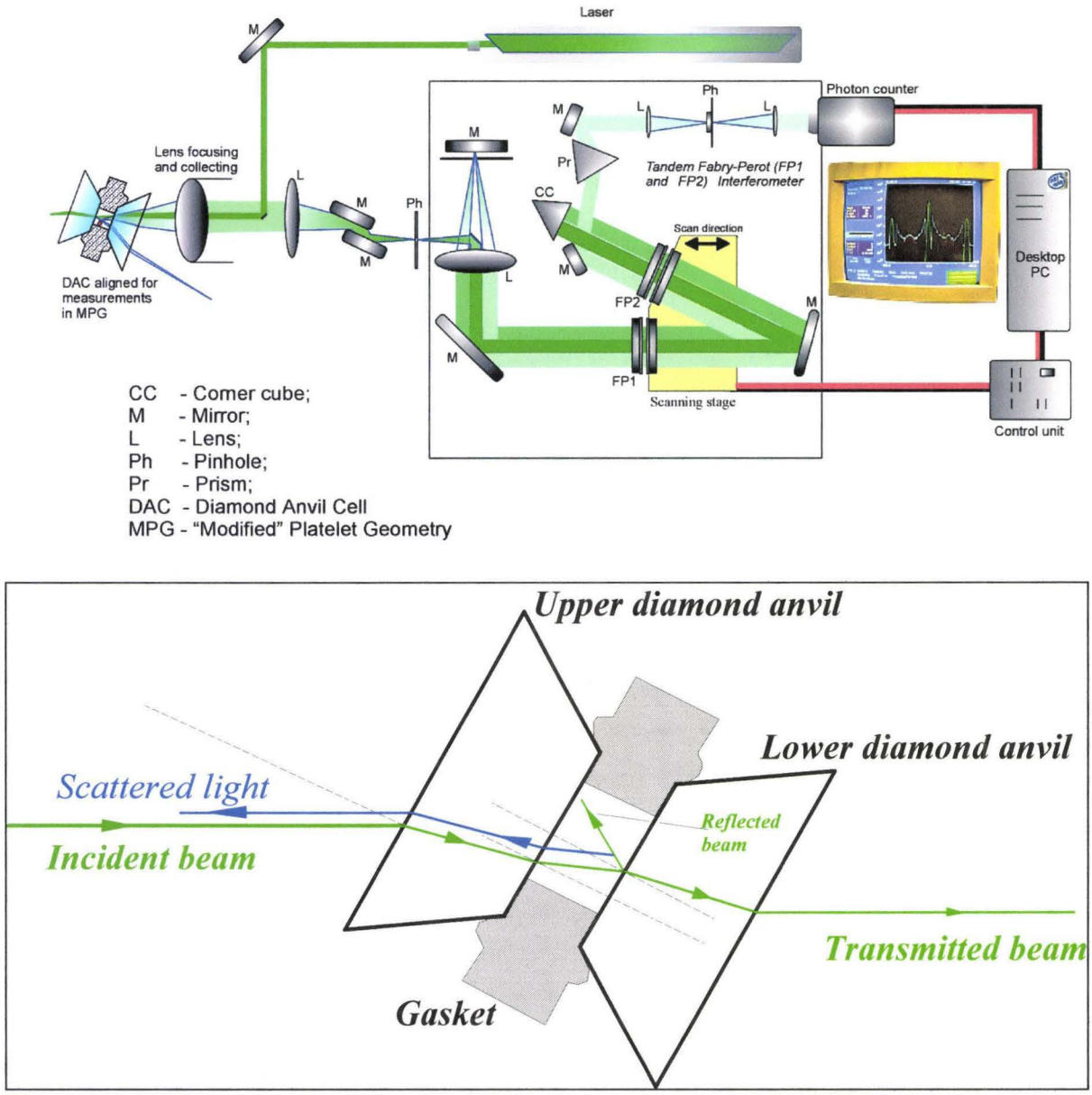

Figure 3.2.

Brillouin scattering spectroscopy experimental setup and "modified" platelet geometry (inset at the bottom in the shaded frame), where dashed lines are normals to the diamond surfaces.

routine are the same ones as those that have been recently utilized for determining the elastic properties of cubic BC_2N [*Tkachev et al.*, 2003a]. A beam from an argon ion laser (λ=514.5 nm and beam power of 100 mW) was focused onto the pressurized sample in a resistively heated diamond anvil cell (DAC) [*Ming et al.*, 1987] with a 1:4 (f =50 mm) lens. Each spectrum was typically accumulated for 1-2 hours.

Since classical backscattering geometry (θ =180°) enables only measurements of nV_P (product of refractive index and longitudinal velocity), and the conventional platelet geometry [*Whitfield et al.*, 1976] utilized in Chapter 2 could not be adopted for use in our high-T DAC, we deployed the "modified" platelet geometry (Fig. 3.2, inset), which is based on probing the sample with the laser beam reflected from the surface of the diamond [*Zha et al.*, 1993, 1994]. The advantage of this approach is that the sound velocity can be obtained independently from the sample's refractive index without changing from ordinary backscattering geometry [*Krüger et al.*, 1998; *Tkachev et al.*, 2003a]. In this case Brillouin shift v is related to the bulk sound velocity V as:

$$V = \frac{\lambda v}{2\sin\Theta} \tag{3.2.1}$$

where Θ is the angle between the incident wave vector and normal (dashed line, Fig. 3.2) to the surface of the diamond.

Figure 3.3 shows the Brillouin spectrum of water obtained in the "modified" platelet geometry. Note that the Brillouin peaks, from which the values of nV_P and V_P can been calculated, are well defined. The calculated V_P and n are plotted in Figure 3.4 for comparison with other independent measurements. A good agreement among the results by the various approaches demonstrates that "modified" platelet geometry is an effective route for independent and reliable determination of V_P and refractive index in

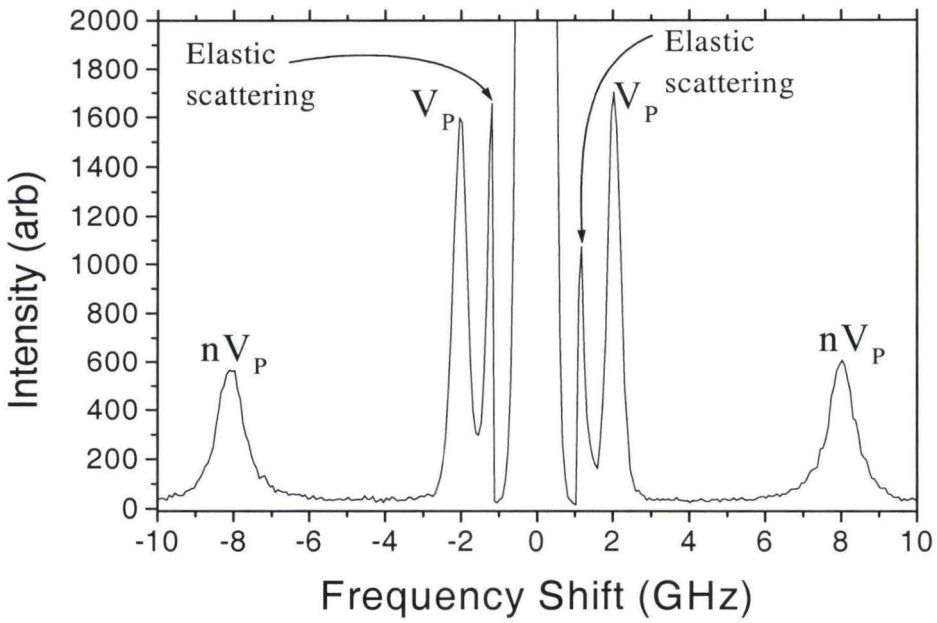

Figure 3.3.

Brillouin spectrum of water in the Diamond Anvil Cell at 0.05±0.03 GPa and room temperature using "modified" symmetric geometry with 20-degree external scattering angle.

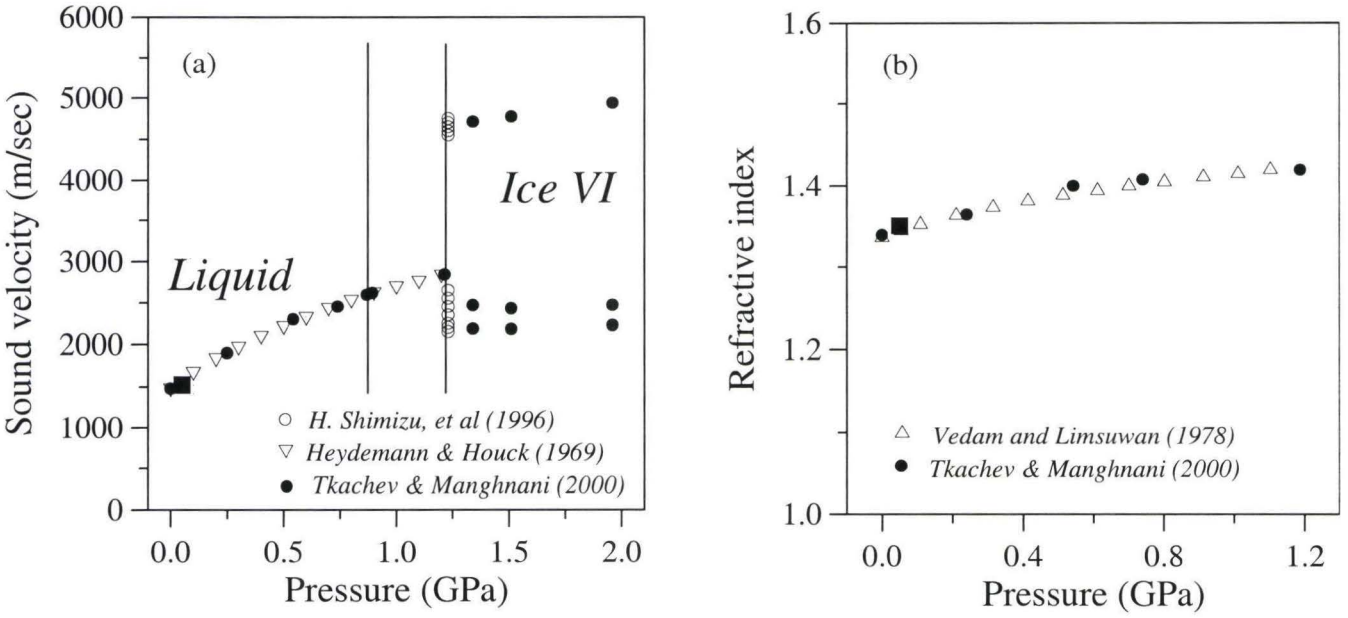

Figures 3.4.a and 3.4.b.

a) V_P and b) n of water as a function of pressure at room temperature. A very good agreement is found among the various Brillouin scattering geometries: "modified" platelet geometry (solid square); backscattering; and conventional platelet 90° scattering geometries (solid and open circles); as well as ultrasonic (inverse triangles), and optical interferometry measurements (triangles).

transparent liquids and solids under high P-T conditions. This geometry has also been used successfully [*Crowhurst et al.,* 2000] in determining the pressure dependence of the elastic properties of glass substrate in the zirconium anvil cell using surface Brillouin scattering technique.

Two types of the samples were employed in this study: (1) anhydrous Na_2O-$2SiO_2$ glass prepared from commercially available ultra-pure SiO_2 and Na_2CO_3 (Alfa Aesar®), following the procedures outlined in *Farber and Williams*, [1996]; and (2) sodium disilicate (Na_2O-$2SiO_2$) solution (containing 18 wt. % of Na_2O and 36 wt. % of SiO_2, density of 1.68 g/cm^3 and viscosity of 70 Pa·s at 20°C) given by the manufacturer (PQ® Corporation). Stoichiometrically, this corresponds to a mixture of Na_2O-$2SiO_2$-$8.5H_2O$. The samples of the aqueous solution were loaded in rhenium gaskets hardened by multi-step pre-indentations from 250 μm to 90-70 μm thickness. On the other hand, only pre-indented Inconel 718 with original thickness of 150 μm allowed the anhydrous sample to be retained under pressure at temperatures exceeding the glass transition, T_g. For each type of starting material, the temperature was increased at the rate of ~10 K/min. The samples were held at the end of every 100 K interval for at least 30 minutes prior to data acquisition. We did not observe any textural or spectral evidence for crystal growth in any of these charges, and melts were never heated above ~885 K to avoid heterogeneous nucleation and rapid growth of crystals [*Farber and Williams*, 1996]. For reference, the ambient pressure calorimetric glass transition of this composition is ~700 K, and there are indications that the glass transition temperature in silicates may decrease with pressure [*Kress et al.,* 1989; *Rosenhauer et al.,* 1978]; glass transitions for aqueous solutions may, however, loosely parallel the melting curve of water [e.g., *Kanno and*

Angell, 1977]. In order to avoid possible sample contamination at high P-T conditions, no pressure-transmitting medium (in contrast to Section 2.2, where mixture of alcohols was used as a pressure-transmitting medium) was utilized: due to a combination of the modest pressure range, the high temperatures, and the low (or zero) shear strength of the starting materials, pressure gradients were not important in these experiments.

Two to three tiny ruby chips, ranging in size from 3 to 7 μm, were placed in a 150-micron gasket hole on the top of the bottom diamond culet for pressure determination. The position of the ruby fluorescence line $\lambda_{P,T}$, which was excited by the same laser used for Brillouin measurements, depends on both pressure P [*Piermarini et al.*, 1975] and temperature T [*Yen and Nicol*, 1992]. Therefore, the wavelength shift $\Delta\lambda_{P,T}$ was expressed via $\Delta\lambda_{P,T}=\lambda_{P,T}-\lambda_{P_0,T_0}=\Delta\lambda_P+\Delta\lambda_T+f(P,T)$, with $\Delta\lambda_P$ and $\Delta\lambda_T$ as pressure and temperature dependent terms at T_0 = 20°C and P_0 = 1 atm, respectively. Because the correction term $f(P,T)$, which describes the pressure dependence of $\Delta\lambda_T$ and the temperature dependence of $\Delta\lambda_P$, is negligibly small [*Shimomura et al.*, 1982], this equation with $f(P,T)=0$ is used to estimate the pressure in a sample chamber using the experimentally established $\Delta\lambda_T$ [*Yen and Nicol*, 1992]. This in situ pressure calibration is of critical importance, as both cell relaxation at high temperatures (producing a decrease of pressure), and thermally-induced shifts in volume of the sample (producing either an increase or decrease in pressure) can occur. As described in the Discussion section below, it appears that the latter effect dominates in these experiments.

We utilized two methods for studying the viscoelastic responses of the sodium silicate glasses and liquids to high P-T conditions. The first consisted of compressing and decompressing (in some cases the specimen was initially pre-compressed at room T to

perform decompression melting at high T) before the aqueous sodium disilicate solution at constant T across the glass transition region (since this is the first time when aqueous sodium disilicate solution is studied under the pressure, no P-T phase diagram is available for this composition). For this particular case, Brillouin measurements were performed using the two types of platelet scattering geometries: conventional alongside with "modified" at ambient temperature - to ensure the consistency of the data acquired in both, and only "modified" at elevated T. The experiments using the conventional type of platelet right-angle geometry were carried out in a Bassett-type DAC redesigned to allow $\pm$ 45° optical access to the sample [*Jayaraman*, 1983]. In the second approach, the Brillouin spectra were collected using the modified platelet geometry during heating of both anhydrous and aqueous samples pre-compressed at room temperature to a certain P.

3.3 RESULTS

Figure 3.5 shows the pressure dependence of the shear (V_S) as well as longitudinal sound velocities, and nV_P of the aqueous solution. The presence of a shear-generated mode [e.g., *Grimsditch et al.,* 1989] implies that these GHz-frequency measurements sample the fluid in an unrelaxed state: the time-frame of the probe is faster than the rate at which the sample is able to attenuate shear excitations. Indeed, relaxation mechanisms in both silicate liquids and aqueous fluids are likely dominated by shear components: volumetric relaxation is typically weak in these fluids [*Kress et al.,* 1989; *Halalay and Nelson,* 1992]. Thus, we anticipate that bulk moduli derived from our study will closely approximate those of the fluid. There are clear indications (bending points on

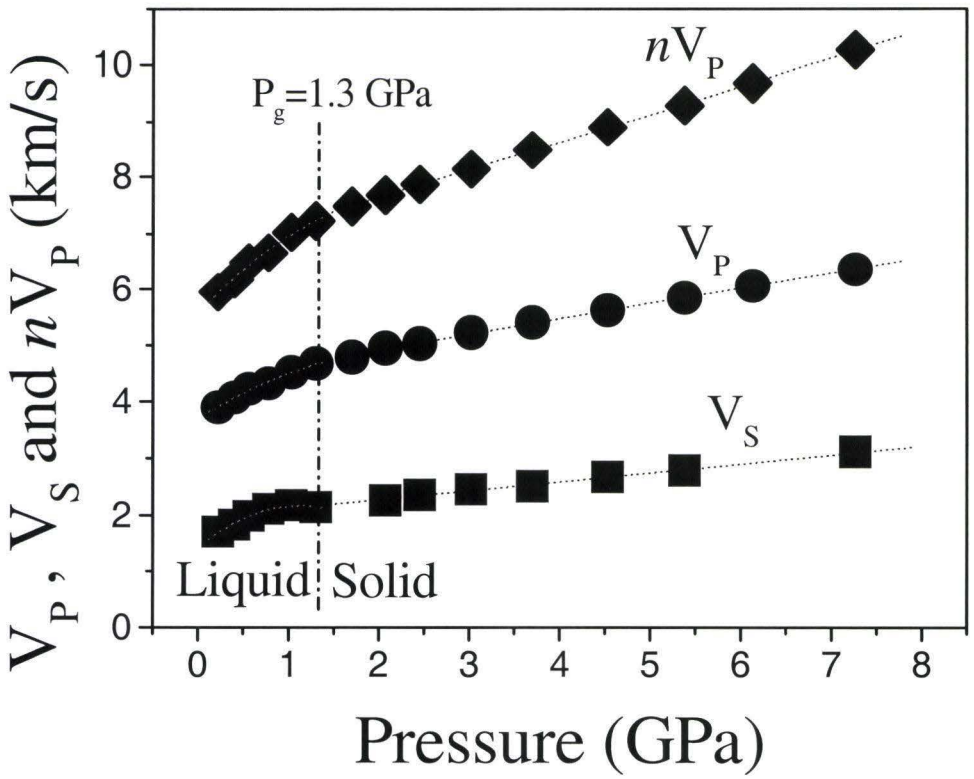

Figure 3.5.

Pressure dependencies of V_P (solid circles), V_S (solid squares), and nV_P (solid rhombs) in aqueous Na-disilicate liquid at ambient T (while experimental errors do not exceed the size of the symbols, the apparent "hump" in the V_S values prior to phase transition is, most likely, an artifact associated with the accuracy limits of the measurements: the shear peaks are both weak and broad within the liquid (Fig. 3.1.a) and substantially more inaccurate determined than the longitudinal peaks. Dotted lines are linear and polynomial fits to the experimental data (only compression cycle is shown). Dash-dotted line represents boundary between two different states.

all curves at about 1.3 GPa) of a liquid-to-solid phase transition (see also: answers to questions 1-3 from Appendix). This is a reversible phase transition (we observed it under both compression and decompression cycles) that reveals a marked change in K_S' (dK_S/dP), which exists between two different thermodynamic states (Fig. 3.6) separated by the glass transition. We associate this break in slope with the onset of glassy behavior of the aqueous solution at Brillouin frequencies (see also: answer to question 4 from Appendix). The universal Vinet equation of state (EOS) was utilized to fit the densities of the liquid and glass by using-ambient pressure values of the adiabatic bulk modulus and its pressure derivative (Fig. 3.6), as iteratively calculated to fit our data: an approach previously applied in glass-forming organic liquids [*Takagi et al.*, 1997]. Except for the assumption that adiabatic and isothermal bulk moduli are equal, similar calculations [*Tkachev and Manghnani*, 2000] have been carried out on pure water with excellent agreement with prior studies (e.g., Fig. 3.4). The notably higher K_S' of the fluid is consistent with the liquid being able to access a wider range of compressional mechanisms (see also: answer to question 6 from Appendix), thus illustrating that the means of compaction of the liquid (K_S'= 6.3) may differ substantially from those of the glass (K_S'= 4.8). However, the unresolvably small change in bulk modulus at the transition point (Fig. 3.6) is consistent with a comparatively minor role of volumetric (as opposed to shear) relaxation mechanisms at the transition to a fully unrelaxed state [*Krisch et al.*, 2002].

Figures 3.7 and 3.8 show results from decompression of the aqueous solution at constant temperature (457 K). The percentage increase in V_P (or, dV_P/V_P) is similar between the low pressure liquid and the high pressure solid; we speculate that the large

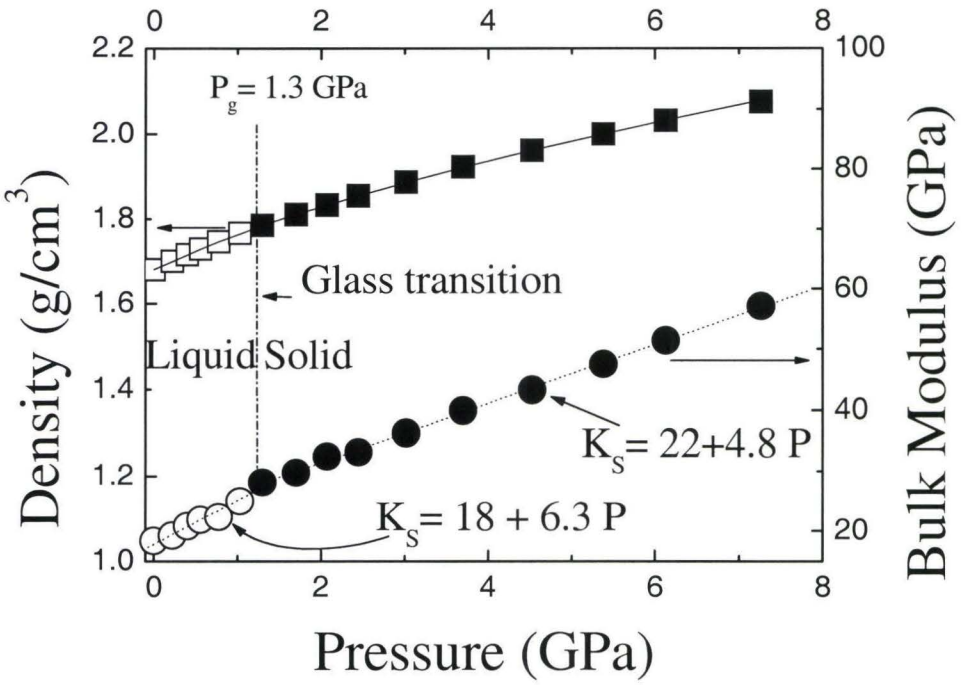

Figure 3.6.

Pressure dependences of density (squares) and bulk modulus (circles) of hydrous Na_2O-$2SiO_2$ at ambient temperature (298 K). Open and solid symbols represent liquid and solid states, respectively (calculation errors do not exceed the size of the symbols). Dotted and solid lines are linear and universal Vinet EOS-type [*Vinet et al.*, 1987] fits (see "Results" for the details) to the calculated data, accordingly. Dash-dotted line separates fields of stability for two different states (only compression cycle is shown).

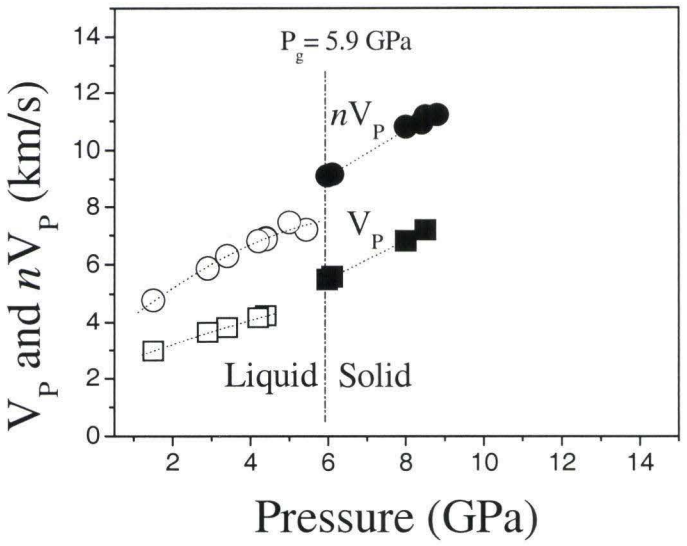

Figure 3.7.

Pressure dependences of V_P (squares) and nV_P (circles) of hydrous sodium disilicate sample at 457 K (experimental errors are the same as on Fig. 3.5). Dotted lines are linear and polynomial fits to the experimental data. Dash-dotted line represents boundary between liquid (open symbols) and solid (solid symbols) states.

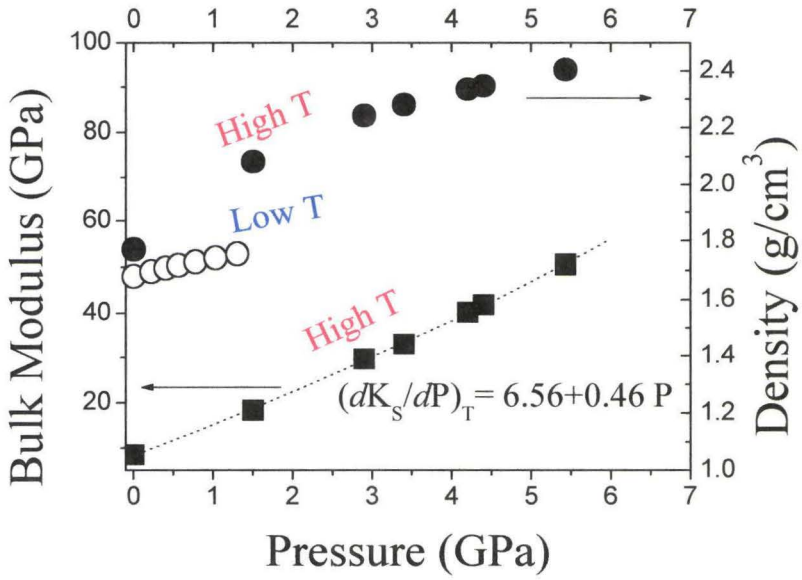

Figure 3.8.

Pressure dependences of density (solid circles) and bulk modulus (squares) of the Na_2O-$2SiO_2$ liquid (hydrous) formed upon decompression melting at 457 K (calculation errors are the same as on Fig. 3.6). Open circles represent density of the sodium disilicate fluid (Fig. 3.6) at ambient T (298 K). Dotted line is a polynomial (K_S = 8.35 + 6.56P + 0.23P^2) fit to the calculated data.

pressure derivative of V_P in the solid may be associated with a coordination transformation of silicon within the glassy aqueous material (see also: answer to question 5 from Appendix), as occurs within the crystalline form within this pressure range [*Fleet and Henderson,* 1977]. Figure 3.8 juxtaposes the pressure dependencies of density and bulk modulus for both high-T isothermal decompression melting (Fig. 3.7) of the hydrous Na-disilicate glass (it was initially pre-compressed to 8.8 GPa at ambient T) and (density only) ambient-T isothermal compression of the corresponding liquid (Fig. 3.6). Due to the structural changes occurring in both liquid and solid [*Farber and Williams*, 1996], the density of the high-T silicate fluid formed at pressure dramatically exceeds that of the same fluid studied at lower temperature (Fig. 3.8). This effect is a tandem consequence of the temperature dependence of the compressibility and the accessing of fully volumetrically relaxed states in the high temperature runs. A subsequent compression cycle did not show any differences in the pressure dependencies of V_P and nV_P within the limits of the experimental errors, implying that this densification is reversible. Accordingly, we attribute this dramatic shift in elasticity (and thus density) primarily to a strong temperature dependence of the elasticity of the aqueous fluid: the zero pressure bulk modulus is reduced by about a factor of two, from 18 to 9 GPa between 300 and 457 K. The weakly positive second pressure derivative of the adiabatic bulk modulus (Fig. 3.8) also indicates that the fluid formed at high P and T experiences gradual structural rearrangements that lead to a greater degree of high pressure compaction than would be inferred from the lower temperature behavior under pressure.

For each temperature in both isothermal compression (Fig. 3.5) and decompression (Fig. 3.7) cycles, Vinet EOS K_{0T} (ambient-pressure isothermal bulk

modulus) and K_{0T}' (ambient-pressure pressure derivative of isothermal bulk modulus) are determined by fitting the calculated values of K_T/ρ, where ρ is the density, to the experimental values of K_S/ρ (correction term between K_T and K_S used in Section 2.1.2 was not considered during the fitting routine due to the lack of literature data for this composition), and calculated values of pressure P_{EOS} to the experimental values of pressure P_{exp}, to minimize the weighted sum of squares (SSQw), which is expressed as $SSQw=\sum\{[(K_T/\rho)_i-(K_S/\rho)_i]/(K_S/\rho)_i\}^2 + \sum\{[(P_{EOS})_i-(P_{exp})_i]/(P_{exp})_i\}^2$. Well-defined minima of the SSQw characterize the uniqueness of the solutions as well as satisfactory accuracy (maximum variation in density values does not exceed ±1% around the smallest contour line of the SSQw minima at the highest pressure reached in the experimental runs) of the fitting procedure (Fig. 3.9.a,b). These calculations would not be possible to accomplish if the density of melt at ambient pressure is unknown. Therefore, after the experimental values of V_P and nV_P had been utilized to determine n at 457 K and ambient pressure, we estimated the zero-pressure density of the melt at 457 K by using the ratio of Lorentz-Lorenz expression at 457 K to the one at ambient T (general view of Lorentz-Lorenz expression is presented by the formula $(n^2-1)/(n^2+2)=4\pi\alpha\rho/(3M)$ with M as the molecular weight and α as the electronic polarizability), assuming that α is constant.

Brillouin scattering measurements of hydrous as well as anhydrous Na_2O-$2SiO_2$ samples (compressed at room temperature to 5.6 GPa and 5.9 GPa, respectively) were also carried out during heating cycles across the corresponding glass transition regions. The typical Brillouin spectra of glass and melt below (Fig. 3.10.a) and above (Fig. 3.10.b) T_g clearly demonstrate not only change in the peak positions but also a marked difference in the linewidths [*Masnik et al.,* 1993] for two thermodynamic states: such shifts in

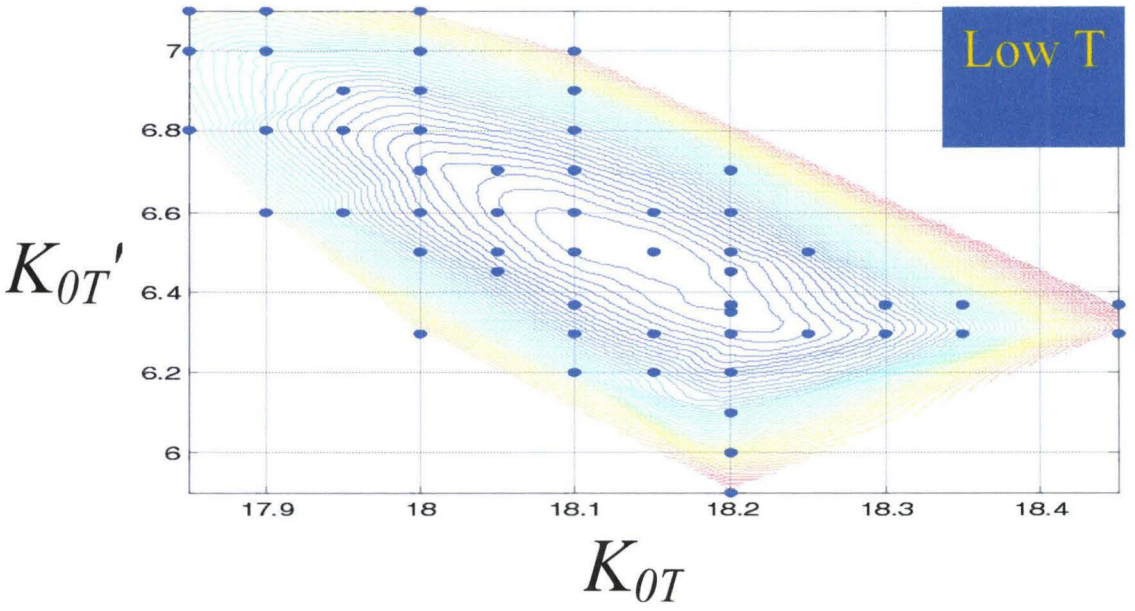

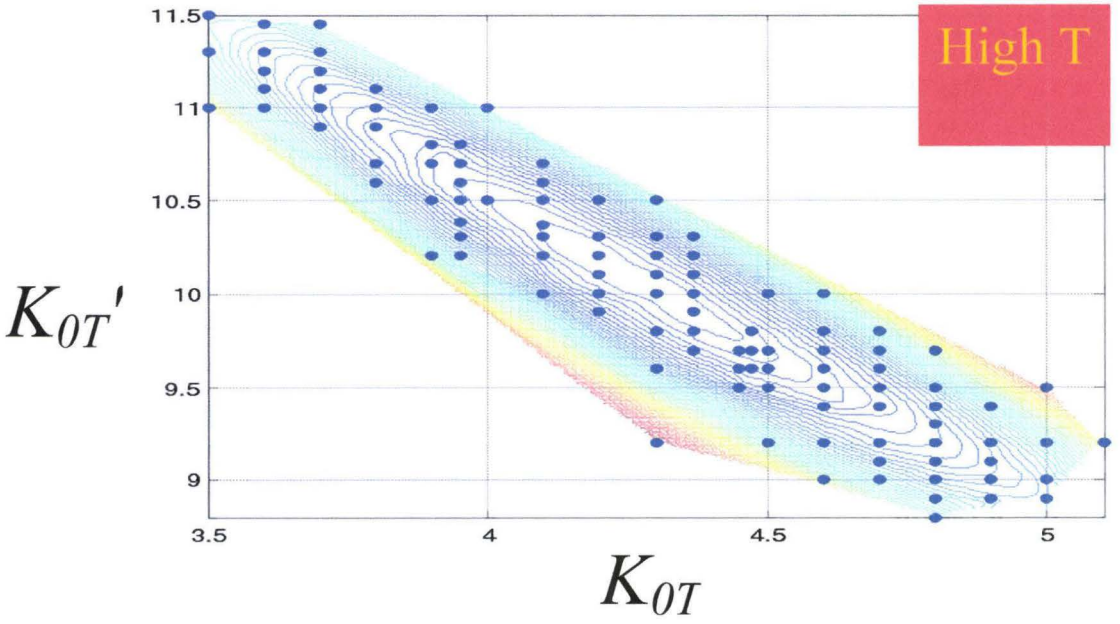

Figures 3.9.a (top) and 3.9.b (bottom).

Vinet EOS K_{0T} (X-axis) and K_{0T}' (Y-axis) contour plots of SSQw (Z-axis) minimization. A set of 50 contour lines and triangle-based cubic interpolation routine have been used to identify the minima in SSQw for both isothermal compression (a) and decompression (b) cycles. Solid circles are data points utilized for the routine.

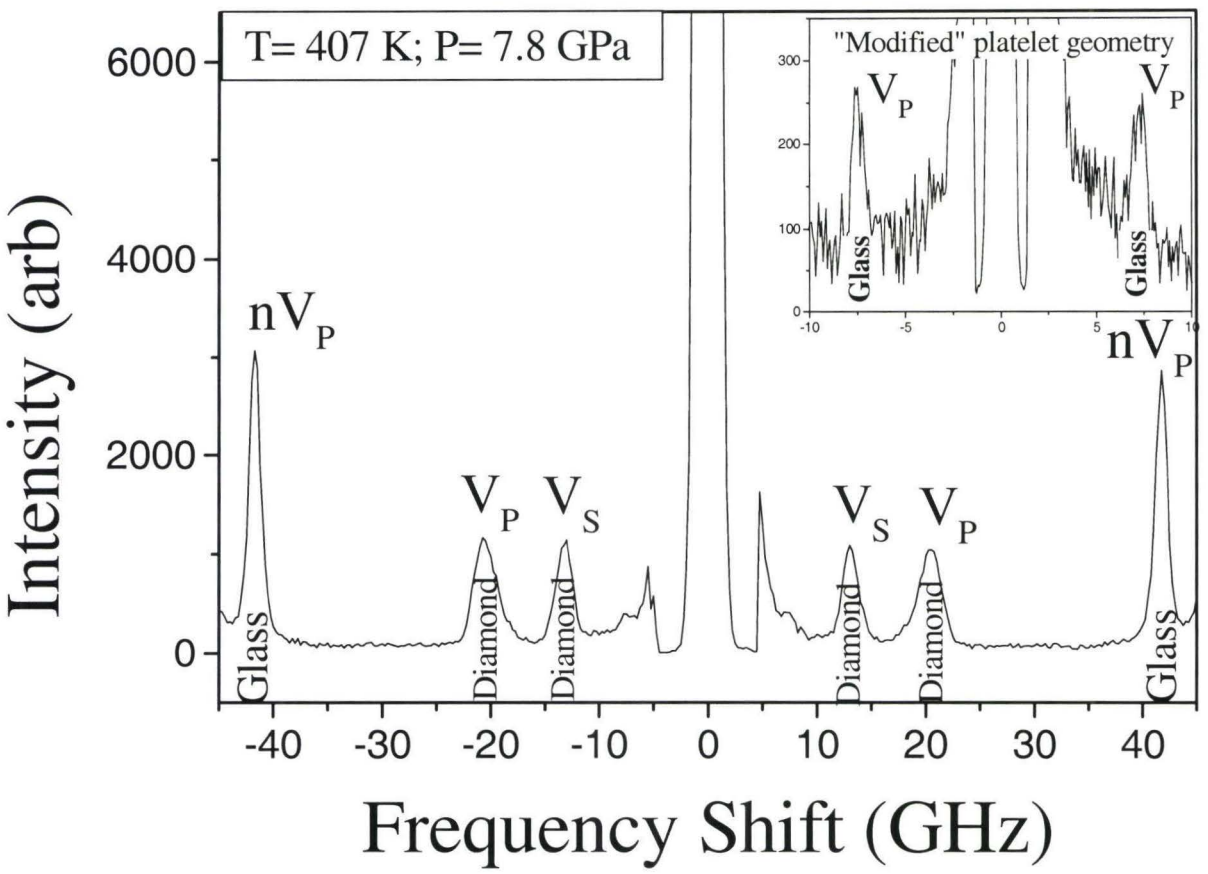

Figure 3.10.a.

Experimental Brillouin spectra of aqueous Na_2O-$2SiO_2$ solution below glass transition T. The V_P and V_S peaks from diamond anvils are marked.

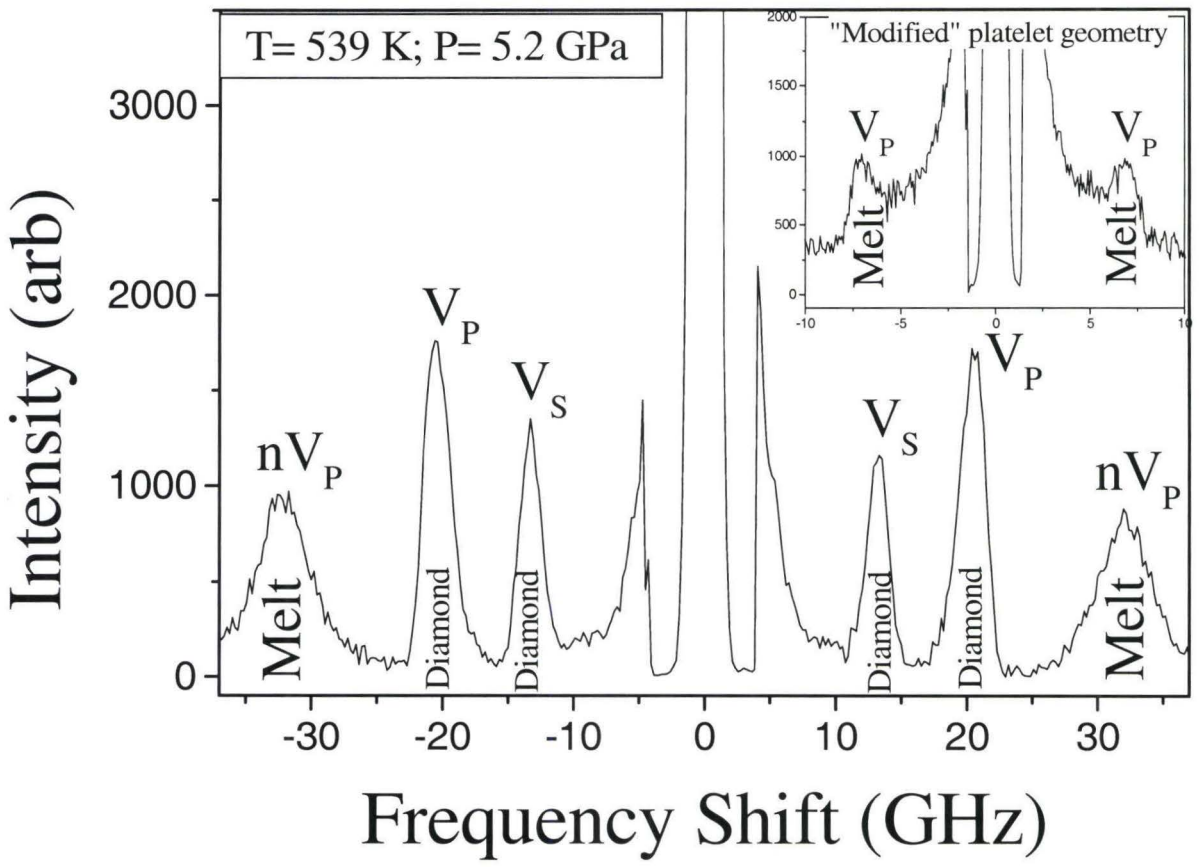

Figure 3.10.b.

Experimental Brillouin spectra of aqueous Na_2O-$2SiO_2$ solution above glass transition T. The V_P and V_S peaks from diamond anvils are also marked.

Brillouin linewidth are well-documented to be associated with shifts in the viscoelastic response associated with the glass transition [e.g., *Pinnow et al.,* 1967]. Experimentally measured temperature dependencies of V_P and nV_P (Fig. 3.11) at high P allowed us to quantitatively evaluate the influence of heating on densities, optical (Fig. 3.12) and elastic (Fig. 3.13) properties in both states separated by the glass transition boundary. These data do, however, depend on the pressure path taken by the cell during the heating process: these changes, while measurable, are neither simple nor readily predictable (Fig. 3.14). The effect of the shifting pressure environment within the cell and its relation to the evolution of the obtained parameters is analyzed in detail in the next section.

3.4 DISCUSSION

3.4.1 *Temperature and Pressure Effects on Liquid and Glass Elasticity*

Our estimated pressure dependence of the density for the aqueous sodium disilicate fluid (Fig. 3.8) indicates that pressure-induced structural changes, which gradually occur in the corresponding glasses on simple compression, are significantly enhanced by increased temperature. As has been experimentally established for amorphous-amorphous transformations in SiO_2 glasses [*El'kin et al.*, 2002], an increase in temperature can decrease the pressure at which structural changes can occur: this may be viewed as hotter liquids being simply able to access a wider suite of structural states [e.g., *Morgan and Spera*, 2001 a, b]. Some of these structural states may be comparatively high density relative to those present in the glassy precursor, or those

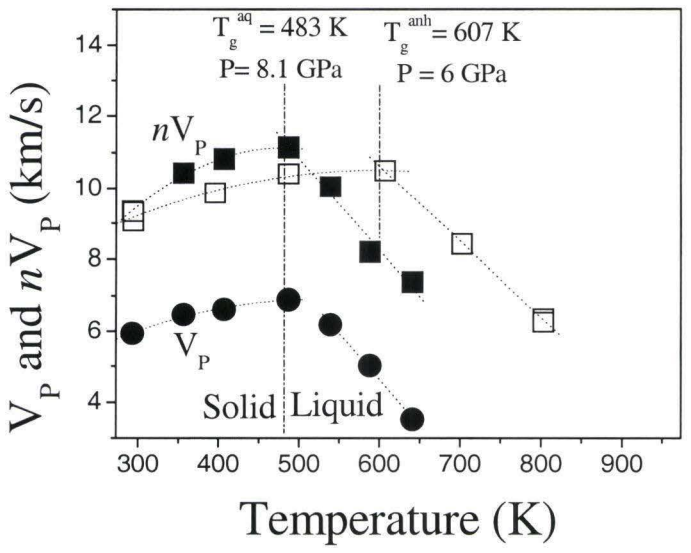

Figure 3.11.

Temperature dependencies of V_P (circles) and nV_P (squares) measured below and above the glass transition temperatures of aqueous (T_g^{aq}) Na_2O-$2SiO_2$ solution (solid symbols) and anhydrous (T_g^{anh}) Na_2O-$2SiO_2$ glass (open symbols). Phase boundaries between solid and liquid are depicted as dash-dotted lines for both types of samples (experimental errors are the same as on Fig. 3.5). Dotted lines are linear (for corresponding liquid state) and 2nd-degree polynomial (for corresponding solid state) fits to the experimental data.

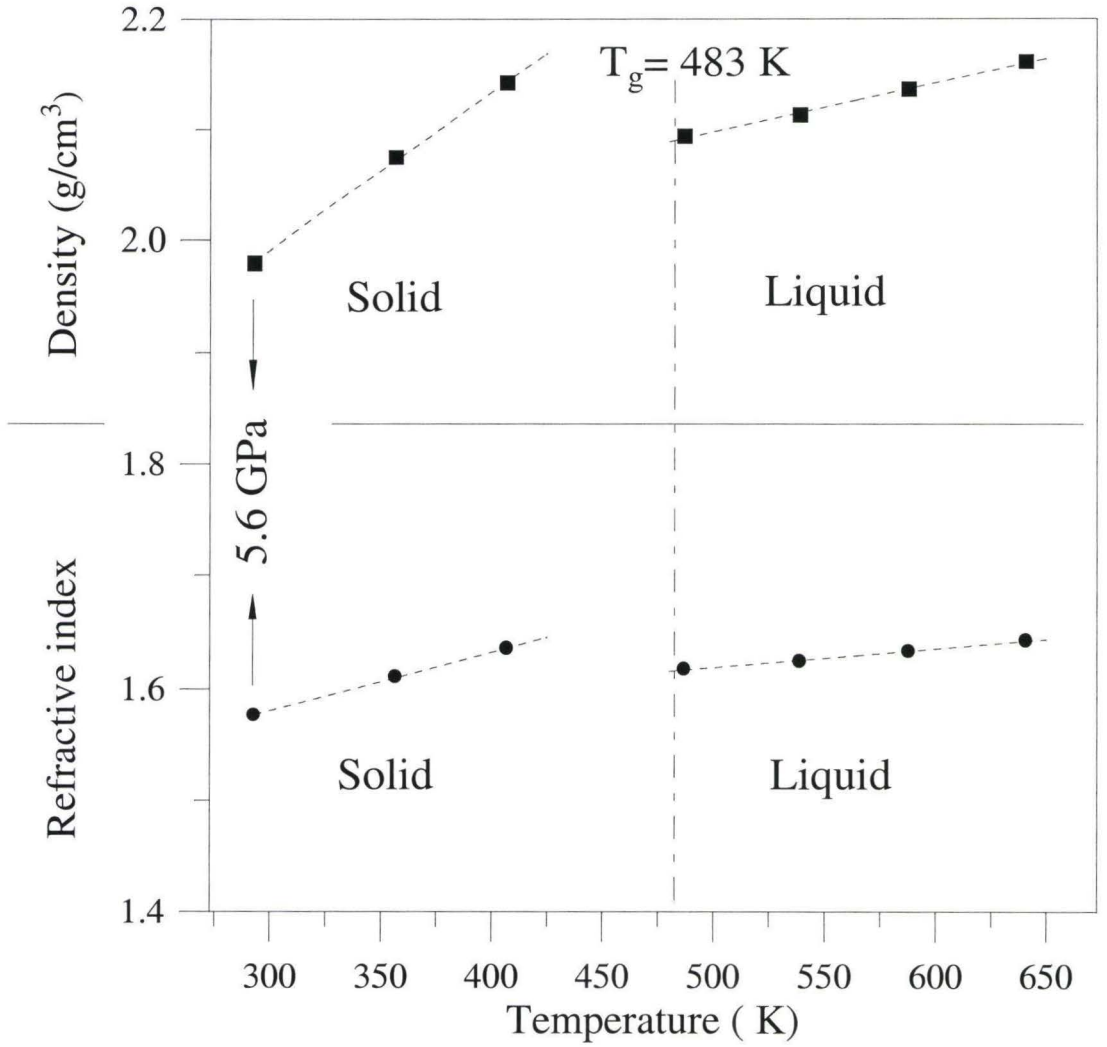

Figure 3.12.

Temperature dependencies of density (squares) and refractive index (circles) in aqueous Na_2O-$2SiO_2$ solution. Dotted lines are linear fits to the measured and estimated data. Dash-dotted line represents boundary between liquid and solid states.

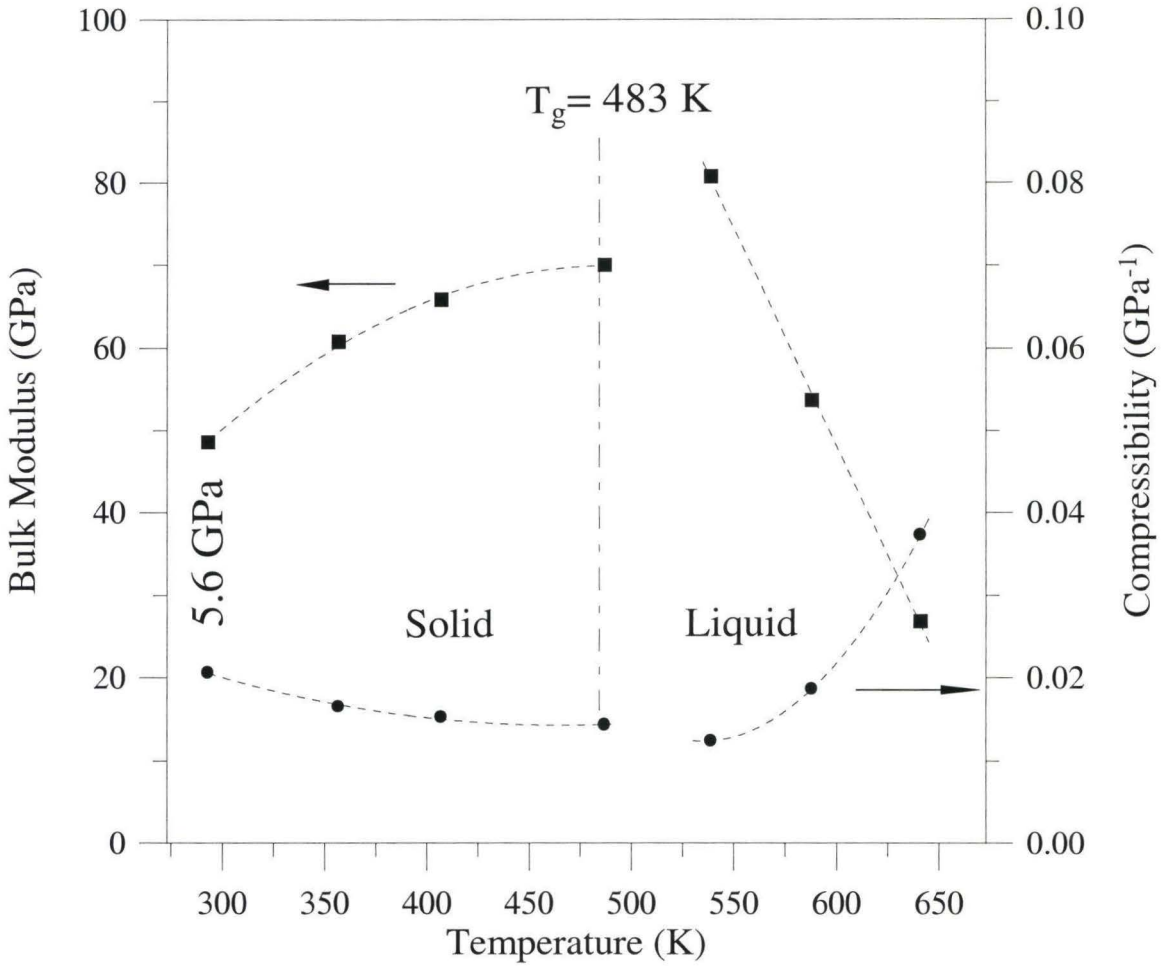

Figure 3.13.

Temperature dependencies of adiabatic bulk modulus (squares) and compressibility (circles) of aqueous Na_2O-$2SiO_2$ solution calculated from the results of sound velocity measurements. Dotted lines are linear and 2nd-degree polynomial fits to the data. Dash-dotted line represents boundary between liquid and solid states.

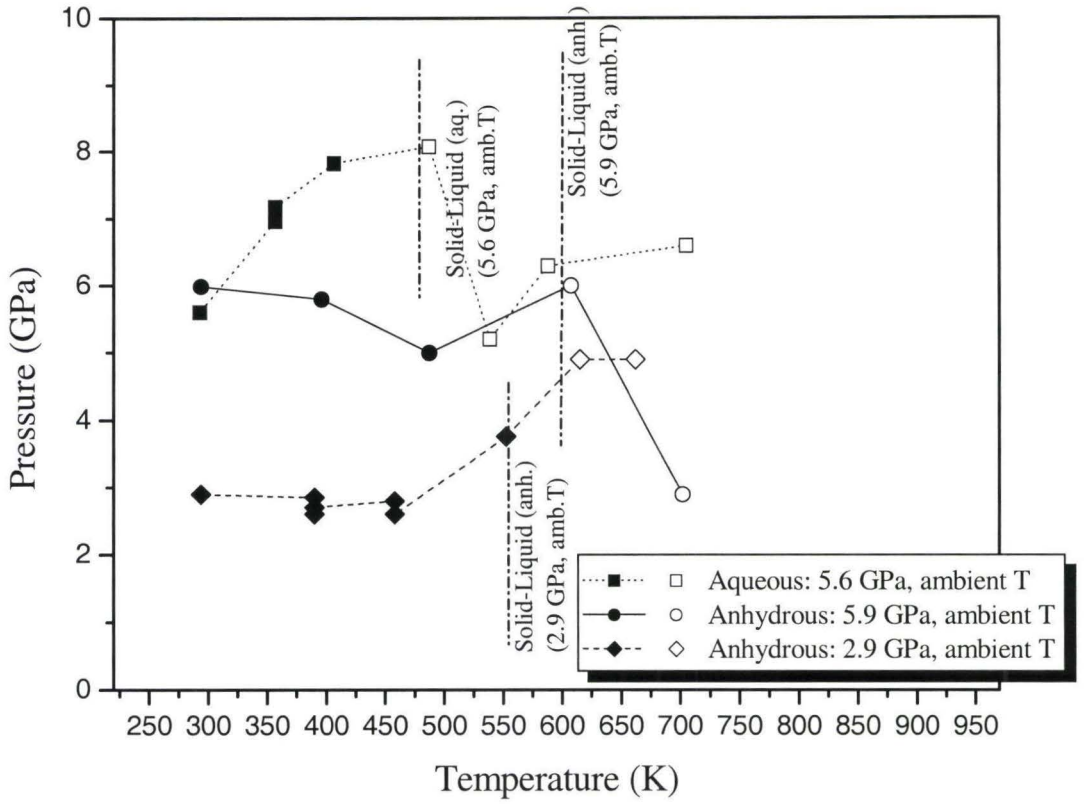

Figure 3.14.

Temperature-induced pressure changes in the sample chamber of DAC for aqueous (squares) and anhydrous (circles and rhombs) sodium disilicates (maximum uncertainty in pressure determination is ±0.2 GPa with maximum uncertainty of ±3 K in temperature determination at highest temperatures). Dotted lines are guides for the eye. Phase boundaries between solid (solid symbols) and liquid (open symbols) are depicted as dash-dotted lines for all types of samples.

present in liquids equilibrated at lower temperatures. The same type of behavior may also characterize hydrous sodium disilicate glasses and, therefore, glasses formed from liquids differ in their densities depending on their pressure-temperature history. In other words, the structural arrangements of atoms, as recorded in the glasses, reflects the density change associated with the corresponding liquids. In the case of the sodium disilicate solution, a higher temperature of melt equilibration at constant pressure produces a substantially higher density of the molten product. Indeed, the present high P-T experimental results (Fig. 3.8) clearly demonstrate that decompression melting at higher temperatures produces liquids with progressively higher densities relative to the ambient temperature liquid. Furthermore, the positive sign of the second pressure derivative of the adiabatic bulk modulus (K_S) at higher T indicates that there exist more efficient mechanisms of sample densification than at lower T (Fig. 3.6). Even though the K_S' of the glass (Fig. 3.6) is comparatively normal (4.8), it produces almost a doubling of its bulk modulus between about 2 and 8 GPa. This is a direct consequence of the markedly low initial K_S associated with the high compressibility of the dissolved water. It is important to emphasize that while a shortening of hydrogen bonds is a major compression mechanism for OH^- and H_2O present in glasses [*Richet and Polian*, 1998], within this pressure range and at ambient temperature the silicate network itself likely compacts primarily via changes in the Si-O-Si angle [*Hemley et al.*, 1986; *Williams et al.*, 1993].

An indirect confirmation of the expected gradual structural changes in glass and its melt can also be shown through an analysis of the temperature-induced changes of pressure (Fig. 3.14) in the sample chamber of DAC. There are two distinctly opposite

types of pressure changes observed across T_g regions during heating cycles in the DAC: a gradual increase (2.9 GPa initial pressure curve) and a substantial drop in pressures (5.6 and 5.9 GPa initial pressure curves) at the onset of the phase transition. These changes are likely associated with a decrease (for higher P) or increase (for lower P) in sample volume, implying that liquids formed from high-P glass melting structurally differ from those generated at lower pressures. This supplementary experimental observation is also in qualitative agreement with the general concept of new densification mechanisms [*El'kin et al.*, 2002, *Farber and Williams*, 1996] induced by high pressure in the silicate glasses and melts.

It is worthwhile to note that the experimentally measured temperature dependencies of V_P and nV_P (Fig. 3.11) as well as the densities, optical (Fig. 3.12) and elastic (Fig. 3.13) properties extracted from these measurements are each subject to the pressure changes inside the DAC chamber during heating cycles. Below 650 K, the total change in pressure is relatively small between the 300-K starting pressure and the pressure at which the glass transition is encountered for the runs with initial pressures of 5.6 and 5.9 GPa: a significant excursion to higher pressure does take place at low temperature (below 450 K) in the 5.6 GPa run, but the sample reverts back to near its starting pressure near the glass transition. In contrast to the anhydrous sodium disilicate glass, which, similar to silica glass, shows an increase in sound velocity at relatively constant pressure, the significant pressure increase (Fig. 3.14) in the DAC sample chamber is one of the reasons for the more dramatic sound velocity increase with temperature in the hydrous material. Therefore, we expect that the density of the melt should be undergoing a larger isobaric increase than that shown in Figure 3.12 when the

observed pressure drop is considered (Fig. 3.14). Accordingly, the results of Figure 3.12 provide a lower bound on the actual density change with pressure of the melt. In other words, the density of the liquids formed upon melting of the glass are shown at lower pressures than their precursors due to the decrease in the volume of the sample associated with the more compact packing of atoms in the high temperature, relaxed form.

The same effect is seen in the temperature dependence of elastic properties (Fig. 3.13). Here, at a temperature corresponding essentially precisely to the glass transition (485 K), the index of refraction, and hence density, show a significant discontinuity (Fig. 3.12). This drop in density, and commensurate pressure decrease, coupled with the near constancy of V_P across this transition (Fig. 3.11), produce a bulk modulus near the glass transition that lies, perhaps fortuitously, on the solid trend (Fig. 3.13). That the results of Figures 3.12 and 3.13 are not under isobaric conditions (a difficult condition to generate within the externally heated diamond cell in systems with large volume changes) makes it important to take into account the crucial role played by a decrease in pressure in generating the apparent negative dK_S/dT for the liquid. While the intercalated effects of changes in sample volume and thermal relaxation of the cell assembly are difficult to separate from one another, the key aspect here is that changes in phase are clearly apparent in such measurements, and robust changes in the behavior of the derivatives of elastic properties are also apparent.

Indeed, precise results on dK_S/dT might be achievable only when the technical problems associated with making measurements at isobaric conditions at high temperatures are fully resolved: a difficult but not impossible experimental task. Alternatively, conducting a large number of measurements at known (but varying)

pressure and temperature conditions and inverting these data for derivatives of elastic properties may prove necessary: given the difficulty of these measurements, such extensive data sets are likely possible, but still require technical improvements in both sample retention at high pressures and temperatures, and likely in the speed/signal-to-noise of the Brillouin measurements.

3.4.2 *The Pressure Dependence of the Partial Molar Volume of Water*

The partial molar volume of water ($\overline{V}_{H2O}$) in the melt has been expressed in terms of a model equation [*Ochs and Lange,* 1997] for hydrous silicate liquids (over the temperature range from 600 to 1873 K and pressures up to 1 GPa) as:

$$\overline{V}_{H2O} = \frac{V^{liq}_{P,T,X_i} - \sum X_j \left\{ \overline{V}_{j,T_{ref}} + \frac{d\overline{V}_j}{dT}(T - T_{ref}) + \left[\left(\frac{d\overline{V}_j}{dP} \right)_{T_{ref}} + \frac{\left(\frac{d\overline{V}_j}{dP} \right)}{dT}(T - T_{ref}) \right] (P - P_{ref}) \right\}}{X_{H2O}} \quad (3.4.1)$$

where V^{liq}_{P,T,X_i} is the molar volume of the liquid, $\overline{V}_{j,T_{ref}}$ is the partial molar volume of each oxide component j (except water), T is the temperature in Kelvins, P is the pressure in bars, P_{ref} is one bar, $\frac{d\overline{V}_j}{dT}$ is the partial molar thermal expansivity of each oxide component j (except water), $\frac{d\overline{V}_j}{dP}$ is the partial molar volume compressibility of each oxide component j (except water), $\left(\frac{d\overline{V}_j}{dP} \right) \Big/ dT$ is the temperature dependence of the partial molar compressibility of each oxide component j (except water), X_j is the mole

fraction of each oxide component j (except water), and X_{H_2O} is the mole fraction of water component. It is possible to estimate the pressure dependence of partial molar volume of water in the hydrated Na_2O-$2SiO_2$ liquid at 457 K by using Equation 3.4.1 in conjunction with the values of partial molar volume, thermal expansivity, compressibility, $\left(\frac{d\overline{V}_j}{dP}\right)\Big/dT$ previously determined for SiO_2 and Na_2O components at T_{ref} = 1673 K, and V^{liq}_{P,T,X_i} recalculated from our density values (Fig. 3.8). The consistency of our present results for the partial molar volume of water (Fig. 3.15) with those obtained by both dilatometry experiments [*Ochs and Lange,* 1997, 1999] and direct density measurements [*Burnham and Davis*, 1971] not only indicates that the range of applicability of the proposed model equation might extend far towards water-rich compositions, but also is qualitatively consistent (for pressures below 0.8 GPa) with the results of studies on the solubility of water in peralkaline silicate and aluminosilicate melts [*Mysen and Acton*, 1999], where values of $\overline{V}_{H_2O}$ are reported to be lower than those derived by Ochs and Lange.

It is important to recognize that the substantial amount of data relating to the pressure dependence of water solubility [*Mysen and Acton*, 1999; *Mysen and Wheeler*, 2000; *Mysen*, 2002] cannot be directly used in the present study to estimate $\overline{V}_{H_2O}$. Nevertheless, the interpolation of both the model equation for hydrous silicate liquids [*Ochs and Lange,* 1997] and the empirical P-$\overline{V}_{H_2O}$-T equation of state [*Burnham and Davis*, 1971] down to 457 K appears to provide a reasonable approximation to this value (Fig. 3.15). Although the $\frac{d\overline{V}_j}{dP}$ obtained by using the data of this study on the pressure

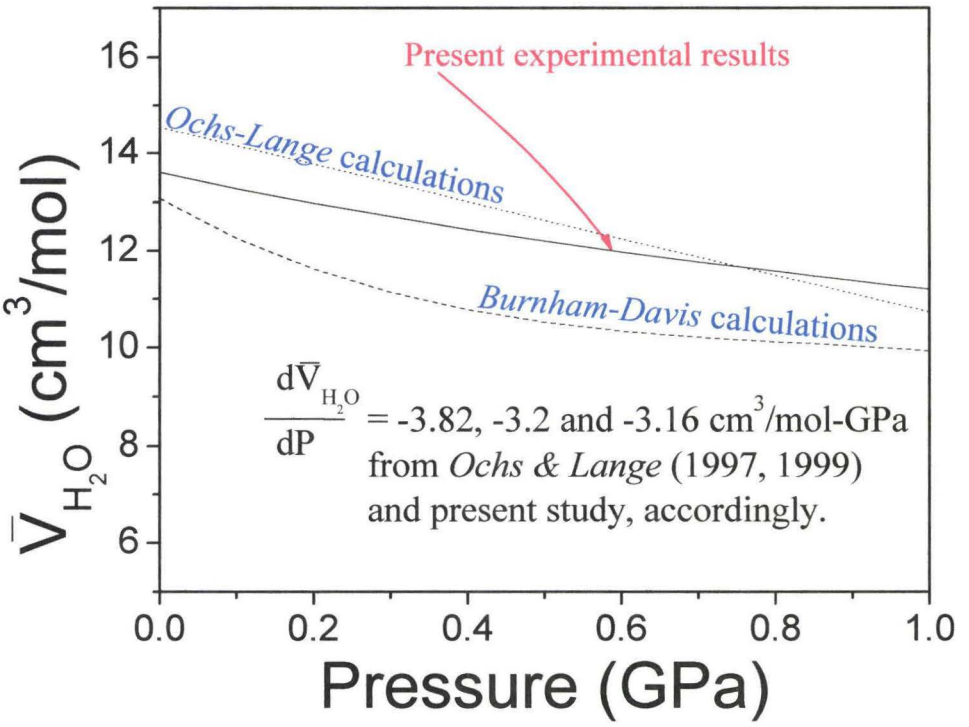

Figure 3.15.

Pressure dependence of $\bar{V}_{H_2O}$ in the hydrated Na_2O-$2SiO_2$ liquid formed upon decompression melting at 457 K. Solid line is present study (maximum error in calculations does not exceed ±1.5 %). Dotted and dashed lines are the interpolations of the model equation for hydrous silicate liquids [*Ochs and Lange,* 1997] and the empirical P-$\bar{V}_{H_2O}$-T EOS [*Burnham and Davis*, 1971] down to 457 K, respectively (measured molar volumes can be recovered with a standard deviation of 0.5 %).

dependence of $\overline{V}_{H_2O}$ agrees well with the earlier reported values [*Ochs and Lange,* 1997, 1999], and the combination of Equation 3.4.1 with our density data (Fig. 3.8) produces a monotonic trend at higher pressures, the extrapolation (Fig. 3.16) of the model equation and the empirical EOS at pressures higher than 1 GPa and low temperatures produce peculiar functional forms and/or zero partial molar volumes for water in silicate melts. Accordingly, we view high temperature and pressure Brillouin experiments as ultimately being perhaps the most viable mechanism for establishing the partial molar volume of water at the pressure conditions of the shallow upper mantle. While we do not view our derived pressure dependence of the partial molar volume of water (Fig. 3.16) as definitive, we believe that it provides a starting point for the assessment of the partial molar volume of water at upper mantle depths, and the temperatures associated with shallow subducted material.

The glass transition temperature (T_g) inferred from the present Brillouin scattering measurements of the hydrous liquid and glass (Fig. 3.11) at high pressure lies within the boundaries of trends of total water content vs T_g for glasses of rhyolitic [*Sowerby and Keppler*, 1999], haplogranitic and albitic [*Shen and Keppler*, 1995; *Dingwell*, 1998] chemistries. The experimentally determined value of T_g of 483 K at a pressure of 8.1 GPa is strikingly close to the T_g of 466 K calculated for hydrous sodium disilicate system using expression $T_g = 1059 - 83.47\ln(c_w)$, where c_w is the water concentration in wt.% [*Dingwell*, 1998]. This excellent agreement supports the idea originally proposed for the felsic melts that the effect of hydration on the glass transition is largely independent of composition [*Sowerby and Keppler*, 1999].

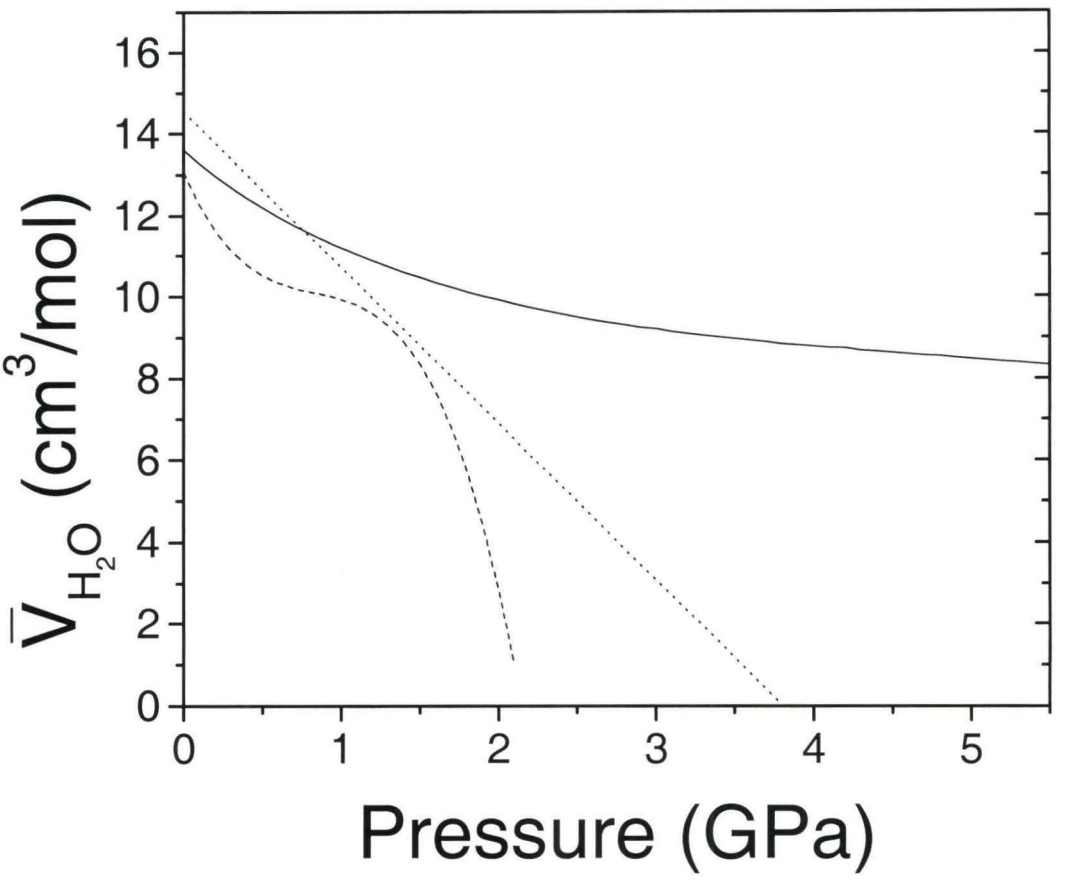

Figure 3.16.

Extended pressure dependence of $\bar{V}_{H_2O}$ in the hydrated Na_2O-$2SiO_2$ liquid formed upon decompression melting at 457 K. Solid line is present study (maximum error in calculations does not exceed ±1.5 %). Dotted and dashed lines are the interpolations of the model equation for hydrous silicate liquids [*Ochs and Lange,* 1997] and the empirical P-$\bar{V}_{H_2O}$-T EOS [*Burnham and Davis*, 1971] down to 457 K, respectively (measured molar volumes can be recovered with a standard deviation of 0.5 %).

The relative importance of water-rich fluids relative to mildly hydrated silicate melts for volatile transport within subduction zones remains uncertain. While such liquids are fully miscible at high pressure and temperature conditions, both the amount of water present and perhaps the wetting/rheologic behavior of the fluid would differ markedly between a comparatively refractory silica-rich liquid and a water-dominated liquid. Indeed, partially molten (and likely hydrated) zones have been seismically inferred to exist at depths between 300 and 400 km [*Revenaugh and Sipkin,* 1994; *Nolet and Zielhuis,* 1994]. Our results demonstrate that the densities and bulk moduli accessed by even a 46 wt% (or 74 mol%) water solution at modest pressures far more closely resemble those of a silicate liquid than those of low pressure water (Figs. 3.6, 3.8). Silicate melts generally have bulk moduli that lie in the 15-25 GPa range [*Rivers and Carmichael,* 1987; *Secco et al.,* 1991], while liquid water at ambient pressure has a bulk modulus less than 2 GPa [*Shimizu et al.,* 1996b]. For comparison, estimates of the bulk modulus of the water component in silicate liquids containing up to 6 wt% water lie near 6 GPa [*Ochs and Lange,* 1997]. Our data show that (at least at modest temperatures), the bulk modulus of a 74 mol% water sodium silicate aqueous solution is near 9 GPa, and increases markedly with compression. Indeed, an extrapolation of the trends in Figure 3.8 implies that under the pressure conditions of the deep upper mantle (10-13 GPa), this aqueous solution will have a bulk modulus of ~100 GPa and a density near 2.8 g/cm^3: values approaching those of a silicate liquid under these conditions. Accordingly, we hypothesize that the seismic signature of a region containing a water-rich fluid may be effectively indistinguishable from that of a partially molten zone with a (nearly anhydrous) silicate liquid.

3.5 CONCLUSIONS

Brillouin spectroscopy using the "modified" platelet scattering geometry can be successfully applied to molten silicate systems at high pressure and temperature conditions. The glass transitions in these systems is manifested by a shift in the pressure derivatives of the sound velocities, and are likely associated with the complete onset of the spectrum of relaxational mechanisms at Brillouin frequencies. This criterion for determining the glass transition temperature produces values in close accord with those inferred from other, longer time-scale probes. Our data allow not only the elastic properties of hydrous and anhydrous sodium silicate liquids to be determined at simultaneous high pressures and temperatures, but also can be used to model the partial molar volume of water in silicate liquids at high pressures. We find that water-rich fluids at deep upper mantle depths may have elastic properties far more similar to those of anhydrous silicate liquids than at low pressure conditions. Thus, while the precise temperature dependence of the density and elasticity of aqueous fluids under the comparatively hot conditions of ambient mantle remains to be determined, our reconnaissance results demonstrate the utility of Brillouin spectroscopy coupled with the externally heated diamond anvil cell in characterizing the elastic behavior of hot, compressed liquid systems.

3.6 FUTURE DIRECTIONS

As a short-term commitment, we plan to perform the Brillouin scattering

measurements of sodium silicate liquids to 600 °C (1000 °C is feasible to achieve if the cubic zirconia anvils are used; the tradeoff is the lower pressure range and increased amount of breakage of such anvils) and ~ 10 GPa in the externally heated DAC. Liquid silicates with the following set of silica-to-alkali weight ratios and viscosities: 3.25 (viscosity: 0.83 Pa·s); 3.22 (viscosity: 0.18 Pa·s); 2.88 (viscosity: 0.96 Pa·s); 2.4 (viscosity: 2.1 Pa·s); 2.00 (viscosity: 0.4 Pa·s); 1.60 (viscosity: 0.28 Pa·s) and the corresponding anhydrous sodium silicates – will be studied in addition to the samples with 2.00 (viscosity: 70 Pa·s) silica-to-alkali weight ratio and the corresponding water-free glass and melt that are already under investigation. The elastic and relaxation properties obtained from the Brillouin measurements will be correlated with Raman spectroscopic data that constrain the degree of polymerization of the liquids. Our goal is to produce a correlation between high pressure elasticity/density and pressure-induced shifts in melt polymerization. Brillouin light scattering results obtained in the "modified" platelet scattering geometry will be verified by the Brillouin measurements at lower pressures up to 2.5 GPa and 1000 °C in the newly designed for symmetric 90^0-scattering geometry DAC (based on hydrothermal DAC [*Bassett*, 2003]) that allows to carry out the experiments in the conventional platelet geometry [e.g., *Tkachev and Bass*, 1996]. The P-T dependences of elasticity and density measured in liquids will be used as analogs for density and elasticity changes in silicate melts at pressures and temperatures of the Earth's lower crust and upper mantle.

Our goals also include measurements of sound velocity in potassium silicate liquids at high T and P of internally heated DAC by Brillouin light scattering. Again, silica-to-alkali weight ratios and water content will be varied and Brillouin data will be

correlated with Raman spectroscopy measurements in order to assess the effect of the degree of polymerization and composition on viscous and elastic properties of silicate liquids under extreme conditions of the Earth's interior. In fact, we have already made an initial effort in the direction of extending our research towards other compositions of silicate liquids by performing Brillouin light scattering measurements at moderate pressures of two sodium silicate solutions with different $Ca(OH)_2$ concentrations [*Phair et al.*, 2004]. The data on sodium silicate liquids will be compared with data on potassium silicates and, if necessary, custom made compositions of silicate liquids with Li oxide network modifiers will be utilized for further Brillouin and Raman measurements. The final data will be directly applied to constrain structural and elastic changes in properties that natural melts are likely to undergo at high pressures.

We recognize that this suite of studies involves an ambitious research plan, which holds the prospect of providing an unprecedented data set of the elasticity of melts at high pressures and temperatures. The compositions, which we have chosen to date, are those that we are confident will undergo major structural changes under pressure, which are readily interpretable from a chemical and microstructural viewpoint using Raman spectroscopy. Examining melts, which have greater chemical complexity and incorporate volatile constituents, are a long-term goal of this set of studies.

Measurements on these materials may be conducted toward the end of this sequence of studies designed to illuminate the microstructural systematics of melt elasticity at pressure, likely utilizing a combination of chemistry and pressure to tune the structure of the melt, while probing its elastic response. Additionally, we recognize that the ultimate goal of such studies is to conduct measurements on actual molten natural

magma compositions at high pressures and temperatures: because of the high temperatures required to access the liquidus of most mafic magmas, we view such studies as demanding a new generation of measurements which couple diamond anvil-cell laser-heating with Brillouin spectroscopy: we believe that our proposed studies provide a logical (and completely necessary) step towards this ultimate goal of studies of melt elasticity.

APPENDIX

Selected answers (A) to some reviewers' critique (Q)

Q1. One question is the use of the term glass transition, with regard to the solidification of the sodium silicate solution. Historically, the term glass transition is used to refer to the transition in a solid from a glass to a higher temperature supercooled liquid in which the structural configuration can easily change. This is still the most common way in which the term is used.

A1. The glass transition as we use it in the context of our sodium silicate solution reflects the transition from a supercooled liquid to a glass through compression: the glass transition is, from a thermodynamic perspective, a second-order transition from a liquid to an amorphous solid (or vice versa). That we encounter this transition on compression is a natural consequence of a positive Clapeyron slope of this transition. There is thus no contradiction in the usage of the term "glass transition" at pressures other than ambient, because pressure only adds another degree of freedom to the system and does not change the physical meaning of the glass transition itself. Accordingly, we believe that our usage of this term is thermochemically correct. Our usage is also in accord with the chemical physics literature, as shown by *Takagi et al.* [1997] (including in their title – referenced in the text of the dissertation), who observe a glass transition in propanol at ambient temperature and ~5 GPa.

Q2. There is an observation of a change in some properties at high pressure, which is interpreted as a transition to an amorphous solid, and that is probably fine. It is referred to

as a glass transition, but it may be very different from the usual sense of a glass transition.

A2. Transition from a liquid to a crystalline state and vice versa are typically associated with a discontinuity in sound velocities at the transition pressure/temperature. We observe only bending points (changes in slope), that are usually characteristic of transitions between amorphous states. Finally, the Brillouin spectra above Tg, are noticeably broader than below Tg, which is one of the confirmations that glass exists below Tg.

Q3. It is true that the "glass" material transmits shear waves, but *Grimsditch et al.*, [1989] has shown that shear waves can be seen in this frequency range even above the melting point. Is what they are observing a glass transition, or a freezing point?

A3. The freezing point is associated with a first order phase transition, which is characterized by discontinuities in pressure or/and temperature dependencies of density and sound velocity. It is also associated with sample crystallinity. Our results demonstrate that there are no discrete jumps in pressure dependencies of sound velocities during the transition from one state to another; neither are there crystals; therefore, the concept of "freezing point" is not valid in our case, and we believe that the evidence is unambiguous that we are observing the glass transition.

Q4. In Figure 3.5, it seems clear that V_S show a different glass transition pressure (about .7 GPa) than V_P or nV_P. These glass transition pressures differ by about a factor of two! This deserves some comment. In terms of density, there is no glass transition at 1.3 GPa (Fig.3.6).

A4. There is an apparent "hump" in Vs values and the explanation is now given in the caption to Figure 3.5 — the simple observation is, as Figure 3.1a shows, that the shear peak is broad and weak, and is thus far more subject to possible errors than V_P. Additionally, as a second order transition, we do not expect to see a change in density at the glass transition; only a shift in its pressure dependence. The latter shows up in both the sound velocity and bulk modulus. Accordingly, density is not very sensitive to the glass transition, and it is not surprising that Figure 3.6 does not have a clear cut bending point in density.

Q5. Figure 3.7 is very interesting. It shows that V_P changes FASTER with pressure in the solid, than it does in the liquid! Wouldn't one expect the liquid to change more rapidly with pressure? Does this contradict the solid versus liquid behavior of K' discussed earlier in the text? This should be addressed. It is either a very interesting physical phenomenon or an error in the data.

A5. The errors in Brillouin spectroscopy measurements do not exceed the sizes of the symbols, so errors are not a potential cause of the trend mentioned above. We believe that the relevant parameter to consider is dV_P/V_P here, which is roughly comparable between

solid and liquid. Nevertheless, we believe this trend may have a straightforward (although speculative) physical explanation, associated with a coordination transformation of silicon within the solid. Characterizing this phenomenon would require Raman experiments at these conditions, as well. These unique experiments are currently in progress, and we hope to fully address this intriguing question in the nearest future.

Q6. It has been asserted that "the notably higher K_S' of the fluid is consistent with the liquid being able to access a wider range of compression mechanisms, thus illustrating..." This is an interesting idea but is it possible to provide some other examples to give some credibility to this argument?

A6. It is an interesting idea. However, it is certainly not new. It was discussed over 17 years ago by one of the collaborators [e.g., *Williams and Jeanloz*, 1988], and formed a basis for interpreting the well-publicized shock experiments on silicate liquids [*Stolper and Ahrens*, 1987]. There are a number of other examples as well, but the fact is that this argument is quite well-precedented; it also makes simple physical sense. We could include copious references, but this argument is really routine at this stage.

Q7. Does it make sense speculating on the existence of a first or second order transition in a system which is not fully equilibrated?

A7. The ability of thermodynamics to treat metastable phases is well-documented, in a broad suite of studies that spans from thermodynamic measurements of thin films to ceramics (as exemplified by the cement literature) to the enormous literature on the

thermodynamics of amorphous solids at ambient or near-ambient pressures. This comment seems to imply that one should only thermodynamically examine phases that have the lowest Gibbs Free Energy (and thus are "fully equilibrated") - which, were we to take it to its logical extreme, indicates that if one wanted to apply thermodynamics to our system (or any amorphous or metastable system), we should just simply crystallize/equilibrate our samples and be done with them. In short, the fact that a phase is metastable (or "non-equilibrium") in no way or form obviates the ability to apply thermodynamics to that phase. This is not to say that amorphous-amorphous transitions (in ice, silicate glass, or otherwise) must be correlated with liquid-liquid transitions; nor that they need to occupy the same portion of the potential energy landscape as the liquid; nor that the time-scales/sample history might play a role in the structural state of the glass; nor that a continuum of (amorphous) structural states might not exist [*Giovambattista et al.*, 2003]. Rather, irrespective of metastability or degree of equilibration, the thermodynamic state of a sample may be specified, and the response to Q7 is thus a resounding "yes".

The underlying subtext of this response to the reviewer's query is important: the recognition that apparent pressure-induced first-order transitions can occur within amorphous/out-of-equilibrium materials (as first described by *Mishima et al.*, [1985]) inspired extensive theoretical and experimental follow-ups and interest (and 312 citations to date in the ISI index). We view our present work documenting apparent pressure-induced second-order transitions in amorphous materials as being of comparable interest to the previous documentations of first-order amorphous-amorphous (and not fully equilibrated) transitions. So, irrespective of our arguments in the paragraph above, the

reviewer's query, on which much of his/her first comment is based, has already been abundantly answered within the current literature of the field.

Q8. The self-contradictory phrase "this pressure-induced second order transition does share characteristics with the glass transition" shows the weak point of the present work. In fact the liquid-glass transition, similar to the glass-glass transition here observed in float glass, is an out-of-equilibrium process and, for this reason, it cannot be recognized either as a first or a second order phase transition.

A8. We disagree, and believe that the entire quote should have been used: "The likely second order transformation we document here is CLEARLY DISTINCT from the well-known thermally activated second-order glass transition. However, this pressure-induced second order transition does share characteristics with the glass transition: it is associated with the glass accessing a different (and, in this instance) pressure-activated set of structural environments...". The full quote exemplifies the disagreement that the reviewer has with our study: our description of the glass transition as second-order. The reviewer is correct that this has been a topic of extensive discussion: from a phenomenological standpoint, the near-universal smeared discontinuities in second-order thermodynamic properties have led a wide suite of investigators, from *Gibbs and DiMarzio* [1958] on to Richard Zallen in his text "The Physics of Amorphous Solids" [1983] to describe the liquid -glass transition as (Zallen's description, p. 19) "an apparent, diffuse, second order transition." More recently, *Nieuwenhuizen* [1997; 2000] has documented that the Ehrenfest relations, when correctly formulated, are satisfied for the best-documented

glass-liquid transitions (and thus that the transition satisfies the thermodynamic criteria for a second order transition). It is with such studies in mind that we referred to the liquid-glass transition as second order.

REFERENCES

Agee, C. B., and D. Walker, Static compression and olivine flotation in ultrabasic silicate liquid, *J. Geophys. Res., 93*, 3437-3449, 1988.

Agee, C. B., Isothermal compression of molten Fe_2SiO_4, *Geophys. Res. Lett., 19*, 1169-1172, 1992a.

Agee, C. B., Thermal expansion of molten Fe_2SiO_4 at high pressure, *Geophys. Res. Lett., 19*, 1173-1176, 1992b.

Agee, C. B., Crystal-liquid density inversions in terrestrial and lunar magmas, *Phys. Earth Planet. Inter., 107*, 63-74, 1998.

Almeida, R. M., and C. G. Pantano, Structural investigation of silica gel films by infrared spectroscopy, *J. App. Phys., 68*, 4225-4232, 1990.

Angell, C. A., P. A. Cheeseman, and S. Tamaddon, Pressure enhancement of ion mobilities in liquid silicates from computer-simulated studies to 800-kilobars, *Science, 218*, 885-887, 1982.

Angell, C. A., Liquid fragility and the glass transition in water and aqueous solutions, *Chem. Rev., 102*, 2627, doi:10.1021/cr000689q, 2002.

Askarpour V., M. H. Manghnani, S. Fassbender, and A. Yoneda, Elasticity of single-crystal $MgAl_2O_4$ spinel up to 1273 K by Brillouin spectroscopy, *Phys. Chem. Miner. 19*, 511-519, 1993.

Askarpour V., and M. H. Manghnani, Elastic properties of breakaway glass and liquid by Brillouin scattering up to 170 ^{0}C, *J. Appl. Phys., 75*, 675-677, 1994.

Bass, J. L., and G. L. Turner, Anion distributions in sodium silicate solutions.

Characterization by ^{29}Si NMR and infrared spectroscopies, and vapor phase osmometry, *J. Phys. Chem. B, 101*, 10638-10644, 1997.

Bassett, W.A., High pressure-temperature aqueous systems in the hydrothermal diamond anvil cell (HDAC), *Eur. J. Mineral., 15*, 773-780, 2003.

Benedek, G. B., and K. Fritsch, Brillouin scattering in cubic crystals, *Phys. Rev. 149*, 647-662, 1966.

Boehler, R., and G. C. Kennedy, Pressure dependence of the thermodynamical Gruneisen parameter of fluids, *J. Appl. Phys., 48(10)*, 4183-4186, 1977.

Bridgman, P.W., Thermodynamic properties of liquid water to 80^{o} and 12000 kgm, *Proc. Am. Acad. Arts Sci., 48*, 307-362, 1913.

Brown, J. M., L. J. Slutsky, K. A. Nelson, and L.-T. Cheng, Velocity of sound and equations of state for methanol and ethanol in a diamond-anvil cell *Science, 241*, 65-67, 1988.

Brückner, R., Properties and structure of vitreous silica. I, *J. Non-Cryst. Solids 5*, 123-175, 1970, Properties and structure of vitreous silica. II, *J. Non-Cryst. Solids 5*, 177-216, 1971.

Bryce J. G., F. J. Spera, and D. J. Stein, Dependence of self diffusivity on P and T in molten $NaAlSi_2O_6$: Comparison of laboratory and molecular dynamics experiments, *Geophys. Res. Lett., 24,* 711-714, 1997.

Burnham, C. W., and N. F. Davis, The role of H_2O in silicate melts I. P-V-T relations in the system $NaAlSi_3O_8$-H_2O to 10 kilobars and $1000^{0}C$, *Am. J. Sci., 270*, 54-79, 1971.

Chen, C.-T., R. A. Fine, and F. J. Millero, The equation of state of pure water determined

from sound speeds, *J. Chem. Phys., 66*, 2142-2144, 1977.

Chmel, A., E. K. Mazurina, and V. S. Shashkin, Vibrational spectra and defect structure of silica prepared by non-organic sol-gel process, *J. Non-Cryst. Solids, 122*, 285-290, 1990.

Circone, S., and C. B. Agee, Compressibility of molten high-Ti mare glass - evidence for crystal-liquid density inversions in the lunar mantle, *Geochim. Cosmochim. Acta, 60*, 2709-2720, 1996.

Cohen, M. H., and G. S. Grest, Liquid-glass transition, free-volume approach, *Phys. Rev. B 20*, 1077-1098, 1979.

Crowhurst, J. C., G. R. Hearne, J. D. Comins, A. G. Every, and P. R. Stoddart, Surface Brillouin scattering from opaque materials at high pressure in *Science and Technology of High Pressure*, Proceedings of the International Conference on High Pressure Science and Technology (AIRAPT-17), edited by M. H. Manghnani, W. J. Nellis and M. F. Nicol, V. 1, pp. 43-46, Universities Press, Hyderabad, India, 2000.

Diefenbacher J., P. F. McMillan, and G. H. Wolf, Molecular dynamics simulations of $Na_2Si_4O_9$ liquid at high pressure, *J. Phys. Chem. B, 102*, 3003-3008, 1998.

Dingwell, D. B., The glass transition in hydrous granitic melts, *Phys. Earth Planet. Inter., 107*, 1-8, 1998.

Döring K., S. Rau, G. Weiss, J. Arndt, and S. Hunklinger, Brillouin scattering of compacted vitreous silica, *Phys. Lett. A 184*, 464-466, 1994.

El'kin, F. S., V. V. Brazhkin, L. G. Khvostantsev, O. B. Tsiok, and A. G. Lyapin, In situ study of the mechanism of formation of pressure-densified SiO_2 glasses,

JETP Lett., 75, 342, doi: 0021-3640/02/7507-0342, 2002.

Fabelinskii, I. L., *Molecular scattering of light*, Plenum Press, New York, 1968.

Farber, D. L., and Q. Williams, An in situ Raman spectroscopic study of $Na_2Si_2O_5$ at high pressures and temperatures: structures of compressed liquids and glasses, *Amer. Min., 81*, 273-283, 1996.

Fine, R. A., and F. J. Millero, Compressibility of water as a function of temperature and pressure, *J. Chem. Phys., 59*, 5529-5536, 1973.

Fleet, M. E., and G. S. Henderson, Structure-composition relations and Raman spectroscopy of high-pressure sodium silicates, *Phys. Chem. Minerals, 24*, 345-355, 1997.

Gaboriaud, F., A. Nonat, D. Chaumont, and A. Craievich, Aggregation and gel formation in basic silico-calco-alkaline solutions studied: A SAXS, SANS, and ELS study, *J. Phys. Chem. B, 103*, 5775-5781, 1999.

Gaboriaud, F., A. Nonat, D. Chaumont, and A. Craievich, Aggregation processes and formation of silico-calco-alkaline gels under high ionic strength, *J. Colloid Interf. Sci., 253*, 140-149, doi: 10.1006/jcis.2002.8522, 2002.

Gibbs, J. H., and E. A. DiMarzio, Nature of the glass transition and the glassy state, *J. Chem. Phys.*, 28, 373-383, 1958.

Giovambattista, N., H. E. Stanley, and F. Sciortino, Potential-energy landscape study of the amorphous-amorphous transformation in H_2O, *Phys. Rev. Lett. 91*, 115504, 2003.

Grimsditch, M., Polymorphism in amorphous SiO_2, *Phys. Rev. Lett. 52*, 2379-2381, 1984.

Grimsditch, M., Annealing and relaxation in the high-pressure phase of amorphous SiO_2,

Phys. Rev. B 34, 4372-4373, 1986.

Grimsditch, M., R. Bhadra, and L. M. Torell, Shear waves through the glass-liquid transformation, *Phys. Rev. Lett., 62*, 2616-2619, 1989.

Grimsditch, M., S. Popova, and A. Polian, Test of the equation of state of water up to freezing at 100 and 200^{0}C, *J. Chem. Phys., 105(19)*, 8801-8803, 1996.

Grimsditch, M., in *Handbook of Elastic Properties of Solids, Liquids, and Gases. Volume I: Dynamic Methods for Measuring the Elastic Properties of Solids*, edited by M. Levy, H. Bass, R. Stern, and V. Keppens, V. I, p. 331, Academic Press, New York, 2001.

Gromnitskaya, E. L., O. V. Stal'gorova, V. V. Brazhkin, and A. G. Lyapin, Ultrasonic study of the nonequilibrium pressure-temperature diagram of H_2O, *Phys. Rev. B 64*, 094205, doi: 10.1103/PhysRevB.64.094205, 2001

Halalay, I. C., and K. A. Nelson, The liquid-glass transition in $LiCl/H_2O$: Impulsive stimulated light scattering experiments and mode-coupling analysis, *J. Chem. Phys., 97,* 3557- 3572, 1992.

Hemley, R. J., H. K. Mao, P. M. Bell, and B. O. Mysen, Raman-spectroscopy of SiO_2 glass at high-pressure, *Phys. Rev. Lett., 57*, 747-750, 1986.

Herzfeld, K. F., and T. A. Litovitz, *Absorption and Dispersion of Ultrasonic Waves,* Academic, New York, 1959.

Heydemann, P. L. M., and J. C. Houck, Self-consistent ultrasonic method for the determination of the equation of state of liquids at very high pressures, *J. Appl. Phys., 40,* 1609-1613, 1969.

Hilbert, R., K. Todheide, and E. U. Franck, PVT data for water in the ranges 20 to 600^{0}C

and 100 to 4000 bar, *Ber. Bunsenges. Phys. Chem., 85*, 636-643, 1981.

Holmquist, T. J., G. R. Johnson, D. E. Grady, G. M. Lopatin, and E. S. Hertel Jr., High Strain Rate Properties and Constitutive Modeling of Glass, *Proceedings of the 15th International Symposium on Ballistics, Jerusalem, Israel, May 1995.*

Holton, G., M. P. Hagelberg, S. Kao, and W. H. Johnson, Jr., Ultrasonic-velocity measurements in water at pressures to 10 000 kg/cm^2, *J. Acoust. Soc. Am., 43(1)*, 102-107, 1968.

Huang, L. P., and J. Kieffer, Amorphous-amorphous transitions in silica glass. I. Reversible transitions and thermomechanical anomalies, *Phys. Rev. B 69*, 224203, doi: 10.1103/PhysRevB.69.224203; Amorphous-amorphous transitions in silica glass. II. Irreversible transitions and densification limit, *Phys. Rev. B 69*, 224204, doi: 10.1103/PhysRevB.69.22403, 2004.

Hughes, T. L., C. M. Methven, T. G. J. Jones, S. E. Pelham, and P. Franklin, The use of Fourier transform infrared spectroscopy to characterize cement poders, cement hydration and the role of additives, *Spec. Pub. R. Soc. Chem., 159*, 99-115, 1994.

Jayaraman, A., Diamond anvil cell and high-pressure physical investigations, *Rev. Mod. Phys., 55*, 65-108, 1983.

Jeanloz, R., Thermodynamics and evolution of the Earth's interior: high-pressure melting of silicate perovskite as an example, *Proceedings of the Gibbs Symposium*, Yale University, 1989.

Kanno, H., and C. A. Angell, Homogeneous nucleation and glass formation in aqueous alkali halide solutions at high pressures, *J. Phys. Chem., 81*, 2639-2643, 1977.

Kanno, H., Double glass transition in aqueous lithium-chloride solutions vitrified at

high-pressures – evidence for a liquid-liquid immiscibility, *J. Phys. Chem., 91*, 1967-1971, 1987.

Kohn, S. C., The dissolution mechanisms of water in silicate melts; a synthesis of recent data, *Miner. Mag., 64*, 389-408, 2000.

Kress, V. C., Q. Williams, and I. S. E. Carmichael, Ultrasonic investigation of melts in the system Na_2O-Al_2O_3-SiO_2, *Geochim. Cosmochim. Acta, 52*, 283-293, 1988.

Kress, V. C., Q. Williams, and I. S. E. Carmichael, When is a silicate melt not a liquid?, *Geochim. Cosmochim. Acta, 53*, 1687-1692, 1989.

Krisch, M., P. Loubeyre, G. Ruocco, F. Sette, A. Cunsolo, M. D'Astuto, R. LeToullec, M. Lorenzen, A. Mermet, G. Monaco, and R. Verbeni, Pressure evolution of the high-frequency sound velocity in liquid water, *Phys. Rev. Lett., 89,* 125502 (4 pages), 2002.

Krüger, J. K., J. Embs, J. Brierley, and R. Jiménez, Brillouin scattering technique for the investigation of acoustic and opto-acoustic properties: application to polymers, *J. Phys. D: Appl. Phys., 31*, 1913-1917, 1998.

Lacks, D. J., Localized mechanical instabilities and structural transformations in silica glass under high pressure, *Phys. Rev. Lett. 80*, 5385-5388, 1998.

Lange, R. L., and I. S. E. Carmichael, Densities of Na_2O-K_2O-CaO-MgO-FeO-Fe_2O_3-Al_2O_2-SiO_2-TiO_2 liquids: new measurements and derived partial molar properties, *Geochim. Cosmochim. Acta, 51*, 2931-2946, 1987.

Lange, R. L., and I. S. E. Carmichael, Thermodynamic properties of silicate liquids with emphasis on density, thermal expansion and compressibility, *Rev. Mineral., 1*, 25-64, 1991.

Li, F. Y., S. S. Fu, R. J. Wang, and M. H. Manghnani, Elastic properties of float glass and $SiO_2 + TiO_2$ glass under high pressure (in Chinese), *Acta Phys. Sin. 49*, 2129-2132, 2000.

Litovitz, T. A., and E. H. Carnevale, Effect of pressure on sound propagation in water, *J. Appl. Phys., 26*, 816-820, 1955.

Manghnani, M. H., Role of silica content in the anomalous elastic behavior of silicate glasses under pressure, *Bull. Am. Ceram. Soc. 48*, 434, 1969.

Manghnani, M. H., and W. M. Benzing, Pressure derivatives of elastic moduli of Vycor glass to 8 kbar, *J. Phys. Chem. Solids 30*, 2241-2245, 1969.

Manghnani M. H., Y. Wang, F. Li, P. Zinin, and W. Rafaniello, Elastic and vibrational properties of B_4C to 21 GPa, in *Science and Technology of High Pressure*, Proceedings of the International Conference on High Pressure Science and Technology (AIRAPT-17), edited by M. H. Manghnani, W. J. Nellis and M. F. Nicol, V. 2, pp. 945-948, Universities Press, Hyderabad, India, 2000.

Marinangeli, A., M. A. Morelli, R. Simoni, and A. Bertoluzza, A Raman and infrared study of aqueous solutions of sodium silicates as a function of pH, *Canad. J. Spectrosc., 23*, 173-177, 1978.

Masnik, J. E., J. Kieffer, and J. D. Bass, Structural relaxations in alkali silicate systems by Brillouin light scattering, *J. Am. Ceram. Soc., 76,* 3073-3080, 1993.

Matsui, M., Molecular dynamics simulation of structures, bulk moduli, and volume thermal expansivities of silicate liquids in the system $CaO-MgO-Al_2O_3-SiO_2$, *Geophys. Res. Lett., 23*, 395-398, 1996.

Meade, C., and R. Jeanloz, Frequency-dependent equation of state of fused silica to 10

GPa, *Phys. Rev. B 35*, 236-244, 1987.

Meade, C., and R. Jeanloz, Effect of a coordination change on the strength of amorphous SiO_2, *Science 241*, 1072-1074, 1988.

Meade, C., R. J. Hemley, and H. K. Mao, High-pressure X-ray diffraction of SiO_2 glass, *Phys. Rev. Lett. 69,* 1387-1390, 1992.

Merrill, L., and W. A. Bassett, Miniature diamond anvil pressure cell for single crystal X-ray diffraction studies, *Rev. Sci. Instrum., 45(2)*, pp. 290-294, 1974.

Miller, G. H., E. M. Stolper and T. J. Ahrens, The equation of state of a molten komatiite. I. Shock wave compression to 36 GPa, *J. Geophys. Res., 96*, 11831-11848, 1991.

Ming, L. C., M. H. Manghnani, and J. Balogh, Resistive heating in the diamond-anvil cell under vacuum conditions, in *High-Pressure Research in Mineral Physics*, edited by M. H. Manghnani and Y. Syono, pp. 69-74, Terra Scientific Publishing Company, Tokyo / American Geophysical Union, Washington, D.C., 1987.

Mishima, O., L. D. Calvert, and E. Whalley, An apparently first-order transition between two amorphous phases of ice induced by pressure, *Nature 314*, 76-78, 1985.

Mishima O., and H. E. Stanley, The relationship between liquid, supercooled and glassy water, *Nature, 396*, 329-335, 1998a.

Mishima O., and H. E. Stanley, Decompression-induced melting of ice IV and the liquid-liquid transition in water, *Nature, 392*, 164-168, 1998b.

Morgan, N. A., and F. J. Spera, A molecular dynamics study of the glass transition in $CaAl_2Si_2O_8$: Thermodynamics and tracer diffusion, *Amer. Min., 86*, 915-926, 2001a.

Morgan, N. A., and F. J. Spera, Glass transition, structural relaxation, and theories of

viscosity: A molecular dynamics study of amorphous $CaAl_2Si_2O_8$, *Geochim. Cosmochim. Acta, 65*, 4019-4041, 2001b.

Mountain, R. D., Spectral distribution of scattered light in a simple fluid, *Rev. Mod. Phys., 38*, 205-214, 1966.

Mysen, B. O., D. Virgo, and F. A. Seifert, The structure of silicate melts: implications for chemical and physical properties of natural magma, *Rev. Geophys., 20*, 353-383, 1982.

Mysen, B. O., Relationship between silicate melt structure and petrological processes, *Earth-Sci. Rev., 27*, 281-365, 1990.

Mysen, B. O., and M. Acton, Water in H_2O-saturated magma-fluid systems: Solubility behavior in K_2O-Al_2O_3-SiO_2-H_2O to 2.0 GPa and 1300^0C, Geochim. Cosmochim. Acta, 63, 3799-3815, 1999.

Mysen, B. O., and K. Wheeler, Solubility behavior of water in haploandesitic melts at high pressure and high temperature, *Amer. Min., 85*, 1128-1142, 2000.

Mysen, B., Water in peralkaline aluminosilicate melts to 2 GPa and 1400^0C, *Geochim. Cosmochim. Acta,66*, 2915-2928, 2002.

Nevins, D., and F. J. Spera, Molecular dynamics simulations of molten $CaAl_2Si_2O_8$: Dependence of structure and properties at pressure, *Amer. Min., 83*, 1220-1230, 1998.

Nieuwenhuizen, Th. M., Ehrenfest relations at the glass transition: solution to an old paradox, *Phys. Rev. Lett., 79*, 1317-1320, 1997.

Nieuwenhuizen, Th. M., Thermodynamic picture of the glassy state, *J. Phys.: Condens. Matter, 12*, 6543-6552, 2000.

Nolet, G., and A. Zielhuis, Low S velocities under the Tornquist-Teisseyeare zone: Evidence for water injection into the transition zone by subduction, *J. Geophys. Res., 99,* 15813-15820, 1994.

Ochs, F. A. III, and R. A. Lange, The partial molar volume, thermal expansivity and compressibility of H_2O in $NaAlSi_3O_8$ liquid: New measurements and an internally consistent model, *Contrib. Mineral. Petrol., 129,* 155-165, 1997.

Ochs, F. A. III, and R. A. Lange, The density of hydrous magmatic liquids, *Science, 283,* 1314-1317, 1999.

Oliver, W. F., C. A. Herbst, S. M. Lindsay, and G. H. Wolf, High-pressure viscoelastic properties and equation of state of liquids derived from Brillouin data, Phys. Rev. Lett., 67, 2795-2798, 1991.

Oliver, W. F., C. A. Herbst, S. M. Lindsay, and G. H. Wolf, A general method for determination of Brillouin linewidths by correction for instrumental effects and aperture broadening: Application to high-pressure diamond anvil cell experiments, *Rev. Sci. Instrum., 63*, 1884-1895, 1992.

Ortego, J. D., Y. Barroeta, F. K. Cartledge, and H. Akhter, Leaching effects on silicate polymerization. An FTIR and ^{29}Si NMR study of lead and zinc in Portland cement, *Environ. Sci. Technol., 25*, 1171-1174, 1991.

Phair, J. W., S. N. Tkachev, M. H. Manghnani, and R. A. Livingston, Elastic and structural properties of alkaline-calcium silica hydrogels, *J. Mater. Res., 20*, 344-349, 2005.

Piermarini, G. J., and S. Block, Ultrahigh pressure diamond-anvil cell and several semiconductor phase transition pressures in relation to the fixed point pressure

scale, *Rev. Sci. Instrum., 46(8)*, 973-979, 1975.

Piermarini, G. J., S. Block, J. D. Barnett, and R. A. Forman, Calibration of the pressure dependence of the R1 ruby fluorescence line to 195 kbar, *J. Appl. Phys., 46*, 2774-2780, 1975.

Pinnow, D. A., S. J. Candau, J. T. LaMacchia and T. A. Litovitz, Brillouin scattering: Viscoelastic measurements in liquids, *J. Acoust. Soc. Am., 43*, 131-142, 1967.

Pistorius, C. W. F. T., E. Rapoport, and J. B. Clark, Phase diagram of H_2O and D_2O at high pressures, *J. Chem. Phys., 48(12)*, pp. 5509-5514, 1968.

Polian, A., and M. Grimsditch, Brillouin scattering from H_2O: Liquid, ice VI, and ice VII, *Phys. Rev. B, 27*, 6409-6412, 1983.

Polian A., and M. Grimsditch, Room-temperature densification of α-SiO_2 versus pressure, *Phys. Rev. B 41*, 6086-6087, 1990.

Polian A., and M. Grimsditch, Sound velocities and refractive index of densified α-SiO_2 to 25 GPa, *Phys. Rev. B 47*, 13979-13982, 1993.

Polian A., D. Vo-Thanh, and P. Richet, Elastic properties of α-SiO_2 up to 2300K from Brillouin scattering measurements, *Europhys. Lett. 57*, 375-381, 2002.

Poole, P. H., F. Sciortino, U. Essmann, and H. E. Stanley, Phase behavior of metastable water, *Nature, 360*, 324-328, 1992.

Rai, C. S., M. H. Manghnani, and K. W. Katahara, Ultrasonic studies on a basalt melt, *Geophys. Res. Lett., 8*, 1215-1218, 1981.

Rau S., S. Baeßler, G. Kasper, G. Weiss, and S. Hunklinger, Brillouin scattering of vitreous silica under high pressure, *Ann. Phys. 4*, 91-98, 1995.

Revenaugh, J., and S. A. Sipkin, Seismic evidence for silicate melt atop the 410-km

discontinuity, *Nature, 369,* 474-476, 1994.

Richet, P, and A. Polian, Water as a dense icelike component in silicate glasses, *Science, 281*, 396-398, 1998.

Rigden, S. M., T. J. Ahrens, and E. M. Stolper, Densities of liquid silicates at high pressures, *Science, 226*, 1071-1074, 1984.

Rigden, S. M., E. M. Stolper, and T. J. Ahrens, Shock compression of molten silicates: Results for model basaltic composition, *J. Geophys. Res., 93,* 367-382, 1988.

Rigden, S. M., T. J. Ahrens, and E. M. Stolper, High-pressure equation of state of molten anorthite and diopside, *J. Geophys. Res., 94*, 9508-9522, 1989.

Rivers, M. L., and I. S. E. Carmichael, Ultrasonic studies of silicate melts, *J. Geophys. Res., 92,* 9247-9270, 1987.

Rose, J. H., J. Ferrante, and J. R. Smith, Universal binding energy curves for metals and bimetallic interfaces, *Phys. Rev. Lett., 47*, 675-678, 1981.

Rosenhauer, M., C. M. Scarfe, and D. Virgo, Pressure dependence of the glass transition temperature in glasses of diopside, albite, and sodium trisilicate composition, *Carn. Inst. Yrbk., 78,* 556-559, 1978.

Rouch, J., C. C. Lai, and S. H. Chen, Brillouin scattering studies of normal and supercooled water, *J. Chem. Phys., 65(10)*, 4016-4021, 1976.

Rustad, J. R., D. A. Yuen, and F. J. Spera, Molecular dynamics of liquid SiO_2 under high pressure, *Phys. Rev. A, 42*, 2081-2089, 1990.

Rustad, J. R., D.A. Yuen, and F.J. Spera, Molecular dynamics of amorphous silica at very high pressures (135 GPa): Thermodynamics and extraction of structures through analysis of Voronoi polyhedra, *Phys. Rev. B, 44*, 2108-2121, 1991.

Sandercock, J. R., Trends in Brillouin scattering: studies of opaque materials, supported films, and central modes, In: *Light Scattering in Solids, III: Recent Results*, edited by M. Gardona and G. Guntherodt, Topics in applied physics, V. 51, pp. 173-206, Berlin, New York, Springer-Verlag, 1982.

Sato, S., and M. H. Manghnani, Ultrasonic measurements of Vp and Qp: relaxation spectrum of complex modulus on basalt melt, *Phys. Earth Planet. Inter., 41*, 18-33, 1985.

Secco, R. A., M. H. Manghnani, and T. -C. Liu, The bulk modulus-attenuation-viscosity systematics of diopside-anorthite melts, *Geophys. Res. Lett., 18,* 93-96, 1991.

Shen, A. H., and H. Keppler, Infrared spectroscopy of hydrous silicate melts to 1000°C and 10 kbar: direct observation of H_2O speciation in a diamond anvil cell, *Amer. Min., 80*, 1335-1338, 1995.

Shen, A. H., and H. Keppler, Direct observation of complete miscibility the albite-H_2O system, *Nature, 385*, 710-712, 1997.

Shimizu, H., N. Nakashima, and S. Sasaki, High-pressure Brillouin scattering and elastic properties of liquid and solid methane, *Phys. Rev. B 53*, 111-115, 1996a.

Shimizu, H., T. Nabetani, T. Nishiba, and S. Sasaki, High-pressure elastic properties of the VI and VII phase of ice in dense H_2O and D_2O, *Phys. Rev. B, 53,* 6107-6110, 1996b.

Shimomura, O., S. Yamaoka, H. Nakazawa, and O. Fukunaga, Application of a diamond-anvil cell to high-temperature and high-pressure experiments, in *Advances in Earth and Planetary Sciences: High-Pressure Research in Geophysics*, V. 12, edited by S. Akimoto and M. H. Manghnani, pp. 49-60, Reidel, Tokyo, 1982.

Sowerby, J. R., and H. Keppler, Water speciation in rhyolitic melt determined by in-situ infrared spectroscopy, *Amer. Min., 84*, 1843-1849, 1999.

Stacey, F. D., *Physics of the Earth,* Ch. 10, 414 p., New York: Wiley, 1977.

Stebbins, J. F., Identification of multiple structural species in silicate glasses by ^{29}Si NMR, *Nature 330*, 465-467, 1987.

Stebbins, J. F., NMR evidence for five-coordinated silicon in a silicate glass at atmospheric pressure, *Nature 351*, 638-639, 1991.

Stolper, E. M., and T. J. Ahrens, On the nature of pressure-induced coordination changes in silicate melts and glasses, *Geoph. Res. Lett., 14*, 1231-1233, 1987.

Takagi, Y., M. Ahart, T. Yano, and S. Kojima, The liquid-glass transition in n-propanol: the pressure dependence of the Brillouin spectra, *J. Phys.: Condens. Mat., 9*, 6995-7002, 1997.

Tkachev, S. N., R. M. Nasimov, and V. A. Kalinin, New experimental data on ice VI, ice VII and liquid water phase boundaries (in Russian), *Doklady Akademii Nauk (Reports of Russian Academy of Sciences), 342(1)*, 108-110, 1995a.

Tkachev, S. N., J. D. Bass, and A. G. Kalinichev, Viscoelastic properties of liquid water up to 12 kbar by Brillouin spectroscopy. *Eos. Trans. AGU, 76(46)*, F545, 1995b.

Tkachev, S. N., R. M. Nasimov, and V. A. Kalinin, Phase diagram of water in the vicinity of the triple point, *J. Chem. Phys., 105*, 3722-3725, 1996.

Tkachev, S. N., and J. D. Bass, Brillouin scattering study of pentane at high pressure, *J. Chem. Phys., 104(24)*, 10059-10060, 1996.

Tkachev, S. N., and M. H. Manghnani, Sound velocity and attenuation in stable and metastable liquid water to 1.2 GPa by Brillouin spectroscopy, in *Science and*

Technology of High Pressure, Proceedings of the International Conference on High Pressure Science and Technology (AIRAPT-17), edited by M. H. Manghnani, W. J. Nellis and M. F. Nicol, V. 1, pp. 137-140, Universities Press, Hyderabad, India, 2000.

Tkachev, S. N., V. L. Solozhenko, P. V. Zinin, M. H. Manghnani, and L. C. Ming, Elastic moduli of the superhard cubic BC_2N phase by Brillouin scattering, *Phys. Rev. B, 68*, 052104, doi: 10.1103/PhysRevB.68.052104, 2003a.

Tkachev S. N., M. H. Manghnani, Q. Williams, L. C. Ming, Compressibility of Na_2O-$2SiO_2$ Liquid and Melt to 8 GPa Using Brillouin Scattering, *Eos. Trans. AGU, 84(46)*, Fall Meet. Suppl., Abstract V42A-0328, 2003b.

Trachenko, K., and M. T. Dove, Compressibility, kinetics, and phase transition in pressurized amorphous silica, *Phys. Rev. B 67*, 064107, doi: 10.1103/PhysRevB.67.064107, 2003.

Vacher, R., and L. Boyer, Brillouin scattering: A tool for the measurement of elastic and photoelastic constants, *Phys. Rev. B, 6*, 639-673, 1972.

Vedam, K., and P. Limsuwan, Piezo- and elasto-optic properties of liquids under high pressure. I. Refractive index vs pressure and strain, *J. Chem. Phys., 69,* 4762-4771, 1978.

Viart, N., D. Niznansky, and J. L. Rehspringer, Structural evolution of a formamide modified sol - Spectroscopic study, *J. Sol-Gel Sci. Technol., 8*, 183-187, 1997.

Vinet, P., J. Ferrante, J. H. Rose, and J. R. Smith, Compressibility of solids, *J. Geoph. Res., 92*, 9319-9325, 1987.

Wasserman, E. A., D. A Yuen, and J. R Rustad, Molecular dynamics study of the

transport properties of perovskite melts under high temperature and pressure conditions, *Earth and Planet. Sci. Lett., 114*, 373-384, 1993.

Webb, S. L. and P. Courtial, Compressibility of melts in the CaO-Al_2O_3-SiO_2 system, *Geochim. Cosmochim. Acta*, 60, 75-86, 1996.

Williams, Q., R. J. Hemley, M. B. Kruger, and R. Jeanloz, High pressure infrared spectra of α-quartz, coesite, stishovite and silica glass, *J. Geophys. Res., 98*, 22157-22170, 1993.

Williams, Q., and R. Jeanloz, Spectroscopic evidence for pressure-induced coordination changes in silicate glasses and melts, *Science, 239,* 902-905, 1988.

Whitfield, C. H., E. M. Brody, and W. A. Bassett, Elastic moduli of NaCl by Brillouin scattering at high pressure in a diamond anvil cell, *Rev. Sci. Instr., 47*, 942-947, 1976.

Wolf, G. H., D. J. Durben, and P. F. McMillan, High-pressure Raman spectroscopic study of sodium tetrasilicate ($Na_2Si_4O_9$) glass, *J. Chem. Phys. 93*, 2280-2288, 1990.

Wolf, G. H., and P. F. McMillan, Pressure effects on silicate melt - structure and properties, in *Reviews in Mineralogy: Structure, Dynamics and Properties of Silicate Melts*, edited by J. F. Stebbins, P. F. McMillan, and D. B. Dingwell, V. 32, pp. 505-561, Mineralogical Society of America, Washington, D.C., 1995.

Xu, J. A., Brillouin scattering and ultrasonic studies at high temperature and high pressure, *Chem. Geol. 128*, 17-24, 1996.

Xu, J., and M. H. Manghnani, Brillouin-scattering studies of a sodium silicate glass in solid and melt conditions at temperatures up to 1000 ^{o}C, *Phys. Rev. B, 45*, 640-

645, 1992.

Xue, X. Y., J. F. Stebbins, M. Kanzaki, P. F. McMillan, and B. Poe, Pressure-induced silicon coordination and tetrahedral structural changes in alkali oxide silica melts up to 12 GPa: NMR, Raman, and infrared spectroscopy, *Am. Mineral. 76*, 8-26, 1991.

Yen, J., and M. Nicol, Temperature dependence of the ruby luminescence method for measuring high pressures, *J. Appl. Phys., 72*, 5535-5538, 1992.

Zallen, R., *The physics of amorphous solids*, New York: Wiley, 1983.

Zha, C. -S., T. S. Duffy, H. -K. Mao, and R. J. Hemley, Elasticity of hydrogen to 24 GPa from single-crystal Brillouin scattering and synchrotron x-ray diffraction, *Phys. Rev. B, 48*, 9246-9255, 1993.

Zha, C. -S., R. J. Hemley, H. -K. Mao, T. S. Duffy, and C. Meade, Acoustic velocities and refractive index of SiO_2 glass to 57.5 GPa by Brillouin scattering, *Phys. Rev. B, 50*, 13105-13112, 1994.

Zotov, N., I. Ebbsjö, D. Timpel, and H. Keppler, Calculation of Raman spectra and vibrational properties of silicate glasses: Comparison between $Na_2Si_4O_9$ and SiO_2, *Phys. Rev. B 60*, 6383-6397, 1999.

http://www.btinternet.com/~martin.chaplin/anmlies.html

http://www.sunmanagement.com/Ats129.pdf